Master Thesis, Department of Geosciences

Development of Hollendardalen Formation (Svalbard); with emphasis on sedimentological and petrographical analysis.

Christian Sætre

UNIVERSITY OF OSLO

FACULTY OF MATHEMATICS AND NATURAL SCIENCES

Development of Hollendardalen Formation (Svalbard); with emphasis on sedimentological and petrographical analysis.

Christian Sætre

Master Thesis in Geosciences

Discipline: Geology

Department of Geosciences

Faculty of Mathematics and Natural Sciences

University of Oslo

June 1st, 2011

Acknowledgments

First of all I want to thank my supervisor Professor Henning Dypvik at the Department for Geoscience, UiO. Thanks for always having time for questions and discussions and being supportive at all times.

I want to thank North Energies and Lundin for making this project possible. Thanks to Store Norske Spitsbergen Kullkompani (SNSK), and Malte Jochman for providing cores, facilities and field transportation. Thanks to Professor William Helland-Hansen (UiB) for good field teaching and great spirit during the field seasons.

I also want to thank Eivind Patrik Hanevik (UiB) for good stories and good company in two great field seasons on Svalbard.

Thanks to Professor Jenö Nagy (UiO) and his nephew Jonathan Nagy for help with core logging in Longyearbyen. Thanks to Berit Løken Berg for good help with XRD and SEM analysis. Professor Ray Ferrell, Louisiana State University, deserves great thanks for excellent help with XRD analysis.

Great thanks to all of you that have read my thesis and correcting my spelling errors. Especially Wiley Bogren, for always having time to read, and being a good friend at all times. Thanks to Maria Philippa Rossi for motivating mails and proofreading.

Finally my family deserves great thanks for always being supportive.

Oslo, 1st. June 2011

Christian Sætre

Abstract

Hollendardalen Fm. is a shallow marine sandstone unit in the Van Mijenfjorden Group within the Central Basin on Spitsbergen. No detailed systematic mapping, sedimentological or petrographic studies of Hollendardalen Fm. have been conducted before this study.

The sedimentological logs display an upwards shallowing development through the Hollendardalen Fm. Internally Hollendardalen Fm. consists of two upwards coarsening parasequences, which have been recognized throughout the basin. The thickest sediment accumulations are found in the west, with a decreasing development eastwards. Observed structures, lithology and stacking of sedimentary units within the Hollendardalen Fm. indicate a depositional environment of wave and tide dominated delta.

Paleocurrent measurements indicate a northwestern infill in western areas, progressing to a northeastern infill direction in the east. K-feldspar/plagioclase ratio increases from 0,08 in west to 0,51 in east. This is probably a result of a source rock enriched in K-feldspar relative to plagioclase located north in the basin feeding the eastern areas. This is further supported by an increase in the total feldspar/total clay ratio from proximal parts in the west to distal parts in the east.

Heavy mineral assemblages in Grumantbyen, Hollendardalen and Battfjellet formations are not similar. These observed differences indicate that there are different types of parent rocks feeding the system. Change in provenance source between Grumantbyen Fm. and Hollendardalen Fm. is related to a change in regional provenance from an eastern sediment source for Grumantbyen Fm. and a western source for Hollendardalen Fm. Unroofing of source rock under the rising West Spitsbergen Orogen give an explanation for heavy mineral differences between Hollendardalen and Battfjellet formations.

Contents

1 Introduction

This master thesis uses field observations and petrographysical studies to give a sedimentological and petrographic description of Paleogene deposits of the Central Basin on Spitsbergen with a special emphasis on Hollendardalen Fm (Figure 2 - 1, Figure 2 - 3 and Figure 2 - 4).

This thesis is part of a joint international research project named pACE (www.wun.ac.uk/research/pace). The pACE project deals with reconstruction of paleo-climate and paleo-environmental conditions in the Arctic across the Paleocene-Eocene transition. The author and Eivind Patrik Hanevik, a master student at the University of Bergen (UiB), cooperated with field studies and sedimentologic descriptions of Hollendardalen Fm. Eivind Patrik Hanevik writes a thesis with a special emphasis on log correlations, depositional environments and paleo-geometrical evolution of Hollendardalen Fm.

In two field seasons 22 outcrops and five boreholes cores have been logged (Figure 3 - 1). Key outcrops have been studied in detail using field data, in combination with XRD and thin section analysis, along with studies of the heavy mineral composition and geochemical parameters. The acquired data are used to give a sedimentological and petrophysical description of Grumantbyen, Hollendardalen and Battfjellet formations.

2 Regional setting

This chapter presents the tectostratrigraphical development of Svalbard and the lithostratigraphical setting of the Central Basin (Figure 2 - 1, Figure 2 - 3). The study area is located in the Central Basin which is represented by the Van Mijenfjorden Group (Figure 2 - 3, Figure 2 - 4). Other sedimentary basins will briefly be mentioned, but with a special attention to the Van Mijenfjorden Group.

2.1 Tectostratigraphic development

Talwani and Eldholm (1977) studied the evolution of the Norwegian-Greenland Sea by in particular using magnetic anomalies. They concluded that the opening of the Norwegian-Greenland Sea began about 60 to 63 m.y. ago, between magnetic anomaly 24 and 25. The sea floor spreading started about 38 m.y. ago (anomaly 13). In the first phase the sea floor spreading Greenland had a northwesterly motion relative to Eurasia. At this time the Norwegian Sea started to open, but the Greenland Sea remained closed. Greenland slid past Svalbard in a northwesterly motion (Figure 2 - 1). Thereafter a change in pole of rotation occurred and Greenland moved westwards relative to Eurasia (Steel et al. 1985). Land contact was established between Greenland and Svalbard until the opening of the Greenland Sea at 38 m.y. ago (Talwani and Eldholm 1977). The transform motion of Greenland relative to Svalbard in the Paleogene produced the structure named the De Geer Line (Figure 2 - 1). From late Eocene – Oligocene until present Greenland has moved westward with respect to Eurasia, producing a extensional regime at the western side of Svalbard (Steel et al. 1985).

Paleogene sedimentary succession on Svalbard are present in five isolated basins; Bellsund, Forlandsundet, Kongsfjorden, the Northern Spitsbergen and the Central Tertiary Basin, the latter is referred to as the Central Basin in this text (Figure 2 - 3). The Central Basin is the largest and most prominent of the Paleogene basins (Livsic 1992, Dallmann et al. 1999). It constitutes a 200 km long NNW-SSE and 60 km wide E-W synclinorium in the southern and central parts of Svalbard (Figure 2 - 3). The Central Basin deposits comprise an approximate 2.3 km thick succession of siliciclastic rocks which unconformably cover Cretaceous formations (Harland 1969, Dallmann et al. 1999). A considerable amount of material has been eroded and transported away since the Eocene, an 1.7 km thick succession is proposed (Steel et al. 1985).

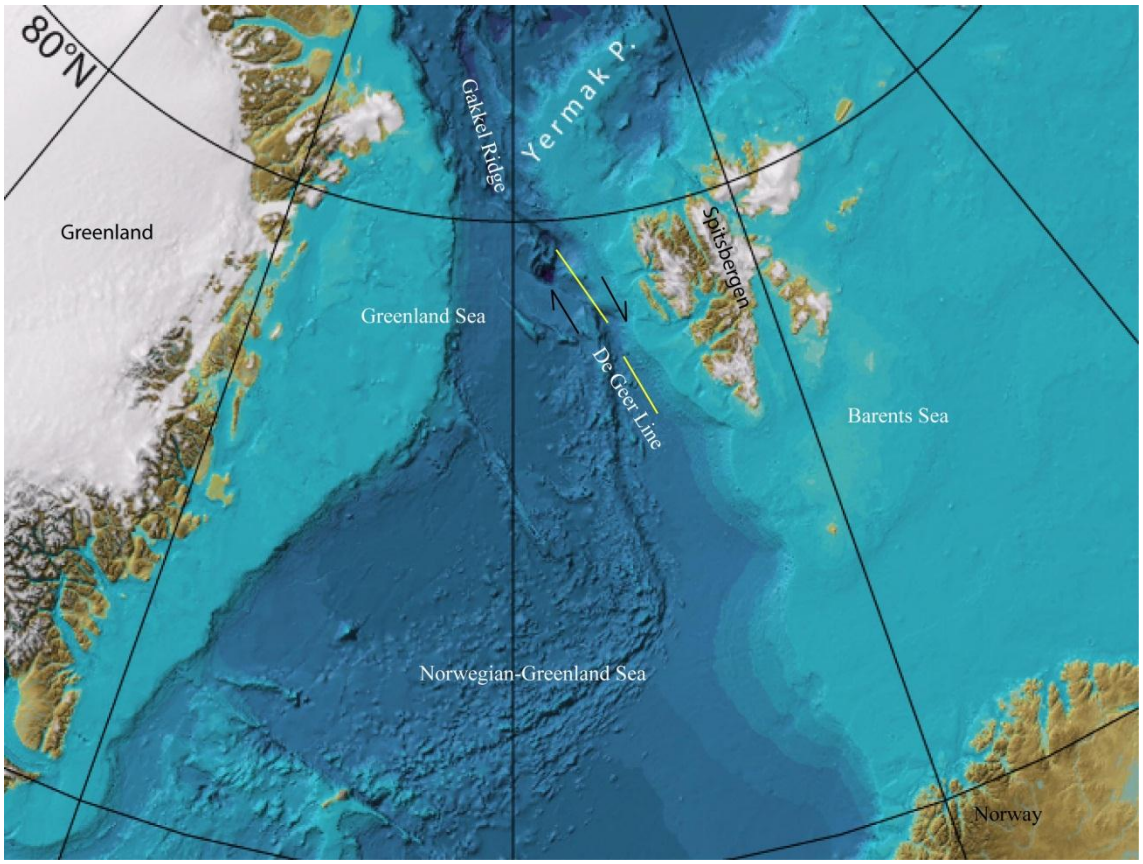

Figure 2 - 1: Present position of Svalbard and Greenland, with major morphological features. Modified from (Jakobsson et al. 2008).

The development of the Central Basin can be divided in two phases; an Early to mid-Paleocene phase and a second one of Late Paleocene – Early Eocene age. The first stage demonstrated an extensional tectonic setting, as e.g. by the thickening of sediments towards the De Geer Line. Ash layers in the Firkanten Formation indicate igneous activity and there is no clear-cut evidence for tectonic uplift (Steel et al. 1985). The second phase of evolution show a major change in the tectonic configuration. Sediments deposited in the early to late Paleocene were most likely derived from the east and northeast (Figure 2 - 2-A to D), while the late Paleocene deposits were derived from more westerly directions (Figure 2 - 2-E). This change in infill pattern suggests an uplift of the western margin of the Central Basin (Steel et al. 1985). Bruhn and Steel (2003) claims that the development can be explained with on compressional phase, where the Central Basin is a foreland basin analogue (Bruhn and Steel 2003) (Figure 2 - 2).

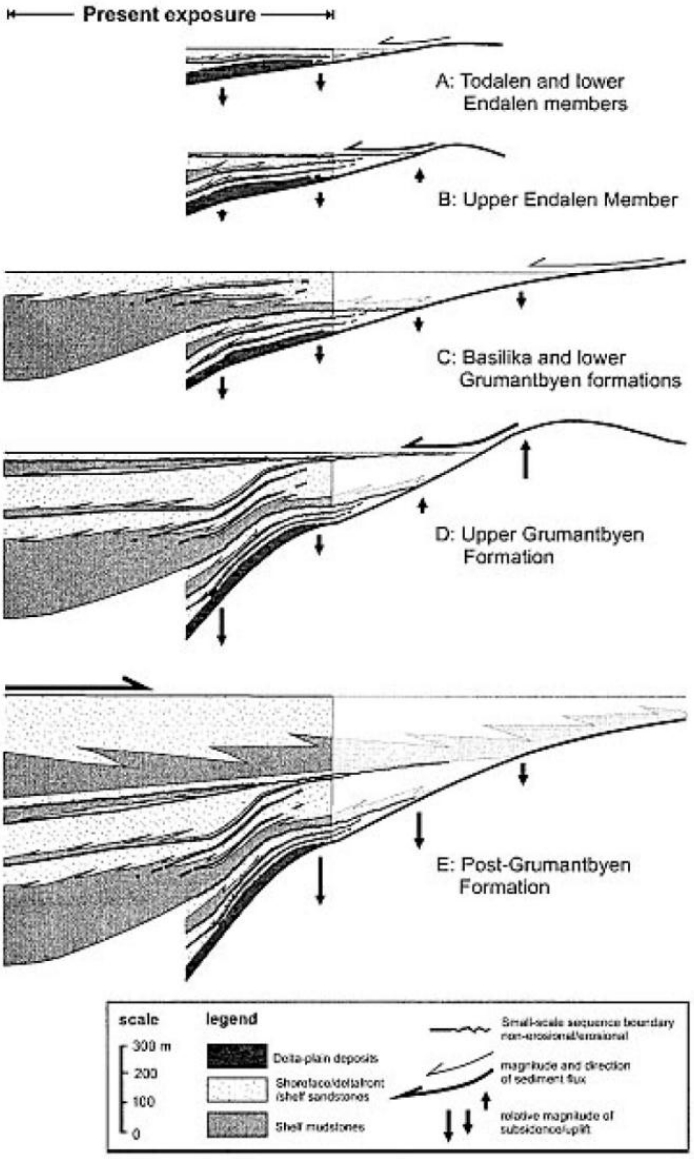

Figure 2 - 2: Figure from (Bruhn and Steel 2003), displaying the development of the Central Basin with a peripheral bulge in east.

Along the southwestern part of Spitsbergen a fold and thrust belt stretches out, named the West Spitsbergen Orogeny (Harland 1969). The West Spitsbergen Orogen is a result of the shift in tectonic setting from phase 1 to phase 2 described by Steel et al. (1985). It develops by the dextral slip along the De Geer Line producing a wrench regime with compression and wrench faults, thrust faults and asymmetric folds (Lowell 1972, Steel et al. 1985). The orogen must be younger than the Van Mijenfjorden Group because the sediments are affected by the orogen. Consequently the orogen may be of post-Oligocene-Miocene age (Harland 1969, Lowell 1972).

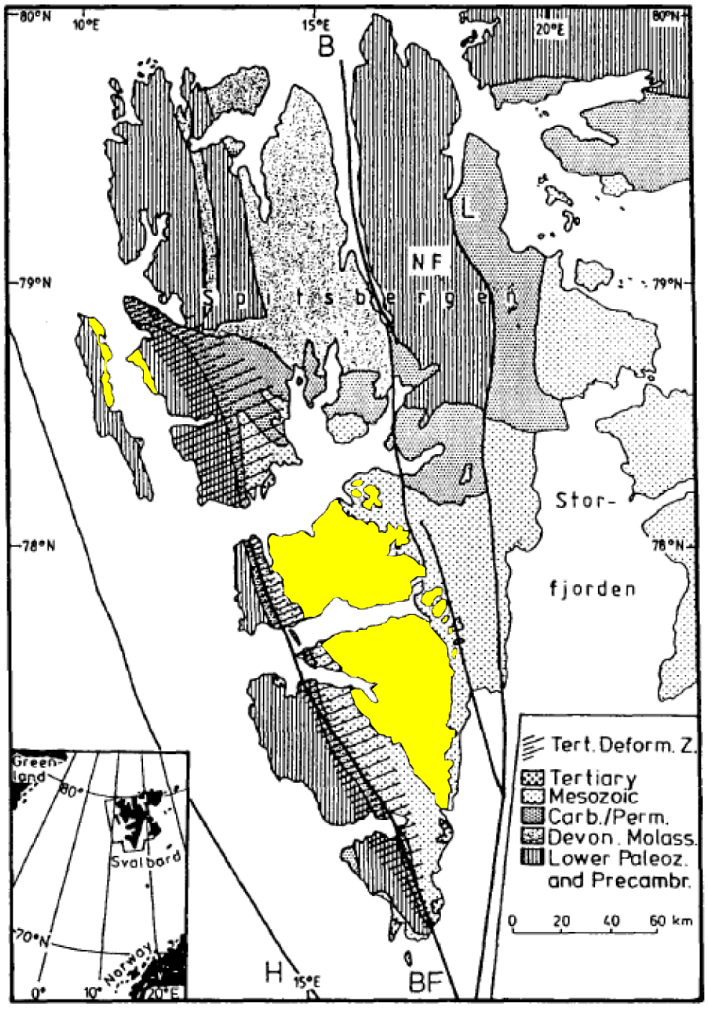

Figure 2 - 3: General geological map of Vest Spitsbergen (Svalbard).Yellow = Tertiary deposits. BF = Western Boundary Fault, H = Hornsund Fault Zone, L = Lomfjorden Fault Zone, NY = Ny Friesland (Müller and Spielhagen 1990).

2.2 Lithostratigraphic setting of the Central Basin

Nathorst (1910) was the first to describe the sedimentary units of the Central Basin of Svalbard, however his work will not be discussed further in this text. The Paleogene deposits of the Central Basin are represented by the Van Mijenfjorden Group (Figure 2 - 4). Along the base of the group there is an unconformity towards underlying Cretaceous units (Harland 1969). The unconformity is the result of a regional uplift and peripheral-bulge uplift. In total the Van Mijenfjorden Group consists of about 2100m of sediments which were deposited in a transgressive regressive trend (Bruhn and Steel 2003). The Cenozoic succession can be divided into seven formations. Firkanten, Basilika and Grumantbyen formations constitute the Paleocene succession, while Frysjaodden, Hollendardalen, Battfjellet and Aspelintoppen

formations make up the Eocene part of the succession. These sediments represent a foreland basin setting, a result of the West Spitsbergen Orogeny (Bruhn and Steel 2003).

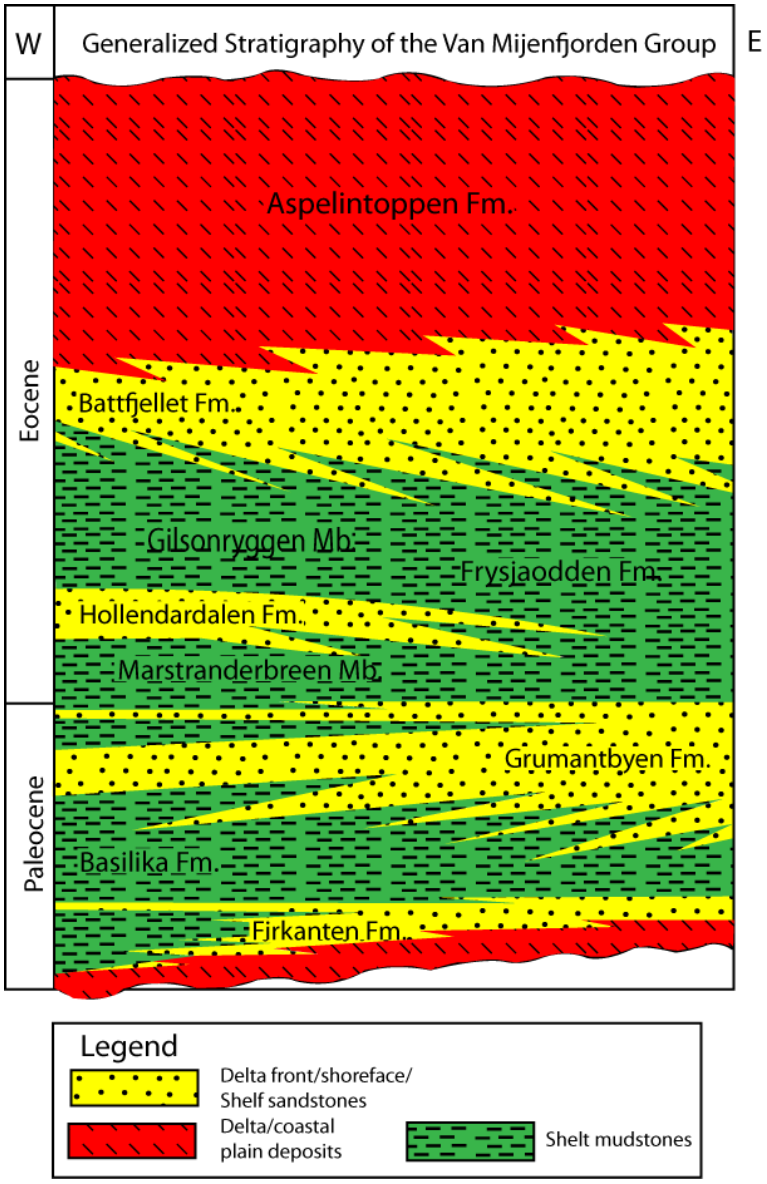

Figure 2 - 4: Stratigraphy of the Van Mijenfjorden Group. Modified from (Bruhn and Steel 2003, Jakobsson et al. 2008).

2.2.1 Firkanten Formation

This formation was probably deposited over a time span of 7 million years and displays an overall transgressive development (Figure 2 - 4). It consists primarily of delta plain to prodelta sandstones, siltstones and shales, derived from the east, west and north (Helland-Hansen 1990, Nagy 2005). Firkanten Fm. is from 80 to 200 m in thickness, increasing towards the west, between Isfjorden and Van Mijenfjorden. Along the base of the Firkanten

Fm. there is a thin basal unit of conglomerates present in the western parts of the basin. This conglomerate is composed of well-rounded pebbles of fluvial origin (Kellogg 1975). The basal conglomeratic is succeeded by three members (Müller and Spielhagen 1990) from the base and upwards:

- **Todalen Member**: It displays a transgressive development with delta-plain and tidal deposits at the base overlain by mouth-bar sandstones and shoreface sandstones at the top (Bruhn and Steel 2003). At the base there is a basal clast-supported conglomerate, which is overlain by a shale/siltstones dominated package. The rest of the Todalen Mb. shows an upwards coarsening trend towards the topmost sandstones (Nagy 2005).

- **Kalthoffberget Member**: This member consists of shelf deposits and contains series of repeated upwards coarsening parasequences; from shale/silt to silt/fine-grained sandstones (Bruhn and Steel 2003, Nagy 2005). This is the southernmost equivalent of the Endalen Member (Müller and Spielhagen 1990).

- **Endalen Member**: Endalen normally comprises series of 4 to 5 upwards coarsening parasequences, it consist mainly of medium-grained sandstones with some silty intervals (Nagy 2005). It represents a prograding storm and wave-dominated shoreface deposits along a deltaic coastline (Dallmann et al. 1999).

2.2.2 Basilika Formation

The Basilika Fm. is the second depositional cycle in the Paleogene succession (Figure 2 - 4). It overlies the coarser sandstones of the Firkanten Fm., and consists of mainly silty shales with small pyrite nodules and pebbles throughout the formation (Müller and Spielhagen 1990). The transition from the Firkanten Fm. sandstones to the shales of Basilika Fm. occurs in 1 – 5 m thick zone. The formation is up to 430 m thick along the western margin, but is rapidly thinning towards the north and northeast (Kellogg 1975). The shales are interpreted to represent an offshore shelf mud complex. This is further supported by presence of lenses of shells and foraminifera, often related to storm activity. Lack of bioturbation and the presence of pyrite in separate levels indicate periods of anoxic conditions (Müller and Spielhagen 1990).

2.2.3 Grumantbyen Formation

This formation overlies the silty shales of the Basilika Fm. often a graded transition from Basilika (Steel et al. 1985). Primary structures seen in this formation are infrequent ripple lamination and load casts. The structures are disturbed by heavy bioturbation and storm events. The lack of structures might be due to thorough sea bottom bioturbation (Frey and Pemberton 1985). Grumantbyen Fm. consists of several sand sheets which are organized in six different sequences. The lower of these sequences are made up of storm deposits and are heavily bioturbated. The upper sequences reflect deposition at or above the storm wave base, seen by hummocky cross-stratification, planar lamination and wave-ripple lamination (Bruhn and Steel 2003).

2.2.4 Frysjaodden Formation

The Frysjaodden Fm. represents the third major depositional cycle in the Central Basin (Figure 2 - 4). It comprises two members: Marstranderbreen Mb. and the Gilsonryggen Mb. A sand formation, Hollendardalen Fm., is wedged in-between these two members (Dallmann et al. 1999). The lower boundary of Frysjaodden Fm. is a sharp shale contact towards the siltstones of Grumantbyen Fm. The Frysjaodden Formation range from 200 to 400 m in thickness and thickens towards the south- and southwestern parts of the Central Basin. The Frysjaodden and Hollendardalen formations represent a change in the drainage pattern from the earlier Paleogene successions (Dallmann et al. 1999).

- **Marstranderbreen Member**: This is the lowermost member of the Frysjaodden Fm. (Figure 2 - 4). It consists of dark shales deposited at deep water, in a foreland basin setting. It comprises dispersed siltstone layers and laterally interfingers with the Hollendardalen Fm. (Dallmann et al. 1999).

- **Gilsonryggen Member**: Gilsonryggen Member (Figure 2 - 4) overlies the coarser sandstones of Hollendardalen Fm. (Dallmann et al. 1999) and it is only defined in areas where Hollendadalen Fm. is present (Dallmann et al. 1999). It is dark grey shale, with a few siltstone and bentonite layers, deposited in an offshore environment (Kellogg 1975, Helland-Hansen 1990, Dallmann et al. 1999).

2.2.5 Hollendardalen Formation

This sandstone formation interfingers with the Gilsonryggen and Marstranderbreen members of the Frysjaodden Fm. (Figure 2 - 4) (Dallmann et al. 1999). The formation measures up to 150 m in thickness in western parts of the basin and progressively thins eastwards until it disappears (Dalland 1979, Steel et al. 1981). Hollendardalen Fm. has been interpreted to be a shallow marine, tidally-influenced delta (Steel et al. 1985, Dallmann et al. 1999). The Hollendardalen Fm. consists of upwards coarsening units, where the lower part consists of alternating sandstone and siltstone beds where the sandstone beds contain current ripples. The middle part of the formation consists of low angle cross-stratified sandstones, while the upper part has cross-bedded sandstone of medium grain size. The upper part is also characterized by root structures and thin coal layers (Dalland 1977). The eastward thinning and paleocurrent measurements indicate that the sediments are derived from a westerly source (Helland-Hansen 1990, Dallmann et al. 1999). The sandstones of Hollendardalen Fm. are the first sandstones that are derived from the rising West Spitsbergen Orogen (Steel et al. 1981, Dallmann et al. 1999).

2.2.6 Battfjellet Formation

This sandstone dominated unit covers the much finer-grained sediments of the Frysjaodden Fm. (Figure 2 - 4). The sediments of the Battfjellet Fm. are typically fine to medium sand and formation thicknesses vary from 60 to 100m (Kellogg 1975, Steel et al. 1985, Helland-Hansen 1990, Dallmann et al. 1999). The formation is organized in several upwards coarsening units, each unit ranging from 10 to 30 m in thickness (Helland-Hansen 1990). The units display hummocky cross-stratification, horizontal and wave ripple laminated structures in the lower part, indicating storm and wave influence. Higher up in the formation trough- and planar cross-stratification are seen, indicating a current influenced deposition (Helland-Hansen 1990, Dallmann et al. 1999). Helland-Hansen (2010) concluded, on basis on observed structures and stacking pattern, that Battfjellet Fm. was formed by shifting delta lobes on a shelf.

2.2.7 Aspelintoppen Formation

The lower boundary of Aspelintoppen Fm. is defined where the first coals or thicker shaly intervals appear over the last sandstone intervals of the Battfjellet Fm. (Dallmann et al. 1999). Aspelintoppen Fm. is the youngest sedimentary deposit preserved in the Central Basin (Figure

2 - 4) (Kellogg 1975). The formation reaches thicknesses over 1000 meters south of Van Mijenfjorden (Kellogg 1975, Helland-Hansen 1990, Dallmann et al. 1999). In this formation the alternating beds of sandstones and siltstones, mudstones and thin coals are dominating. The sandstone intervals have often undergone soft sediment deformation and are rich in organic remains, such as of plant fragments (Helland-Hansen 1990, Dallmann et al. 1999). The upper part of the Aspelintoppen Fm. clearly shows terrestrial depositional influence, crevasse splays and swamp deposits (Kellogg 1975, Helland-Hansen 1990, Dallmann et al. 1999). This formation is interpreted to be of a deltaic or coastal plain origin based on the presence of coal seams, lack of marine fauna and the presence of canalized sandstones and fining upwards successions (Steel et al. 1985).

3 Methods and material

3.1 Field work and core logging

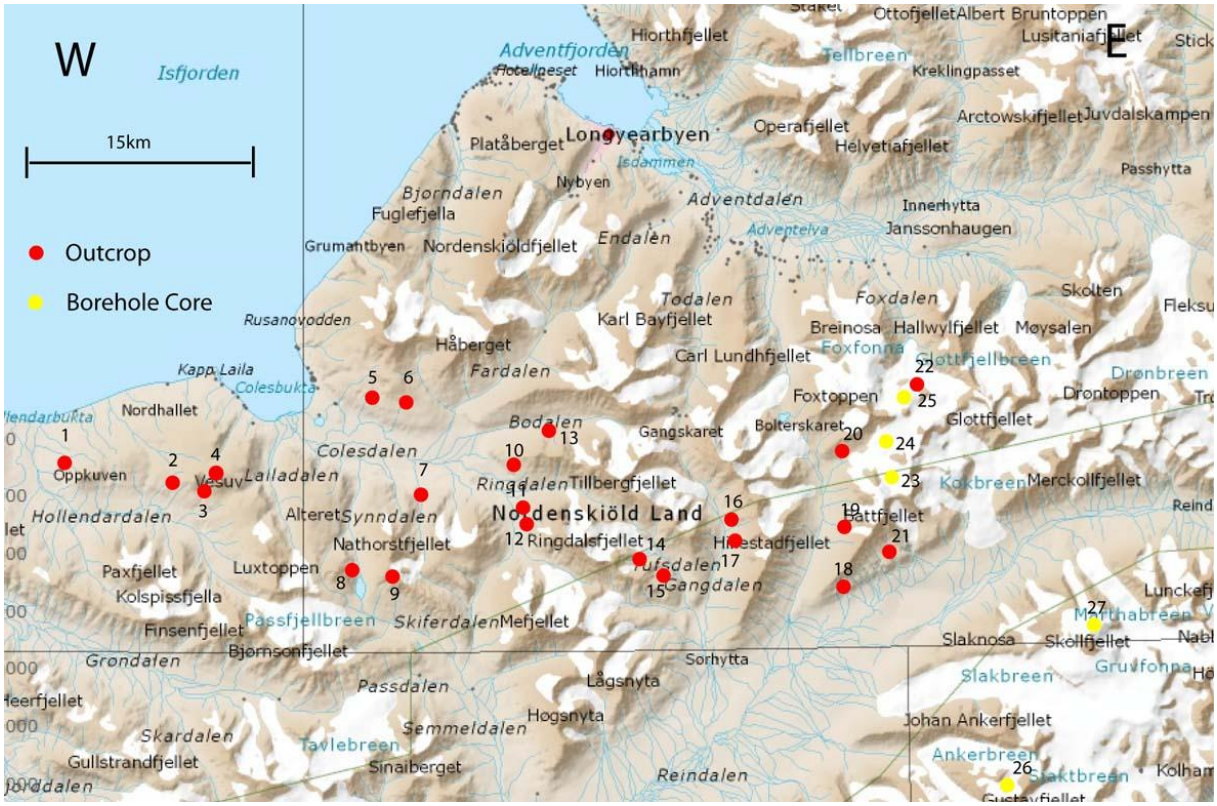

Figure 3 - 1: Overview of outcrops and boreholes studied. Red dots are outcrops and yellow are boreholes. 1 = Oppkuvbekken, 2 = Vestalbekken, 3 = Vesuv Sør, 4 = Vesuv, 5 =N-E of Kapp Laila, 6 = Russekollen, 7 = Trodalen, 8 = Holmsenfjellet, 9 = Istjønnelva, 10 = Tillbergfjellet Vest, 11 = Ringdalsfjellet Øst 2, 12 = Ringdalsfjellet Øst, 13 = Bødalen, 14 = Tufsbreen, 15 = Bromdalsnosa, 16 = Gangdalen Nord, 17 = Gangdalen Sør, 18 = Reindalen Sør, 19 = Tverrdalen, 20 = Gilsonryggen Sør, 21 = Reindalen Nord, 22 = Foxbreen, 23 = BH 9/06, 24 = BH 6/06, 25 = BH 8/06, 26 = BH 10/06, 27 = BH 7/08.

Fieldwork and core logging was executed during the summers of 2009 and 2010.

Professor Arne Dalland (unpublished work) mapped outcrop localities in the Central Basin. His unpublished map was put at our disposal and was a great contribution in our search for the very best sections.

In 2009 eight outcrop sections where logged in the Coles Bay area by the author and Eivind Patrik Hanevik a master student from the University of Bergen (UiB). Professor Henning Dypvik (UiO) and Professor William Helland-Hansen (UiB) supervised the first days of study. Each section was logged in 1:50 scale on a standard log sheet (Appendix 6), overview

and close up photos were taken of each outcrop (Figure 3 - 1). In addition five cores were logged at the core storage of Store Norske Kullkompani in Endalen. Each core was cleaned with water, carefully inspected and logged in 1:20 scale on a standard log sheet.

In 2010, 14 outcrops were logged from Oppkuvbekken in northwest to Foxbreen in southeast (Figure 3 - 1). Logs were made by Eivind Patrik Hanevik and the author. Outcrops were carefully inspected, photographed and logged in 1:50. The first four days we were under supervision of Professor William Helland-Hansen.

3.2 Sampling

478 samples were collected from outcrops and boreholes. Each field sample about fist size, vertical orientation was marked with an arrow.

3.3 Facies description and facies associations

Classification of sedimentary rocks follows the Wentworth grain-size classification (Wentworth 1922) (Table 3 - 1). Folk (1954) provides a further classification based on sand, clay and silt content. Sandstones contain 90 % or more grains of very fine - very coarse grain size, 10% to 50 % silt defines as silty sandstone, 50 % to 90 % silt defines as sandy siltstone, over 90 % silt defines as a siltstone. Field observations, thin section analysis and photos were used to define facies on basis of lithology, texture and structures. Facies lithology and structures are allowed to vary to give a better correlation and understanding of depositional environment. Facies are grouped together in facies associations which representing specific depositional environments,

Table 3 - 1: The Wentworth grain-size classification (Wentworth 1922)

Size range (mm)	Phi units	Wentworth size class
256 - ∞	∞ - 8	Boulder
64 – 256	-6 - -8	Cobble
4 – 64	-2 - -6	Pebble
2 – 4	-1 - -2	Granule
1 – 2	0 - -1	Very coarse sand
0,5 – 1	1 - 0	Coarse sand
0,25 – 0,5	2 - 1	Medium sand
0,125 – 0,25	3 - 2	Fine sand
0,0625 – 0,125	4 - 3	Very fine sand
0,031 – 0, 0625	5 - 4	Silt
∞ **- 0,0039**	1/∞ - 8	Clay

3.4 Digitalizing of sedimentary logs

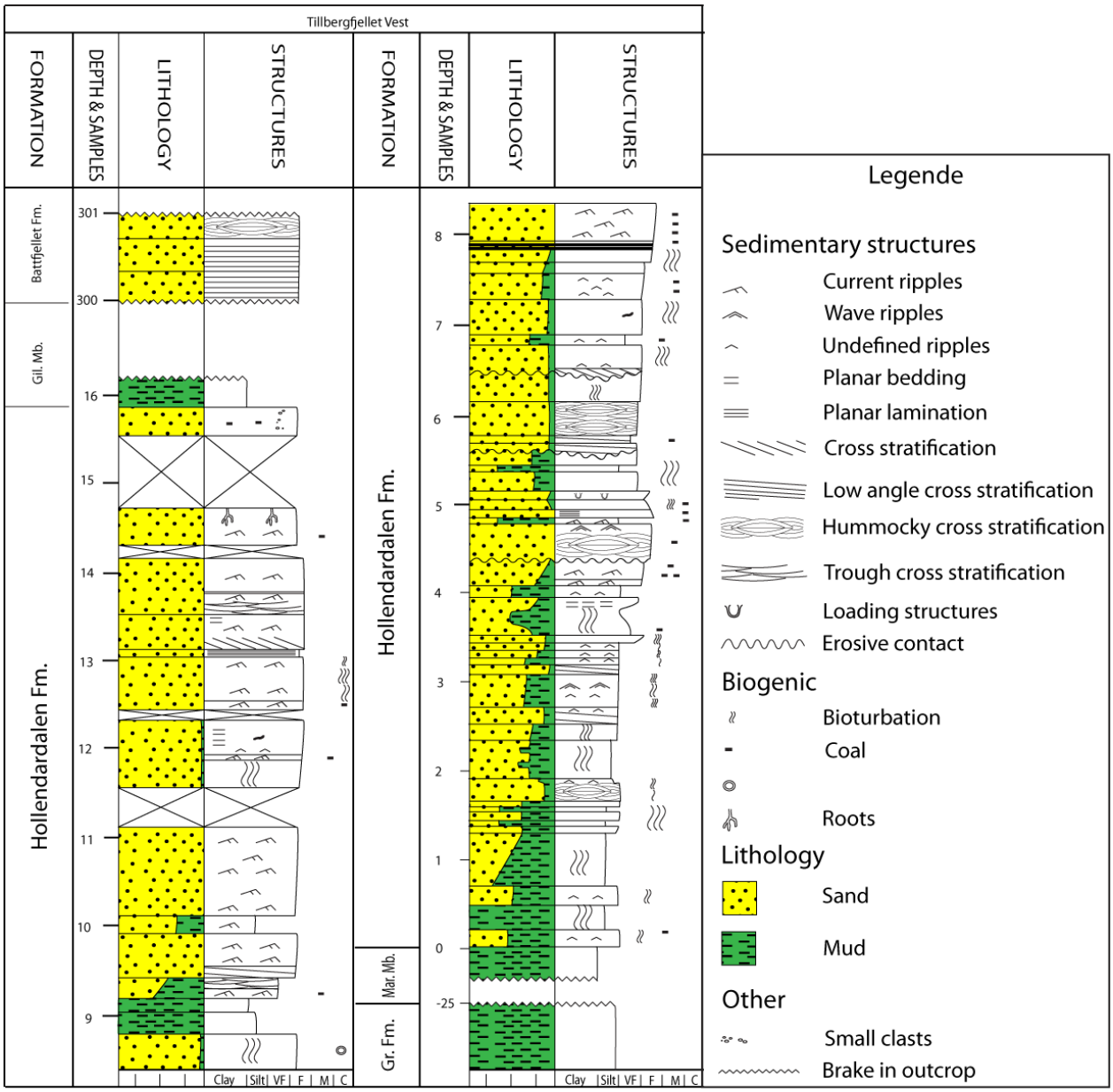

Figure 3 - 2: Example log from Tillbergfjellet Vest section. The log display the normal observed development of Hollendardalen Fm. with two upwards coarsening parasequences and a general increased sand content. Observed structures are normally ripples and Hummocky cross-stratification with root structures and coal beds from the middle of the section and upwards.

All field logs were digitalized by the writer and Eivind Patrik Hanevik. Adobe Illustrator and Corel Draw were used (Figure 3 - 2).

3.5 Laboratory work

3.5.1 Rock grinding

Material for XRD, TOC/TC and Rock-Eval analysis were crushed by the writer at UiO. A slinging mill was used to grain each sample to a rock powder. The mill was careful cleaned and dried with ethanol between each sample.

3.6 Thin section

Key outcrops and cores were selected to keep amount of thin sections to a reasonable level. 83 samples were selected and sent for thin section preparation. Of these were 69 studied in detail.

Thin sections were made by molding samples stained in blue epoxy before grinding and polishing down to 30 µm. Lars Kirksæther at IFE Petrosec prepared the thin sections.

3.6.1 Point counting

Qualitative mineral analyses were performed before point counting. A Nikon petrographic microscope was used for thin section analysis. 400 points were counted for all 69 thin sections using a Swift automatic counter.

Based on the qualitative analysis, twelve different minerals or mineral groups were considered to compose the bulk mineralogy. 1) Monocrystalline quartz, 2) Polycrystalline quartz, 3) Opaque minerals, 4) Plagioclase, 5) Other feldspars, 6) Illite, 7) Other clay minerals, 8) Muscovite, 9) Chlorite, 10) Glauconite, 11) Heavy minerals, 12) Other minerals. Quartz and feldspar have similar optical properties and are difficult to distinguish. Muscovite, paragonite and talc are not differentiated and grouped together as white mica. Pyrite and organic material shows similar optical properties, therefore grouped together as opaque minerals.

3.7 SEM

Key thin sections were examined using a scanning electron microscope (SEM) at the UiO. A SEM study produces an energy dispersive x-ray spectrum (EDX), reflecting the elemental composition. The SEM was operated by the author under supervision of Berit Løken Berg. By comparing elemental composition with known mineral elemental composition, a precise mineral identification could be obtained. SEM Petrology Atlas (Welton 1984) was used for mineral identification. Combining back scatter electron microscopy and secondary electron microscopy provides a method to discover quartz overgrowth.

3.8 XRD analysis

86 XRD-analysis was conducted by Berit Løken Berg at UiO.

During XRD analysis, a monochromatic ray is transmitted on the crystal lattice, whereupon the diffraction angle depends on the crystal lattice structure. Rays transmit at various angles, corresponding diffracted angles are recorded and a difractogram is produced. The different angles recorded correspond to lattice distance related to orientation of the crystal planes. Minerals produce a specific signature that can be recognized in the difractogram (Moore and Reynolds 1989). The theory behind this procedure is based on Bragg's law:

$$2dsin\theta = n\lambda \quad \text{Equation 1, after (Bragg and Bragg 1913)}$$

d equals the spacing between the planes in the crystal lattice, θ is the angle between the incident ray and the reflecting plane, and λ is the wave length of the incident ray (Bragg and Bragg 1913).

3.8.1 MacDiff

All XRD-samples were analyzed using MacDiff (Petschick 2004). Qualitative analysis requires a thorough inspection of XRD-plots. Minerals where identified on basis of d-spacing (Table 3 - 2) for minerals and associated d-spacing (Moore and Reynolds 1989). Based on the qualitative analysis, a subprogram containing three minerals (Quartz, plagioclase and K-feldspars) were made in MacDiff, to automatically measure their peaks. Kaolinite, chlorite, illite and mica have complex peaks, and a manual analysis is necessary to obtain a good peak fit. Kaolinite and chlorite shear their 100 % intensity peak at 7 Å, by measuring their peaks

kaolinite (3,58 Å) and chlorite (3,54 Å) peaks, their internal ratio were calculated. Their ratios are multiplied with the 7 Å peak to acquire their respective XRD intensities. Calcite was searched for, but was not observed in any studied samples. Professor Ray E. Ferrell assisted with the qualitative and quantitative analysis (Ferrell 2010, personal communication). Peak intensity measurements give XRD%, considered as semi-quantification. XRD-values are best used to see changes in relative mineral proportions.

Table 3 - 2: Minerals and associated d-spacing (Moore and Reynolds 1989)

Mineral	D-spacing
Quartz	4,26 Å
K-feldspar	3,24 Å
Plagioclase	3,29 Å
Kaolinite	3,58/7 Å
Chlorite	3,54 Å
Illite + Mica	10,07 Å

3.9 TOC/TC

21 crushed samples were analyzed for total organic carbon (TOC) and total carbon (TC) content by Mufak Naoroz at UiO.

TOC and TC samples were analyzed with the Carbon Analyzer LECO (CR-412). Material was heated in a combustion chamber with a pure oxygen atmosphere. During heating all C-bearing (carbon-bearing) compounds were broken down to free C in an oxidative-reduction process. Heating 0,35 g material to 1350ºC, all free carbon oxidizes to form CO_2. The CO_2 content was measured in an infrared cell and the carbon content was calculated. TOC samples were treated with HCl at 40-50ºC to remove inorganic carbon. HCL treated material was rinsed with distilled water and left to dry at 80ºC for a few hours before run in the LECO instrument. TC samples were done without any pretreatment before being run in the LECO instrument (Naoroz 2010).

3.10 Heavy mineral analysis

23 samples were sent to HM Research in England for heavy mineral analysis. Samples were selected in the very fine fraction in strategic outcrops to get a northwest to southeast coverage.

Heavy minerals are defined as high-density components (density greater than 2,8 g/cm^3) in siliciclastic sediments. Heavy liquid settling separates heavy minerals from other material.

Minerals that have specific gravity greater than the liquid will sink, the rest will float. Provenance studies using heavy mineral composition is based on the principle that a change of provenance rock will result in shift in heavy mineral composition. This is dependent on provenance-sensitive parameters such as hydraulic and diagenetic behavior of minerals. Heavy mineral correlation of sandstones requires use of stable heavy mineral ratios which are unaffected by hydraulic and diagenetic processes (Table 3 - 3). Heavy mineral indexes are produced by determining the relative proportions of heavy minerals in a sample, a count of 200 to 300 detrital minerals are used. (Morton and Hurst 1995, Morton and Hallsworth 1999).

Table 3 - 3: Provenance sensitive heavy mineral indexes, modified from Morton and Hallsworth 1999. ATi = apatite:tourmaline index, GZi = garnet:zircon index, RZi = TiO2 minerals:zircon index, RuZi = rutile:zircon index, MZi = monazite:zircon index, CZi = chrome:spinel index.

Index	Definition
ATi	apatite–tourmaline index
GZi	garnet–zircon index
RZi	TiO2 group–zircon index
RuZi	rutile–zircon index
MZi	monazite–zircon index
CZi	chrome spinel–zircon index

3.11Rock-Eval pyrolysis

21 samples were sent for Rock-Eval pyrolysis at Geolab Nor in Trondheim.

In the Rock Eval pyrolysis crushed material is gradually heated in an inert atmosphere of nitrogen or helium (Peters 1986). A FID (flame ionization detector) detector measures all organic compounds that are pyrolysed during heating. These peaks are registered S1, S2 and S3. S1 equals the thermally distilled free hydrocarbons (mg HC/g rock), further heating pyrolyse kerogen to hydrocarbons (S2 peak (mg HC/g rock)) and CO_2 (S3 peak (mg CO_2/g rock)). Maximum generation of hydrocarbons occur at the S2 peak, at the corresponding temperature Tmax is measured (Peters 1986, Sykes and Snowdon 2002).

The amount of hydrocarbons (S2) generated relative to the total organic carbon (TOC) in a given amount of rock is expressed by the hydrogen index (HI). The oxygen index (OI) equals the amount of CO2 produced (S3) relative to the TOC (Peters 1986).

$$\left(\frac{S2}{TOC}\right) \times 100 = HI$$ Equation 2 (Peters 1986).

$$\left(\frac{S3}{TOC}\right) \times 100 = OI$$ Equation 3 (Peters 1986).

4 Results

In two field seasons 22 outcrops and five boreholes (cores) were logged (Figure 3 - 1). In this section eight outcrops. Outcrops lie in a northwest to southeast transect, (Figure 3 - 1). Borehole BH7/08 was sampled and studied more carefully than other boreholes. It has been concluded that Hollendardalen Fm. is not present in the borehole, therefore it will not be discussed further. Digitalized logs not presented here are placed in Appendix cd.

4.1 Facies description and facies associations

4.1.1 Facies

Based on criteria in chapter 3.3 14 facies with subgroups were identified (Table 4 – 1). Facies are divided in subgroups with similar sedimentological appearance. In the facies presentation it is continuously referred to mapped outcrops (Figure 3 - 1).

Facies i. Siltstone:

This siltstone facies contain poorly developed lamination and a varying degree of bioturbation (Figure 4 - 8). It has a dark grey color and some coal fragments. The facies i is found in the Marstranderbreen Mb. at all outcrops, where it dominates the base. In the Hollendardalen Fm. it interbeds with sandstones of varying facies. The thickness range from 5 to 60 cm.

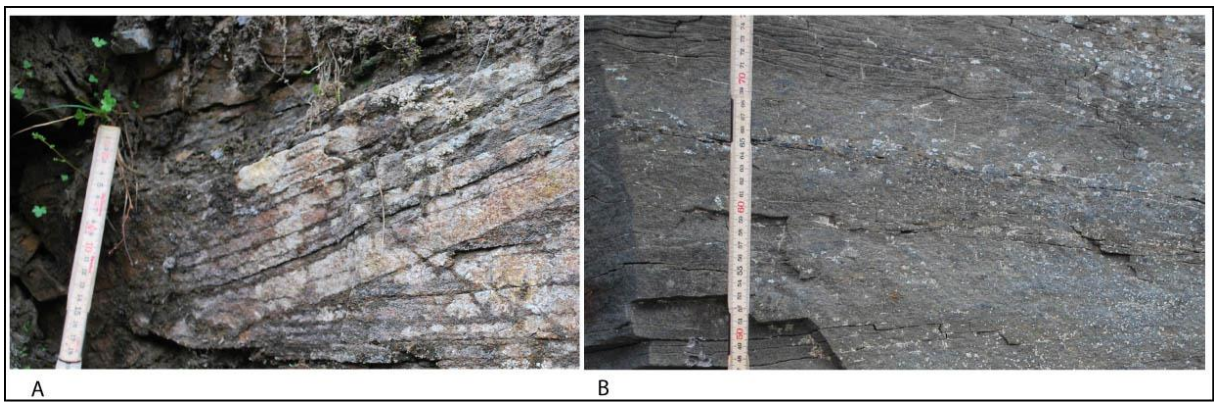

Figure 4 - 1: A) Cross-bedded sandstone facies ii.a (Oppkuvbekken). B) Low angle cross-stratification of sandstone facies ii.b (Holmsenfjellet).

Table 4 - 1: The sedimentary facies classes found in the studied sections.

Facies nr.	Facies	Grain size	Physical and biogenic structures	Figure
i	Siltstone	Clay to silt	Poorly developed lamination. Coal fragments, varying degree of bioturbation. Dark grey color.	Figure 4 - 8
ii.a	Cross stratified sandstone	Very fine to fine sand	Cross-bedding, foreset are planar and nontangential, 1 cm thick foreset beds.	Figure 4 - 1-A
ii.b	Cross stratified siltstone/sandstone	Silt to fine sand	Low angle cross-bedding. Foresets beds are 1 cm thick. Some organic draping.	Figure 4 - 1-B
ii.c	Cross stratified sandstone	Fine sand	Trough cross stratification. Grey color.	Figure 4 - 2-A
ii.d	Cross stratified sandstone	Medium to coarse sand	Tangential with erosive lower boundaries. Foresets beds are sigmoidal- or planar. Some clay clasts and pebbles, coal fragments.	Figure 4 - 2-B
iii.a	Ripple laminated sandstone	Very fine to fine sand	Asymmetrical ripple lamination, slightly bioturbated. Coal fragments, some clay or organic draping.	Figure 4 - 10-D
iii.b	Ripple laminated sandstone	Very fine to fine sand	Symmetrical ripple lamination, some bioturbation. Coal fragments. Grey color.	Figure 4 - 3-A
iii.c	Ripple laminated sandstone	Very fine to medium sand	Bidirectional ripples. Some coal and leaf fragments.	Figure 4 - 3-B
iii.d	Ripple laminated sandstone	Very fine to fine sand	Unspecified ripple lamination. Structures partly destroyed by bioturbation. Some coal fragments.	Figure 4 - 9-D
iv	Hummocky cross stratified sandstone	Very fine to fine sand	Hummocky cross stratification. Sometimes ripples towards the top or soft bed deformation. Coal fragments. Grey color.	Figure 4 - 9-C
v	Laminated/bedded sandstone	Very fine to medium sand	Plan parallel laminae or bed, some bioturbation, coal fragments.	Figure 4 - 4-A
vi	Undulating sandstone	Very fine sand	Undulating laminae.	Figure 4 - 5-A
vii	Flaser bedded sandstone	Silt to fine sand	Flaser bedding.	
viii	Bioturbated siltstone/sandstone	Silt to fine sand.	All structures are destroyed by bioturbation.	Figure 4 - 9-D
ix	Sandstone with root horizons	Very fine to fine sand	Root horizons, ripple laminated or trough cross stratified sandstone.	Figure 4 - 10-F
x	Coal		Unconsolidated coal. Varying amount of sand content. Black color.	Figure 4 - 4-B
xi	Very poorly sorted sandstone	Fine sand	Very poorly sorted, pebbles and clay clasts, shell and coal fragments. Dark grey color.	Figure 4 - 6-A
xii	Pebble rich sandstone	Fine to medium sand	Up to 15 % rounded pebbles, very poorly sorted. Dark grey color.	Figure 4 - 6-B
xiii	Soft sediment deformed sandstone	Very fine to fine sand	Soft sediment deformation and water escape structures. Ripples and clay clasts.	
xiv	Shell rich sandstone	Very fine to medium sand	Rich in shell and coal fragments. Bidirectional and symmetrical ripples.	Figure 4 - 7

Facies ii. Cross stratified sandstone:

a. This facies is present in central and western parts of the studied area within Hollendardalen Fm. (Figure 4 - 1-A). Facies ii.a consists of nontangential cross-bedded units (10 – 50 cm) of very fine to fine sand. Foresets are planar with 1 cm thick foreset beds. Facies ii.a is often overlain by ripple laminated sandstones (facies iii.b).

b. Sandstones and siltstones units (25 cm) of facies ii.b display low angle-cross bedding (Figure 4 - 1-B). Bounding surfaces are normally non-erosive and planar. Some of the foreset beds have organic draping.

c. Facies ii.c (Figure 4 - 2-A) is characterized by trough cross bedding of fine sand. It is present in central and western parts of the basin within Hollendardalen Fm. Units are from 0,1 m to 1,7 m thick, the thicker units (1 – 1,7 m) are slightly upwards coarsening. At Trodalen (7,5 m) the lower boundary is erosional with rounded pebble sized grains, but except from this lower boundaries are non-erosive.

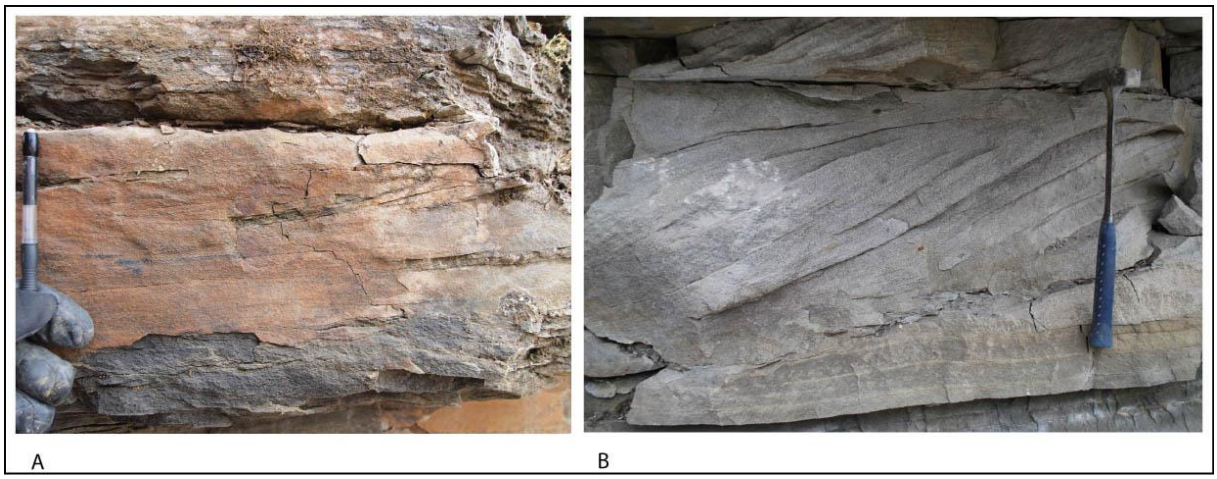

Figure 4 - 2: A) Trough of sandstone facies ii.c (Oppkuvbekken). B) Sigmoidal foresets of sandstone facies ii.d (Vestalbekken).

d. This sandstone facies is 30 to 90 cm in thickness and contains medium to coarse sand with erosive lower boundaries. Small coal fragments are present through the whole facies. Foresets are sigmoidal or planar with reactivation surfaces (Figure 4 - 2-B). Variable foreset bed thicknesses are observed within a unit. Pebble sized grains and clay clasts are present in the lower part of this facies. Foresets are normally tangential. The facies iii.d is only found at the Vestalbekken and Trodalen outcrops.

Facies iii. Ripple laminated sandstone:

a. Facies iii.a was observed in all outcrops. It is ripple laminated very fine to fine sandstone and non to moderate degree of bioturbation (Figure 4 - 10-D). Ripples are asymmetrical and contain some clay or organic draping. Varying amount of coal fragments are found in the sandstones. In the lower part (0 – 4 m) of Oppkuvbekken, Vestalbekken and Holmsenfjellet outcrops the sandstone facies are up to 20 cm thick and make a distinct unit that disrupt siltstones of facies i. When it occur in the upper part (7 m and higher) of the outcrops the sandstone facies iii.a is thicker (0,25 – 1,2 m) and slightly upwards coarsening.

b. This facies is characterized by symmetrical ripple lamination of very fine to fine sand with some coal fragments (Figure 4 - 3-A). It is found in all outcrops in Hollendardalen Fm. In the lower part (0 – 6,2 m) of the outcrops this sandstone facies forms distinct units (10 – 20 cm thick) that interbeds siltstones of facies i or overlies sandstones of facies ii.a. This sandstone facies often overlie facies iv sandstones in the upper part (7 m and higher) of the outcrops. This sandstone facies have non to moderate degree of bioturbation and contain some coal fragments.

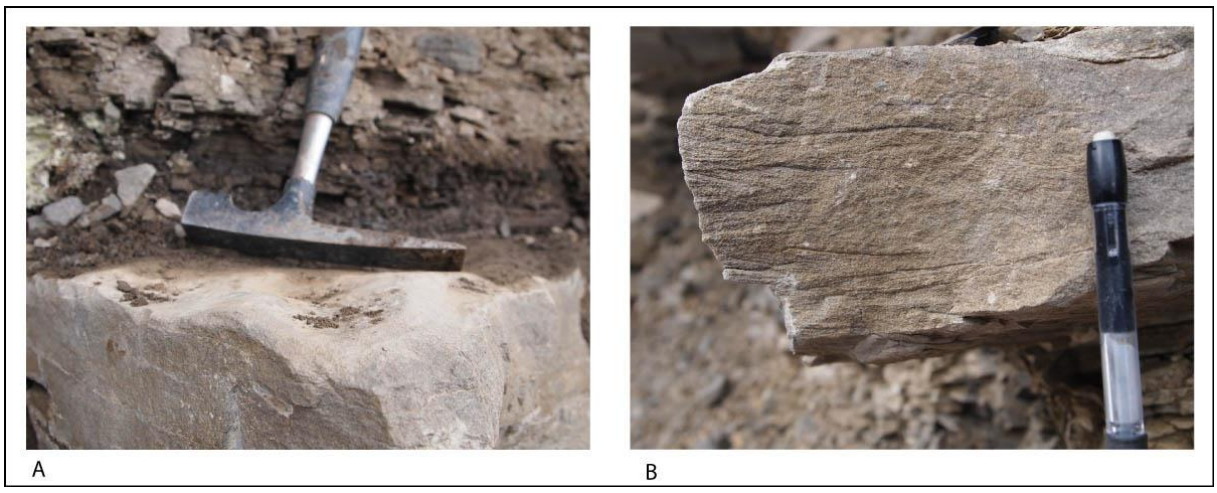

Figure 4 - 3: A) Symmetrical ripples of sandstone facies iii.b (Vestalbekken). B) Bidirectional ripples of sandstone facies iii.c (Vestalbekken).

c. This sandstone facies is found in western and central parts of the basin within Hollendardalen Fm. It form units that are 10 to 25 cm thick, with one exception with a 1,5 m thick unit (12,5 – 14 m) at the Vestalbekken outcrop. The facies iii.c sandstone contains bidirectional ripple lamination and grain size lies between very fine and

medium (Figure 4 - 3-B). Dispersed coal and leaf fragments appear. Single and double mud-drapes have been observed.

d. Sandstone facies iii.d is characterized by a moderate to high degree of bioturbation that partly destroys sedimentary structures. This sandstone facies contains very fine to fine sand with unspecified ripple lamination (Figure 4 - 9-D). It is present in Hollendardalen Fm. at all outcrops of the studied area. Small coal fragments are observed. Unit thickness range from 5 to 40 cm where the thicker units (20 – 40 cm) appearing in upper parts of the logged sections.

Facies iv. Hummocky cross-stratified sandstone (Figure 4 - 9-C):

Facies iv is hummocky cross stratified sandstone with grain sizes between very fine and fine. Ripples and soft sediment deformation are often found in the upper part of the unit. This sandstone facies is found in Hollendardalen Fm. at all outcrops except from Tverrdalen. Small amounts of coal fragments are present. Erosive lower unit boundaries are observed. Unit thickness increase upward in the logged sections. Largest unit thickness (2 m) is found in the west of Vestalbekken and Oppkuvbekken outcrops. In the eastern parts (Gangdalen Sør) unit thickness measures up to 90 cm.

Facies v. Laminated or bedded sandstone (Figure 4 - 4-A):

This sandstone facies is present in Hollendardalen Fm. and Battfjellet Fm. In Battfjellet Fm. it measures between 25 and 90 cm. Sandstone facies v consists of very fine to medium sand with plan parallel laminae or bedding. It is present in all outcrops within Hollendardalen Fm. Thin units (5 – 15 cm) in the lower part (0 – 5m) of the logged sections have moderate bioturbation which partially destroys lamination and bedding planes. Units of facies v with grain sizes between fine and medium sand have erosive boundaries and contain some mud rip up clasts.

Facies vi. Undulating sandstone (Figure 4 - 5-A):

Sandstones of facies vi consist of very fine sand with an undulating appearance. It is found in Hollendardalen Fm. with thickness between 10 and 30 cm. At the Trodalen outcrop (1,5 – 1,7

m) it forms a distinct unit between the siltstones of facies i. The base of the unit is non-erosive.

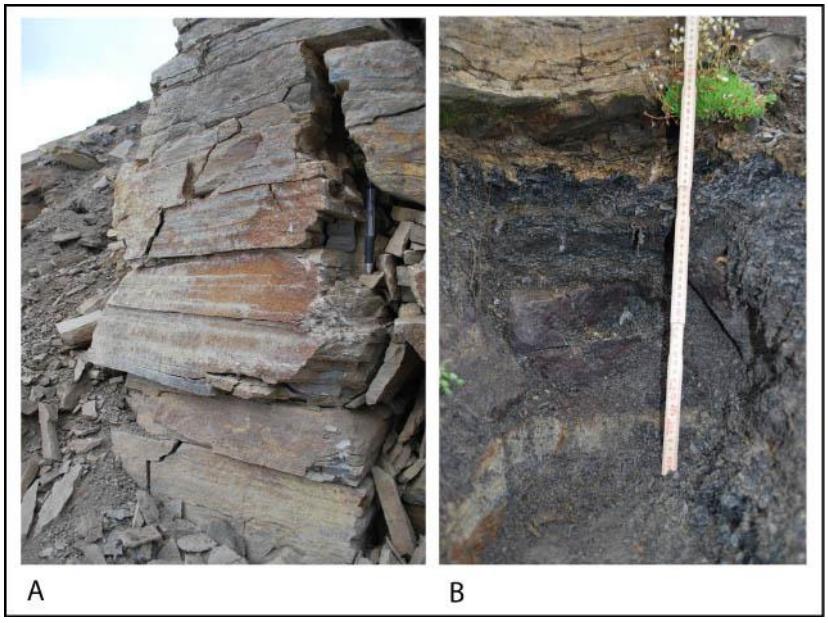

Figure 4 - 4: A) Plan parallel structures of sandstone facies v (Tverrdalen). B) Facies x, unconsolidated coal (Oppkuvbekken).

Facies vii. Flaser-bedded sandstone:

This sandstone is present in Hollendardalen Fm. in the western parts at the Oppkuvbekken and Vestalbekken outcrops. Facies vii contains flaser bedding and grain size lies between silt and fine sand. At Oppkuvbekken (2,8 – 3,0 m) it has an erosive lower boundary and consists of fine sand. Two units (7 – 7,6 m and 10,35 – 10,5 m) are associated with root horizons of the facies ix sandstone. At Vestalbekken one unit is present between 3,8 m and 4,3 m, and it is coarsening upwards from silt to fine sand.

Facies viii. Bioturbated siltstone/sandstone (Figure 4 - 9-D):

Siltstones and sandstones of facies viii are present in Hollendardalen Fm. in all sections of the studied area. It is characterized by bioturbation that destroys all sedimentary structures. Facies viii siltstones are normally associated with the lower 5 meters of the studied sections. Thickness varies from a few centimeters to 60 cm. In the lower 5 meters it forms distinct layers that interbed siltstones of facies i or viii. Higher up (above 5 m) in the studied sections the sandstone facies viii are normally from 10 cm to 85 cm, some pebble sized grains and rip

up mud clasts are observed. At Vestalbekken it is observed two facies viii units (2,8 – 3,5 m and 12,0 – 12,6 m) that are upwards coarsening.

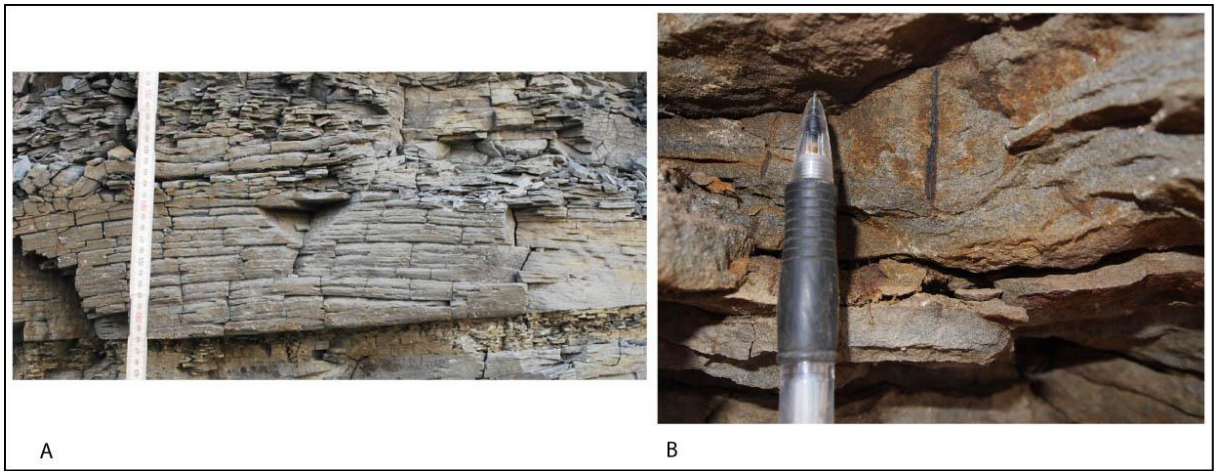

Figure 4 - 5: A) Facies vi sandstone (Holmsenfjellet). B) Root structures of facies ix (Oppkuvbekken).

Facies ix. Sandstone with root horizons (Figure 4 - 5-B):

Characterized by root structures and grain sizes between very fine and fine, ripple lamination and trough cross-bedding might occur. Some units are also associated with hummocky cross stratified sandstones of facies iv. This sandstone facies is observed in Hollendardalen Fm. in western and central parts of the basin at Oppkuvbekken, Vestalbekken, Tillbergfjellet Vest, Trodalen and Holmsenfjellet outcrops. It is observed in the lower part of a coal layer at the Oppkuvbekken (6,5 m) outcrop. Thickness varies between 20 and 50 cm. At the Holmsenfjellet outcrop it appear at the top of the logged section between 26,7 and 26,9 m. An upward coarsening sandstone facies ix occur at the Trodalen outcrop between 18,0 and 18,5 m.

Facies x. Coal (Figure 4 - 4-B):

Facies x is characterized by unconsolidated coals. This facies contains a varying amount of sand and displays a black color. Facies x occurs only in Hollendardalen Fm. at Oppkuvbekken and Tillbergfjellet Vest outcrops. Three units are found at the Oppkuvbekken outcrop (6,6 – 7 m, 14,3 – 14,4 m and 17,0 – 17,4 m), root structures are present in the lower unit (6,6 – 7,0 m) where it penetrate down in the underlying sandstone facies ii.c. At the Tillbergfjellet Vest section two units (5 cm thick) are separated by thin sandstone.

Facies xi. Very poorly sorted sandstone (Figure 4 - 6-A):

Facies xi lithologies are characterized as very poorly sorted fine sandstones. It contains a significant amount of rounded clasts (up to 1,5 cm) of unknown composition, coal and shell fragments. It is present in Hollendardalen Fm. where it normally marks the upper exposure of the formation. Thickness varies between 20 and 30 cm and it has a dark grey color.

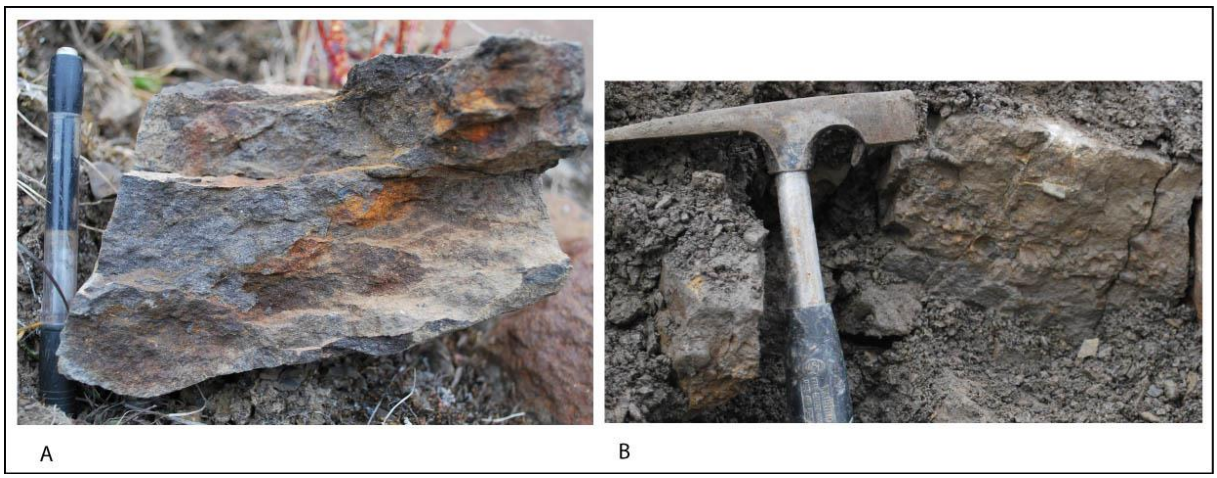

Figure 4 - 6: A) Very poorly sorted sandstone of facies xi (Trodalen). B) Pebble rich sandstone of facies xii (Tverrdalen).

Facies xii. Pebble rich sandstone (Figure 4 - 6-B):

Facies xii consists of 15 to 20 cm thick sandstones of fine to medium grain sizes, it was only observed in Marstranderbreen Mb. It contains 15 to 20 % rounded pebble sized grains of unknown composition. It is found 2,5 to 3,7 m below Hollendardalen Fm. This sandstone facies is observed in the eastern part of the basin in the Gangdalen Sør and Tverrdalen sections. This sandstone facies has a dark grey color and it is upwards fining and very poorly sorted.

Facies xiii. Soft sediment deformed sandstone (Figure 4 - 7):

This sandstone facies is characterized by soft sediment deformation and water escape structures. It consists of very fine to fine sandstones with ripple and parallel lamination. Sandstone facies xiii occur in the Hollendardalen Fm. at all logged sections except from Tverrdalen. Thickness varies between 20 and 80 cm. Pebble sized grains, rip up mud clasts and coal fragments are often observed.

Facies xiv. Shell rich sandstone:

Facies xiv is very fine to medium sandstones that is only found in Hollendardalen Fm. at Oppkuvbekken (20,5 – 21,7 m) and Vestalbekken (15,1 – 16,5 m) section. This sandstone facies is rich in shells up to a few centimeters in size. Coal fragments and ripple lamination are observed. Where present, it marks the upper exposure of Hollendardalen Fm.

Figure 4 - 7: Ball and pillow structure (facies xiii) from Trodalen.

4.1.2 Facies associations

Based on the facies descriptions above (Table 4 – 1), five facies associations, with subgroups, are identified (Table 4 - 2). Definitions and identification of the facies association were done together with Eivind Patrik Hanevik (2011, master thesis UiB).

Table 4 - 2: Facies associations and sub-facies associations of the studied sections, based in facies presented in Table 4 – 1.

.

Facies association	Sub-facies associations	Facies	Figure
FA1		i, xii	Figure 4 - 9
FA2	a	i, iii.a, iii.b, iii.d, iv, viii	Figure 4 - 9-B, Figure 4 - 10 -A
	b	iii.b, iv, v, viii	Figure 4 - 9
	c	i, iii.a, iii.c, viii	Figure 4 - 8
FA3	a	ii.a, ii.d, iii.c, v	Figure 4 - 10-C
	b	ii.c, iii.a, iii.c, iii.d, v, xiii	Figure 4 - 10-E
FA4		iii.c, iii.d, iv, viii, ix, x, xiv	Figure 4 - 10
FA5		xi	Figure 4 - 10

FA1 (Figure 4 - 9- 0,2 m – 2,8m):

The shales of Marstranderbreen Mb. are dominated by siltstones of facies i. Greatest thickness of this facies association is found at the Vestalbekken (41 m) outcrop, where it is thinning progressively eastwards to 6 m at Gangdalen Sør and 8 m at Tverrdalen. The dominating siltstone facies i is locally disturbed by pebble rich sandstones (facies xii). The FA1 facies association underlies the FA2 facies association at all logged sections.

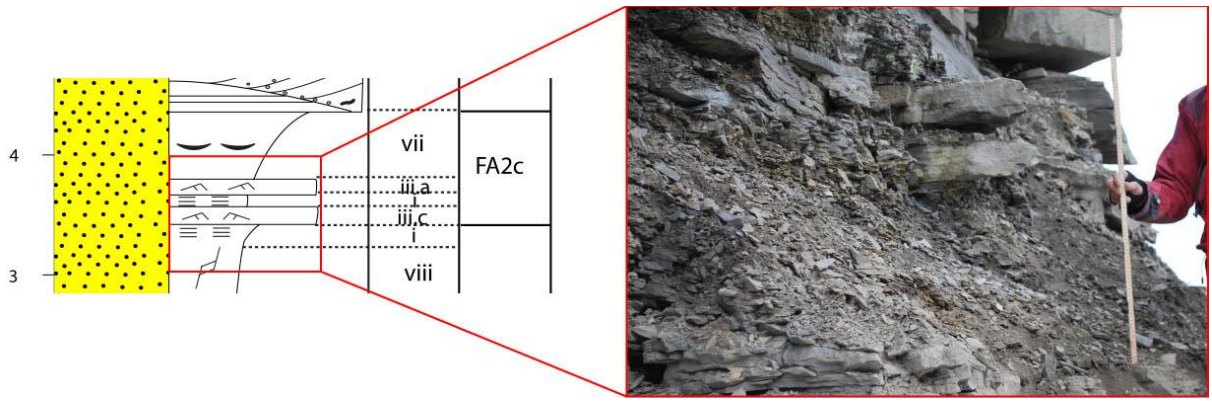

Figure 4 - 8: Example of facies association FA2c with siltsone facies i in the lower part from Vestalbekken.

FA2:

This facies association has been subdivided into three subfacies associations. It is only present in the Hollendardalen Fm.

- **FA2a** (Figure 4 - 10-A): The FA2a facies association is the lowermost facies association in Hollendardalen Fm. Thickness ranges between 2 and 4,5 m. This facies association is present between the underlying FA1 facies association and the overlying FA2b or FA2c facies associations. The transition from the underlying FA1 facies association is marked by the first appearing sandstone facies. The FA2a facies association is characterized by siltstones of facies i and viii, which are interbedded by distinct sandstone beds (facies iii.a, iii.b, iii.d, iv or viii). This sandstone facies normally increase in thickness with height together with increased sand content.

- **FA2b** (Figure 4 - 9– level 7,6 m – 14,8 m): It is present in Hollendardalen Fm. in central western parts of the studied area, occurring in two levels. The lower unit overlies the FA2a facies association with a gradational transition. FA2b lower part is normally upwards coarsening with thicknesses from 60 cm to 2,5 m. The lower FA2b

occurrence has a gradational transition to the overlying FA3 facies association. The upper unit is upwards coarsening at Oppkuvbekken and Vestalbekken, while at Trodalen, Holmsenfjellet and Tillbergfjellet Vest it is upwards fining. Thickness lies between 1,2 m (Tillbergfjellet Vest) and 7 m (Holmsenfjellet).

In eastern parts of the field area (Gangdalen Sør and Tverrdalen) FA2b occurs as one unit with a thickness of 2,5 m (Tverrdalen) and 8,1 m (Gangdalen Sør). At both outcrops it overlies the FA2a facies association. At Gangdalen Sør (6,7 m – 14,8 m) the FA2b facies association begins with an upward coarsening trend (6,7 m – 8,3 m) dominated by hummocky cross stratified sandstones (facies iv). After this it is fining upwards (8,3 m – 14,8 m) accompanied with increased silt content and bioturbation. Ripple laminated sandstones (facies iii.d) and bioturbated sandstones (facies viii) are the main facies. At this locality the upper boundary of the FA2b facies association marks the uppermost exposure of Hollendardalen Fm. In the Tverrdalen outcrop (2 m – 4,4 m) the FA2b unit is slightly upward coarsening consisting of laminated sandstones (facies v) and ripple laminated sandstone (facies iii.b and iii.d). Facies association FA5 overlies the FA2b facies association at the Tverrdalen section.

- **FA2c** (Figure 4 - 8): This facies association occurs only at the Vestalbekken (3,5 m – 4,3 m) section where it overlies a FA2a facies association. It begins with two distinct ripple laminated sandstones (facies iii.a and iii.c) separated by siltstone of facies i. Above this an upwards coarsening flaser-bedded sandstone (facies vii) occurs. A FA3a facies association overlies the FA2c facies association with a sharp boundary.

FA3:

- The FA3 facies association has been subdivided into two subfacies. It is only present in Hollendardalen Fm.

- **FA3a** (Figure 4 - 10– C): The sandstones of this facies association are dominated by sandstones of tangential cross bedding where foresets are planar or sigmoidal (facies ii.d), and sandstones which have planar bedding or lamination (facies v). The grain sizes varies between fine and coarse. FA3a appears at western outcrops (Oppkuvbekken, Vestalbekken, Trodalen and Holmsenfjellet) with thicknesses between 1 and 2 meters. Boundaries towards over- and underlying facies association

are sharp. This facies association consists of two equally thick beds (0,5 m to 1 m) that are separated by an erosive contact containing rip-up mud clasts, pebble sized grains and pockets of fine sand.

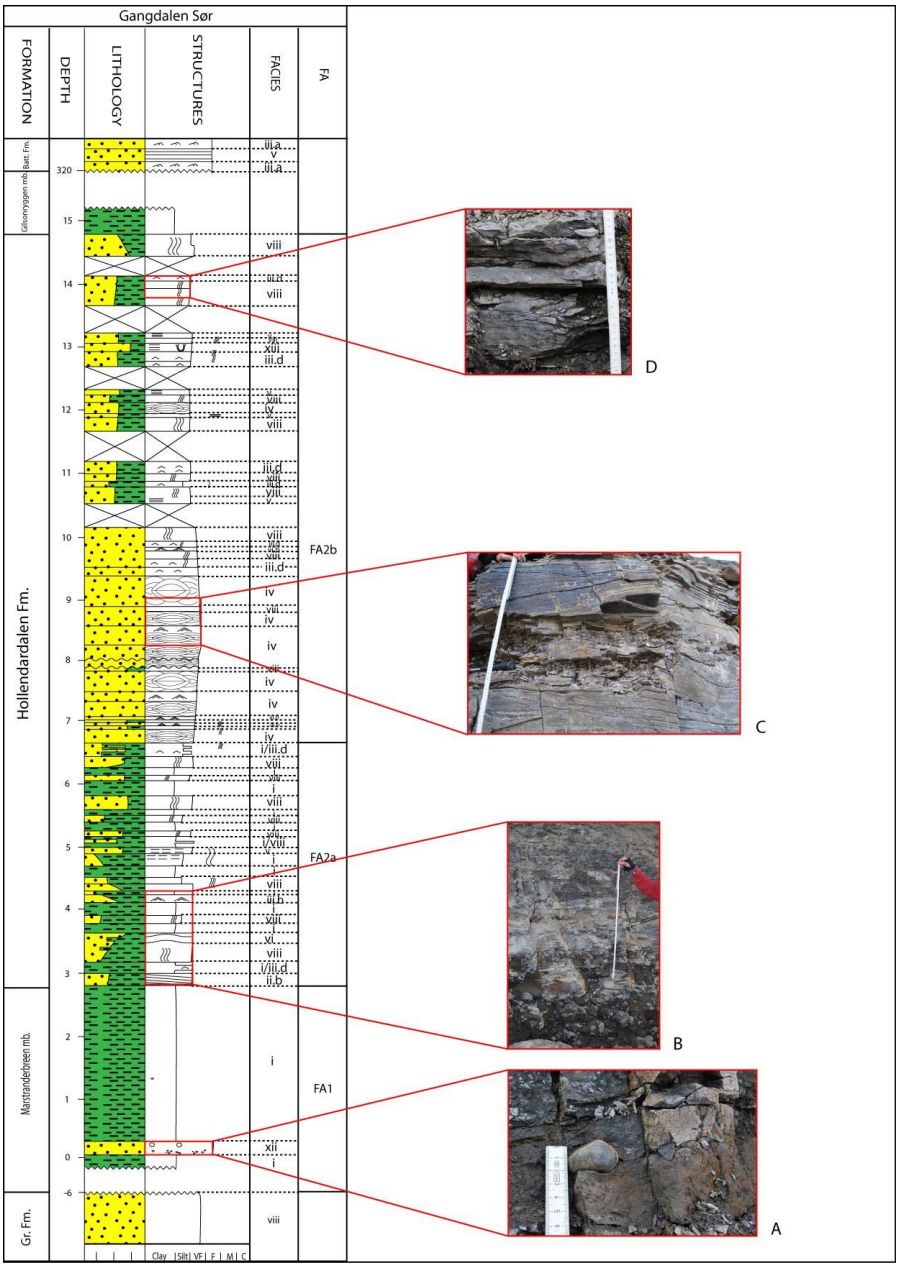

Figure 4 - 9: Facies associations and facies at the Gangdalen section. A) Pebble rich sandstone of sandstone facies xii. B) FA2a facies association. C) Hummocky cross-stratification of sandstone facies iv. D) Sandstone facies iii.d and sandstone facies viii.

- **FA3b** (Figure 4 - 10-E): At the westernmost outcrops (Oppkuvbekken and Vestalbekken) the FA3b facies association appears once. The FA3b facies association is found between FA3a and FA4 facies association at both sections. At Oppkuvbekken it is 3 meters thick (3,4 m – 6,4 m), slightly upwards coarsening and dominated by

trough cross stratified sandstone (facies ii.c) and sandstones of facies ii.a. The lower facies association boundary is erosive. The FA3b facies association at Vestalbekken (6 m – 7,8 m) have an upward increasing sand content. Sandstones facies in the lower part (6 m – 7,2 m) show ripple lamination (facies iii.c) and plan parallel lamination (facies v). Single and double mud-drapes of ripples are observed. The upper part (7,2 m – 7,8 m) consist of a soft bed deformed sandstone (facies xiii).

FA4 (Figure 4 - 10– 17,2 m – 18,8 m):

This facies association is characterized by sandstones with root structures (facies ix), unconsolidated coal layers (facies x) and shell rich sandstones (facies xiv). FA4 normally appears as two subunits in the logged sections.

At Oppkuvbekken the lower unit (6,5 m – 7,6 m) contains a 40 cm thick coal layer overlain by an upward coarsening flaser bedded sandstone (facies vii) and a sandstone containing root structures (facies ix). The upper unit (9,6 m – 21,8 m) contains two coal layers (facies x) at 14,3 m and 17 m, and two sandstones with root structures (facies ix) (9,7 m and 10,1 m). At this outcrop the FA4 facies association ends with a 1,3 m thick shell rich sandstone (facies xiv). At Vestalbekken the lower unit (7,8 m – 8,3 m) consists of coal rich siltstones (facies i) and a bioturbated ripple laminated sandstone (iii.d). The upper unit (11 m – 16,5 m) consists of a sandstone with root structures (facies ix) (11,8 m), ripple laminated sandstones (facies iii.c) and ends with a 1,5 m thick shell rich sandstone (15 m – 16,5 m). The shell rich sandstones mark the upper exposure of Hollendardalen Fm.

Two FA4 units are present at the Holmsenfjellet section (levels 19,8 m and 26,8 m). The thicknesses of these units are unknown because the section is covered by scree material. The FA4 facies association at the Trodalen outcrop appears at the top of the logged section. Here it forms two upward coarsening sandstones of facies ix (17,2 m – 17,8 m and 17,8 m – 18,5 m). At the Tillbergfjellet Vest section two units are present; the lower unit (7,9 m – 8,3 m) is upward coarsening and contains an unconsolidated coal layer (facies x) and a ripple laminated sandstone (facies iii.a) with a high abundance of coal fragments. The upper unit consists of sandstone with root horizons. The thickness of this unit is unknown because the upper boundary is not exposed.

FA5 (Figure 4 - 10– 18,8 m – 19 m):

The FA5 facies association is characterized by a poorly sorted sandstone (facies xi), where the average thickness is 30 cm. FA5 is present at the Trodalen, Tillebergfjellet Vest and Tverrdalen outcrops and marks the upper level of Hollendardalen Fm.

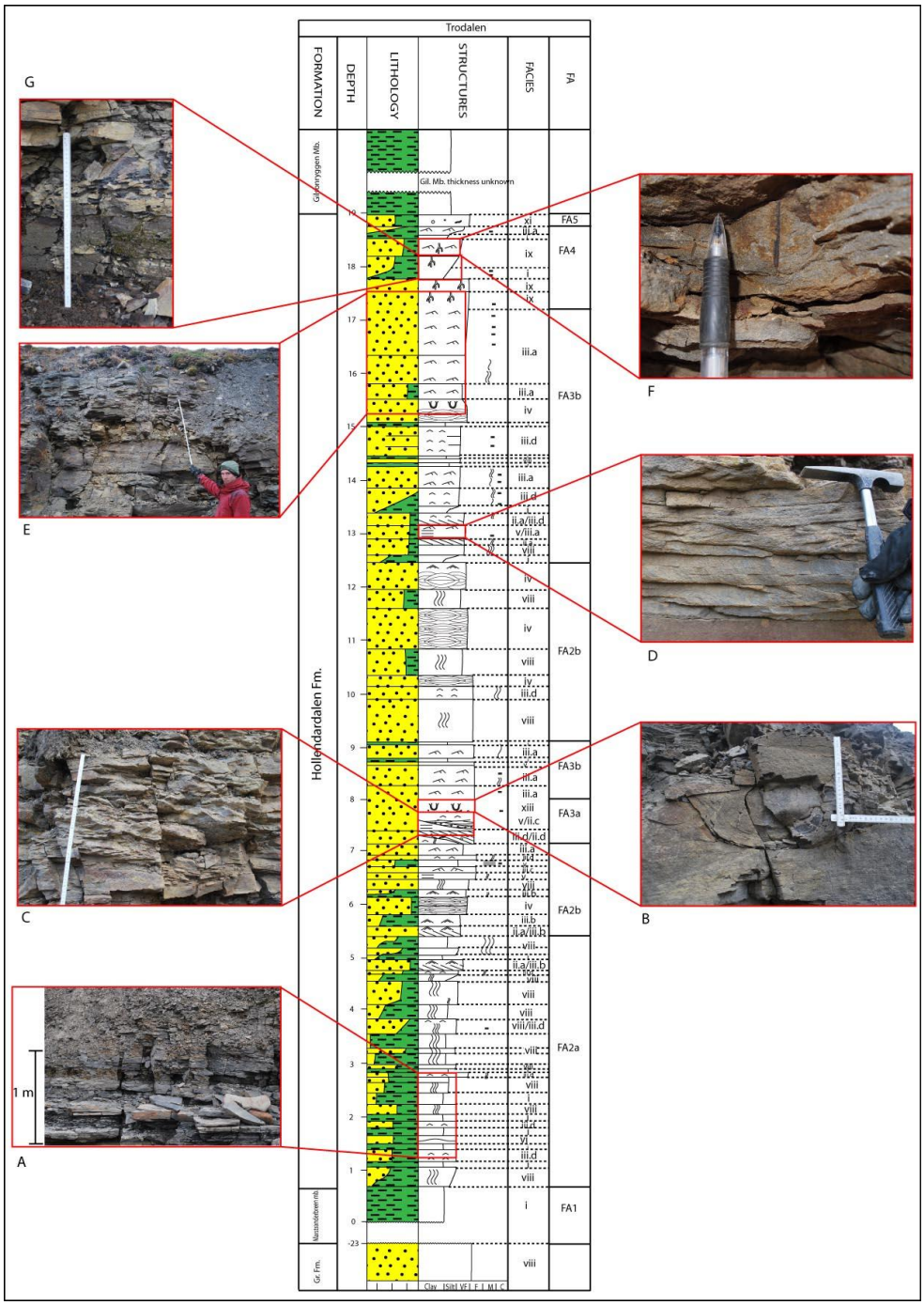

Figure 4 - 10: Facies associations and facies at the Trodalen section. A) Facies association FA2a. B) Ball and pillow structure of sandstone facies xiii. C) FA3a facies association. D) Asymmetrical ripples of facies iii.a. E) Facies association FA3b. F) Root structures in sandstone facies ix.

4.2 Sedimentological and petrographic description

4.2.1 Oppkuvbekken

Oppkuvbekken is the westernmost of the studied localities (Figure 3 - 1), but Hollendardalen Fm. can still be found farther west in the Central Basin with thicknesses up to 150 meters (Steel et al. 1981).

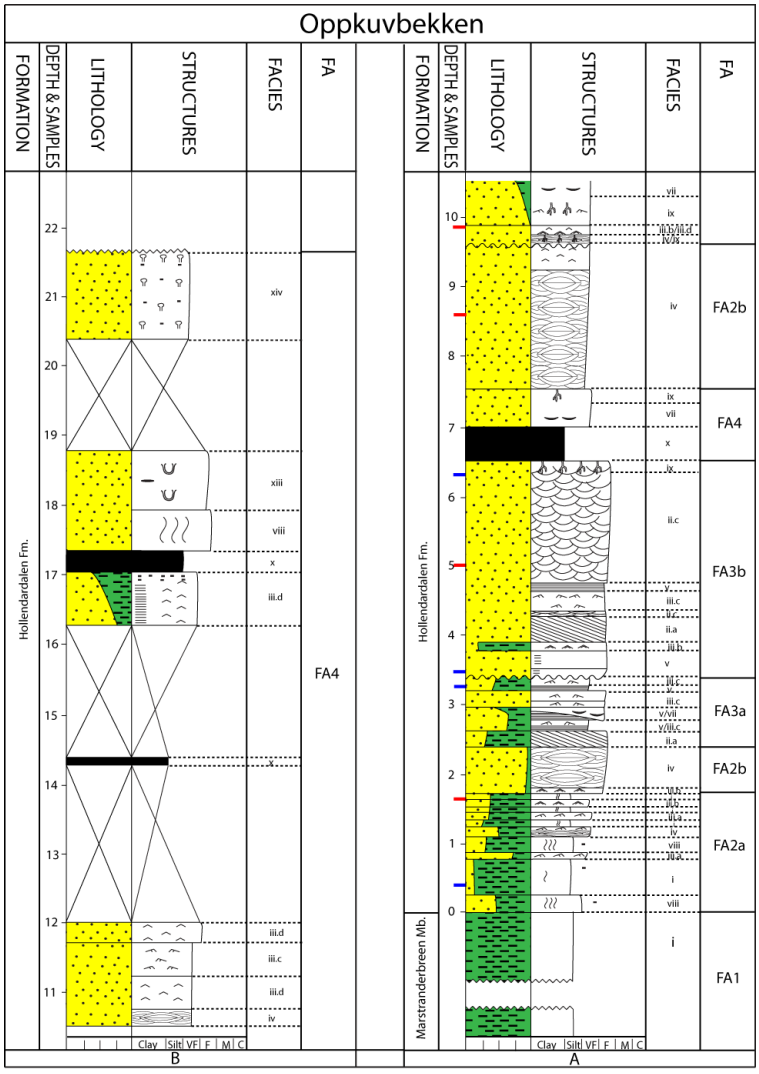

Figure 4 - 11: The Oppkuvbekken section, A) represents the interval between 10,5 m – 21,7 m. B) represents the interval between 0,0 m – 10,5 m FA = facies associations, presented in chapter 4.1.2. Red marks represent XRD and/or thin section analyzed samples, while blue marks are thin section, XRD and heavy mineral analyzed samples.

Sedimentological description

Oppkuvbekken was logged in 2009 and re-logged in 2010 (Figure 4 - 12 and Figure 4 - 11).

Hollendardalen Fm. measures 21,7 m at Oppkuvbekken (Figure 4 - 11). Grumantbyen Fm., Gilsonryggen Mb. and Battfjellet Fm. are not exposed. Grumantbyen Fm., Gilsonryggen Mb. and Battfjellet Fm. are not exposed. Thickness of the Marstranderbreen Mb. is unknown.

Figure 4 - 12: Panorama picture of Oppkuvbekken looking south. Marstranderbreen Mb. covered by scree material in the lower part, sandstones of Hollendardalen Fm. stands out. Exposed outcrop is about 12 meters in thickness.

The Oppkuvbekken section consists of four upward coarsening units (0 m – 2,6 m, 2,6 m – 6,5 m, 6,5 m – 12 m and 16,4 m – 18,8 m) and ends with a shell-rich sandstone (xii, Table 4 – 1) between 20,4 m and 21,7 m (Figure 4 - 11). The lower unit (0 m – 2,6 m) is a FA2a and a FA2b facies association. The FA2a facies association is characterized by bioturbated shales (facies i) interbedded by sandstones (facies iii.a, iii.b and iii.c). The FA2b facies association from 1,7 m to 2,4 m is dominated by hummocky cross-stratified sandstones (facies iv) (Figure 4 - 13). The unit above (2,6 m – 6,5 m) (Figure 4 - 11) is divided into a FA3a and a FA3b facies association. The FA3a facies association consists of sandstones of facies ii.a, iii.c, v and vii with grain sizes varying from very fine to fine. Trough (facies ii.c, Table 4 – 1) and planar cross-bedding (ii.a) dominates the FA3b facies association. An intermediate unit (6,5 m – 12 m) is coarsening up from very fine to fine sand. Between 6,5 m and 7,6 m a FA4 facies association is present, it contains a 40 cm thick coal layer (facies x) and a root horizon (facies ix) (Figure 4 - 11). Above the FA4 facies association a FA2b facies association (7,6 m – 9,7 m), dominated by hummocky cross-stratified sandstones (facies iv), is present. With an erosive contact at 9,6 m (Figure 4 - 11) a FA4 facies association begins, stretching to the rest of the section. The upper unit (16,4 m – 18,8 m) has grain sizes from very fine to fine sand and consist of a FA4 facies association (Figure 4 - 11). The sandstones in this unit are bioturbated, of facies iii.d and viii (Table 4 – 1). An 80 cm thick soft sediment deformed sandstone is present between 18,0 m and 18,8 m. Paleocurrent measurements conducted on asymmetrical ripples and cross-bedding show an infill from southeast (Figure 4 – 13).

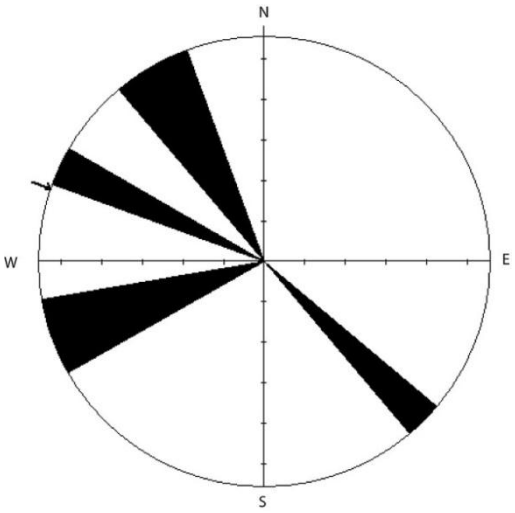

Figure 4 - 13: Paleocurrent measurements of asymmetrical ripples and cross-bedding. Plot made from measurements in Appendix 7.

Petrographic description

All XRD and thin section samples analyzed from the Oppkuvbekken section were sampled from Hollendardalen Fm.

XRD results

Eight samples were analyzed by XRD (Figure 4 - 14).

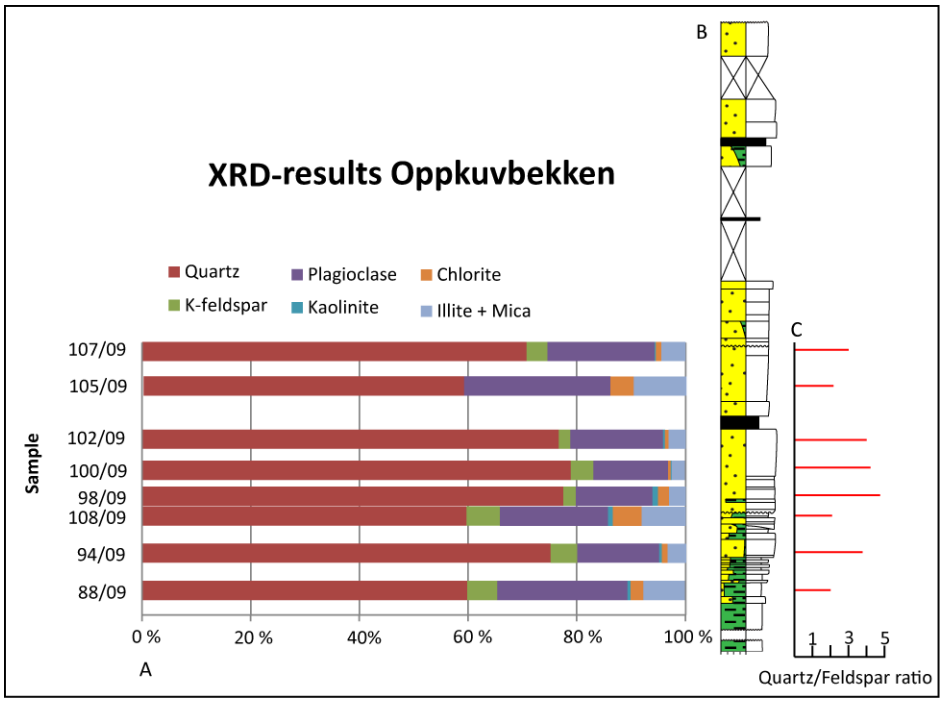

Figure 4 - 14: A) XRD-results, B) simplified log, C) Quartz/feldspar ratio.

Quartz is the main component, with amounts up to 78,9 XRD%. The feldspars constitute up to 29,5 XRD%; subdivided into plagioclase (up to 23,9 XRD%) and K-feldspar (up to 6,1 XRD%) (Figure 4 - 14). Illite and mica make out up to 9,7 XRD%, kaolinite (up to 1,0 XRD%) and chlorite (up to 5,3 XRD%).

Thin section description

Six thin sections from the Oppkuvbekken outcrop were studied. All sandstone samples are grain supported with a low degree of bioturbation. Grains are tightly packed with mainly concave-convex contacts, some tangential and long contacts have been observed (Figure 4 - 15-A).

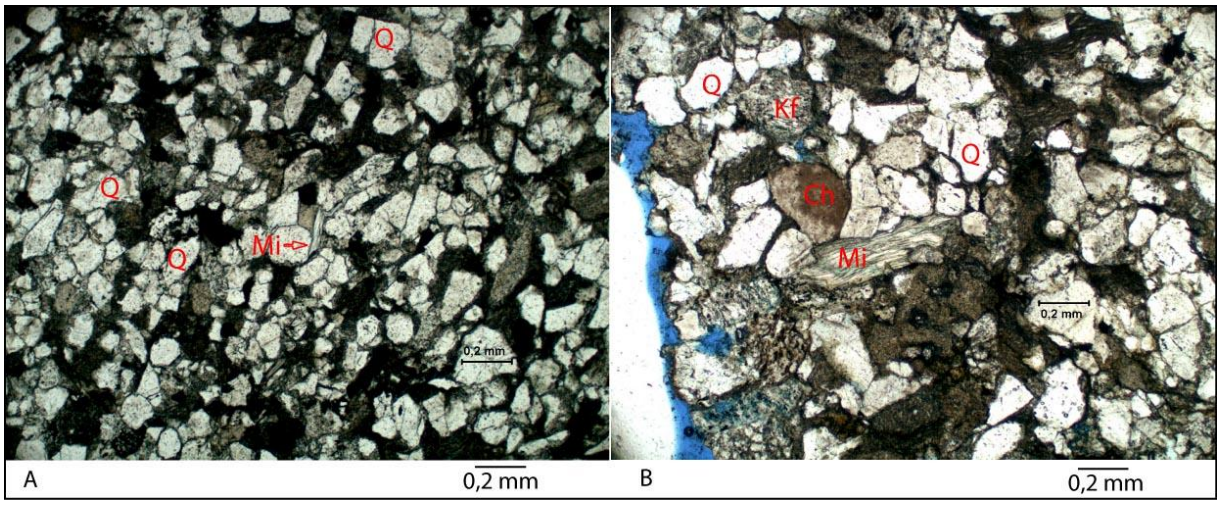

Figure 4 - 15: A) Moderately well sorted sand with bent mica and coal fragments (sample Oppk 94/09, level 1,7 m). B) Poorly sorted sand (sample Oppk 100/09, level 4,9 m).

The majority of grains are sub-rounded, but some angular grains are present (Figure 4 - 15-A). Sorting varies from poor (Figure 4 - 15-B) to moderately well (Figure 4 - 15-A). Shale and siltstone samples normally show a higher degree of bioturbation than sandstones (Figure 4 - 16-A). Monocrystalline quartz is the most abundant mineral with amounts up to 45,9 %. Some polycrystalline quartz (maximum 4 %) and chert (1 %) grains are also observed (Figure 4 - 15-B). In all samples the quartz/feldspar ratio is above 4.

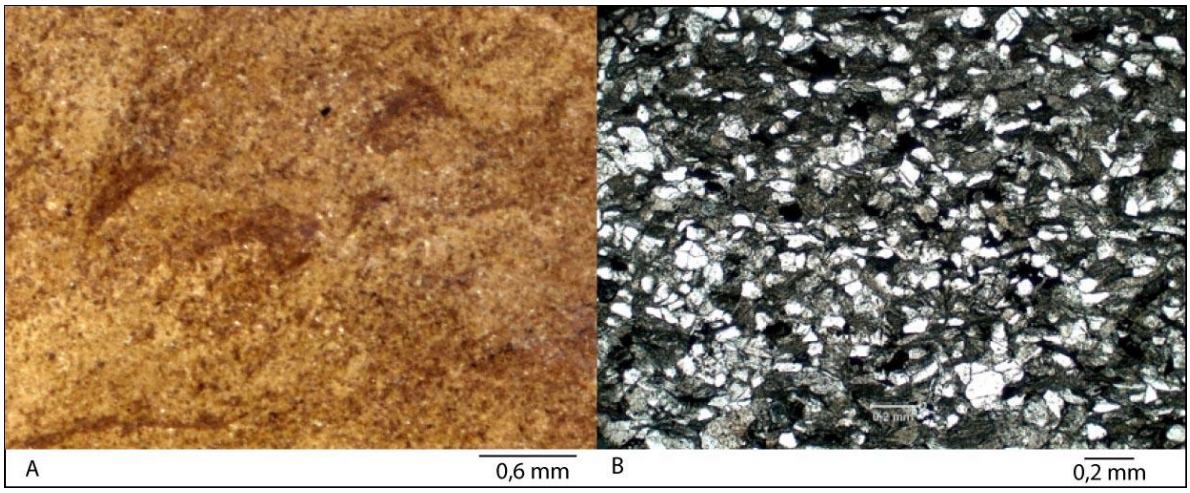

Figure 4 - 16: A) Bioturbated shale (sample Oppk88/09, level 0,4m). B) Preferred orientation of elongated grains (sample Oppk105/09, level 8,5 m).

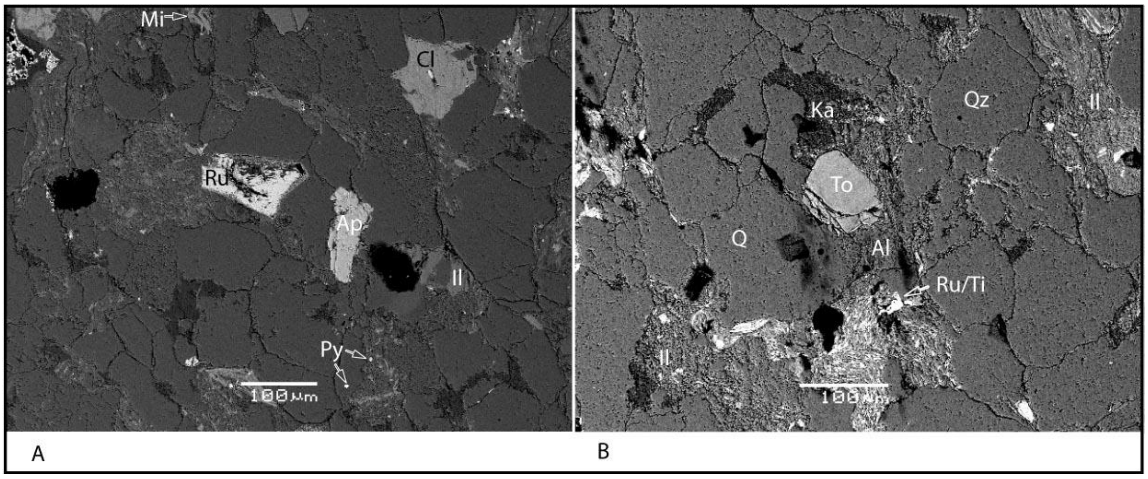

Figure 4 - 17: Qz = quartz, Mi = mica, Al = albite, Cl = chlorite, Il = illite, Ka = kaolinite, Ru = rutile, Ap = apatite, To = tourmaline, Ti = titanite. A) SEM picture with bent mica, framboidal pyrite, heavy minerals, illite and chlorite (sample Oppk 94/09, level 1,7 m). Note concavo-convex and long contacts. B) SEM picture (sample Oppk 94/09, level 1,7 m).

In point counting analysis mostly unspecified feldspars and plagioclase minerals are observed, while SEM studies show the presence of albite (Figure 4 - 17-B). Feldspar grains are partially altered to clay. The amounts of organic content vary, maximum 7,5 % (Appendix 4). Bending of mica flakes (biotite and white mica) between other grains is common (Figure 4 - 15-A and Figure 4 - 17-A). Figure 4 - 16-B show elongated grains with preferred orientation parallel to bedding. Overgrowth of quartz grains is observed in SEM analysis. Small amounts of framboidal pyrite are present in the analyzed samples (Figure 4 - 17-A). Kaolinite, chlorite and illite have been observed in thin sections and SEM studies (Figure 4 - 17-A and B).

4.2.2 Vestalbekken

Figure 4 - 18: Panorama picture of Vestalbekken. Marstranderbreen Mb. covered by scree material in the lower part of the image.

Vestalbekken is located east of Oppkuvbekken (Figure 3 - 1 and Figure 4 - 20).

Sedimentological description

16,5 m was logged, of these 15,3 m were identified as Hollendardalen Fm. Marstranderbreen Mb. is present in this section, however, the exact boundary towards Grumantbyen Fm. was not observed. Grumantbyen Fm., Gilsonryggen Mb. and Battfjellet Fm. are not exposed (Figure 4 - 20).

The first 1,2 m consists of the Marstranderbreen Mb. shales (FA1). The Hollendardalen Fm. is present between 1,2 m and 16,5 m (Figure 4 - 20). It is divided into three upward coarsening units, a lower (1,2 m – 6 m), middle (6 m – 12 m) and an upper unit between 12 m – 16,5 m (Figure 4 - 20). The lower unit between 1,2 m and 6 m consists of FA2a, FA2c and FA3a facies associations, it is coarsening up from silt to medium and coarse sand. The FA2a facies association is characterized by sandstones (facies iii.d, iv and v, Table 4 – 1) that interbed shales of facies viii (Figure 4 - 20). Sandstones of facies iii.d and vii dominate the FA2c facies association (3,5 m – 4,5 m). The lower unit (1, 2 m – 6 m) ends with a FA3a facies association, that contains sandstones of facies ii.d and v with grain sizes from medium to coarse sand (Figure 4 - 20).

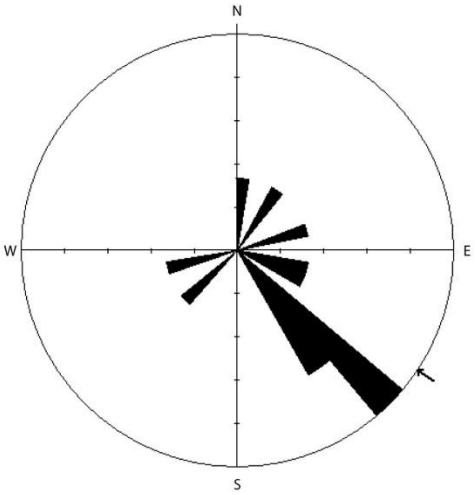

Figure 4 - 19: Paleocurrent measurements of asymmetrical ripples and cross-bedding. Plot made from measurements in Appendix 7.

The middle unit between 6 m and 12 m is coarsening up in the fine grain size. It contains FA3b, FA4 and FA2b facies associations (Figure 4 - 20). Sandstones of facies iii.c and v dominate the FA3b facies association. FA4 facies associations are characterized by shales with a high organic content (facies i) and sandstones with root structures (facies ix). Hummocky and trough cross-stratification (facies iv and ii.c, Table 4 – 1) is observed in the FA2b facies association (Figure 4 - 20). The upper unit (12 m – 16,5 m) is of a FA4 facies association characterized by sandstones of facies iii.c and shell rich sandstone (facies xiv), leaf and coal fragments are observed (Figure 4 - 20). Paleocurrent measurements of symmetrical ripples and cross-bedded sandstones show an infill direction from northwest (Figure 4 - 19).

Petrographic description

14 samples were analyzed by XRD analysis (Figure 4 - 21). Sample 138/09 is from Grumantbyen Fm. The remaining samples are from Hollendardalen Fm. Eleven samples were prepared for thin section studies. Nine were point counted, all from Hollendardalen Fm. Thin sections that were not point counted were either too fine grained or too poorly prepared.

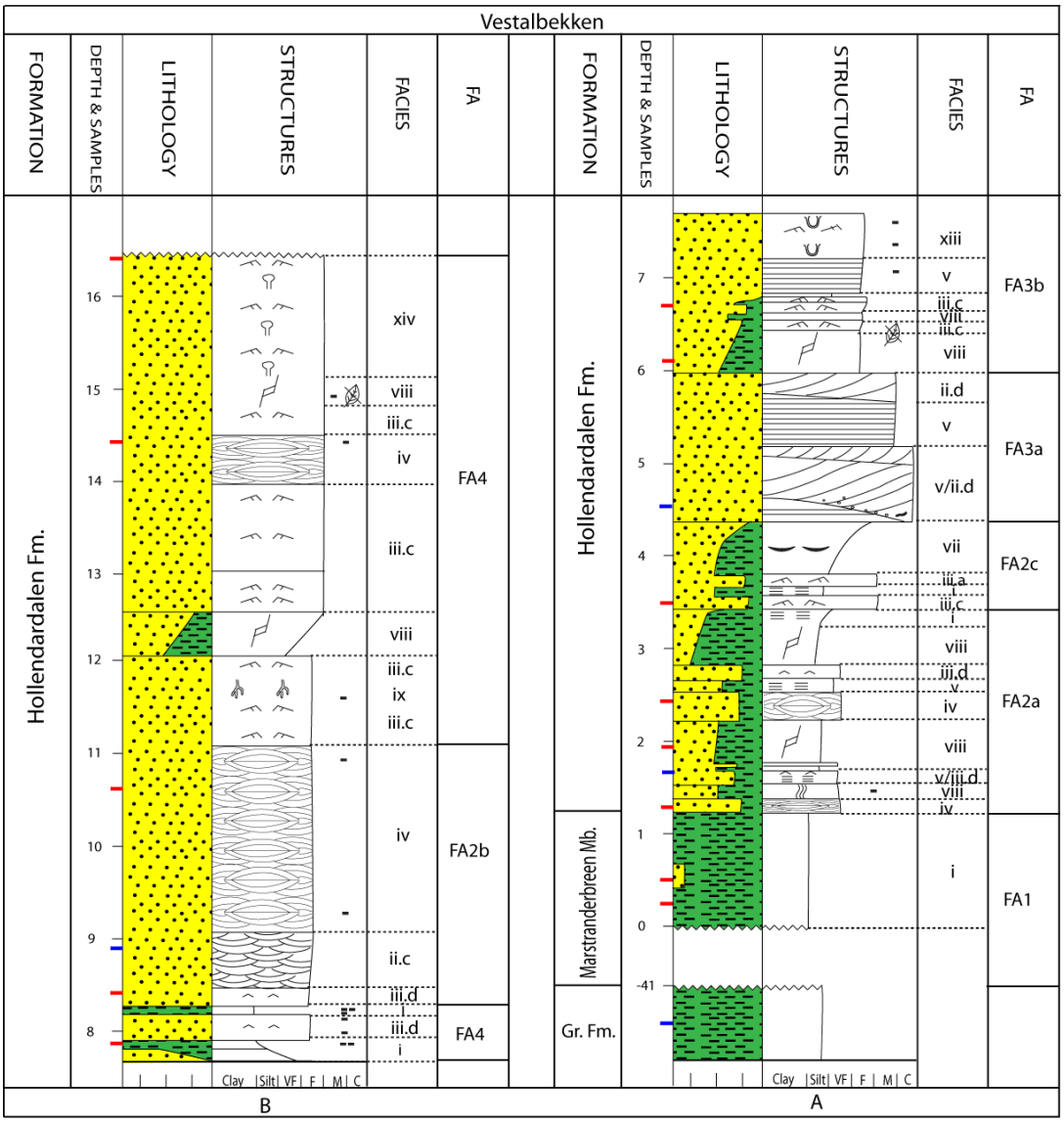

Figure 4 - 20: The Vestalbakken section. A) Represent the interval between -41 m and 7,7 m. B) Represent the interval between 7,7 m and 16,5 m. FA = Facies associations, presented in 4.1.2. Red marks are thin section and/or XRD analyzed samples, blue marks are thins section, XRD and heavy mineral analyzed samples.

XRD results

In sample 138/09 sampled from top Grumantbyen Fm., feldspar minerals contribute with the largest component 55 XRD%, of which plagioclase (44,1 XRD%) and K-feldspar (10,9 XRD%) are found. Quartz makes up 40,5 XRD%. Illite and mica make up 3,8 XRD% and kaolinite 0,3 XRD%, chlorite (0,5 XRD%) (Figure 4 - 21).

Samples from Hollendardalen Fm. consist primarily of quartz with amounts ranging from 54,2 XRD% to 81,7 XRD%. Feldspar content vary from 17,99 XRD% to 28,9 XRD%, divided into plagioclase (up to 21,7 XRD%) and K-feldspar (up to 7,2 XRD%). Illite and

mica amounts make up 2,8 XRD% to 11,8 XRD%. The chlorite amounts varies from 0 XRD% to 8,8 XRD%.

Figure 4 - 21 illustrates the results stratigraphically with Grumantbyen Fm. at the base. The quartz/feldspar ratio changes from Grumantbyen Fm. to Hollendardalen Fm. The ratio in Grumantbyen Fm. equals 0,7. In Hollendardalen Fm. it varies from 2 up to 6.

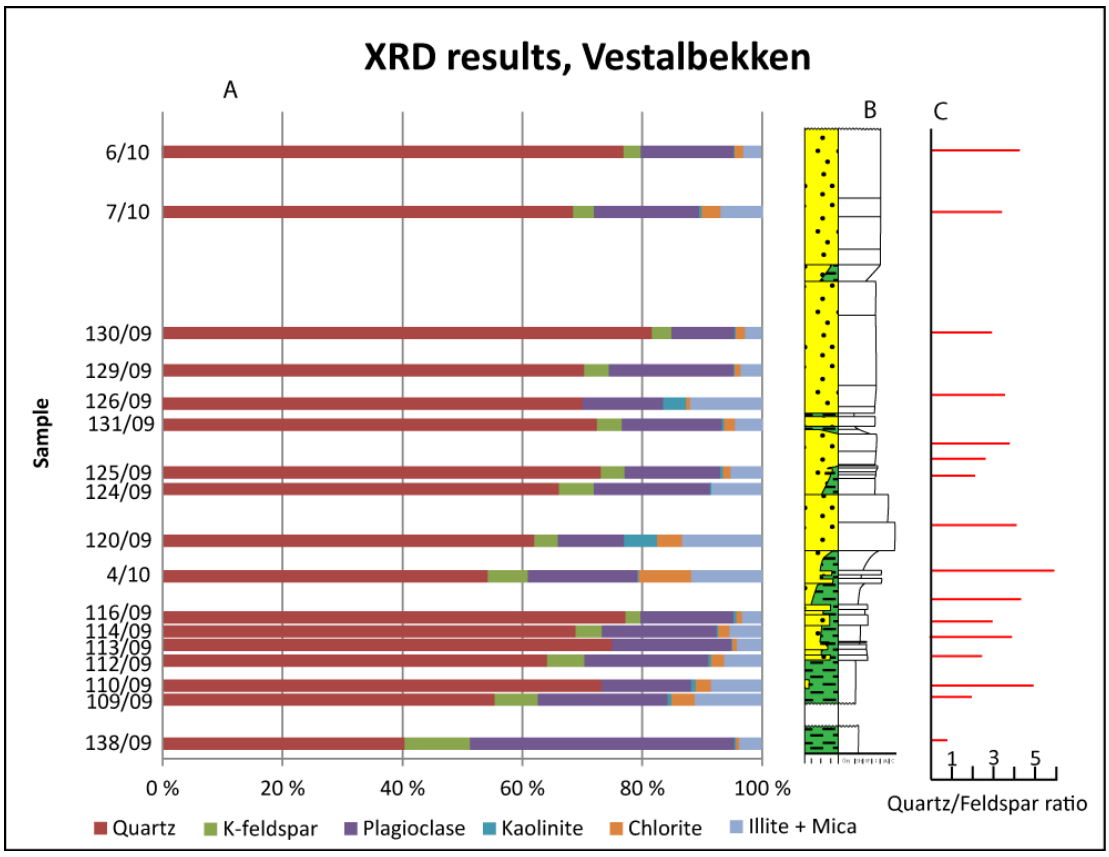

Figure 4 - 21: A) XRD results Vestalbekken. B) Simplified log. C) Quartz/feldspar ratio.

Thin section description

Twelve thin sections were prepared from Hollendardalen Fm., of these were nine point counted.

Sample 138/09 was sampled 3 meters from the top Grumantbyen Fm. It is a highly bioturbated shale. Sand grains are sub-rounded and float in a clay-sized matrix.

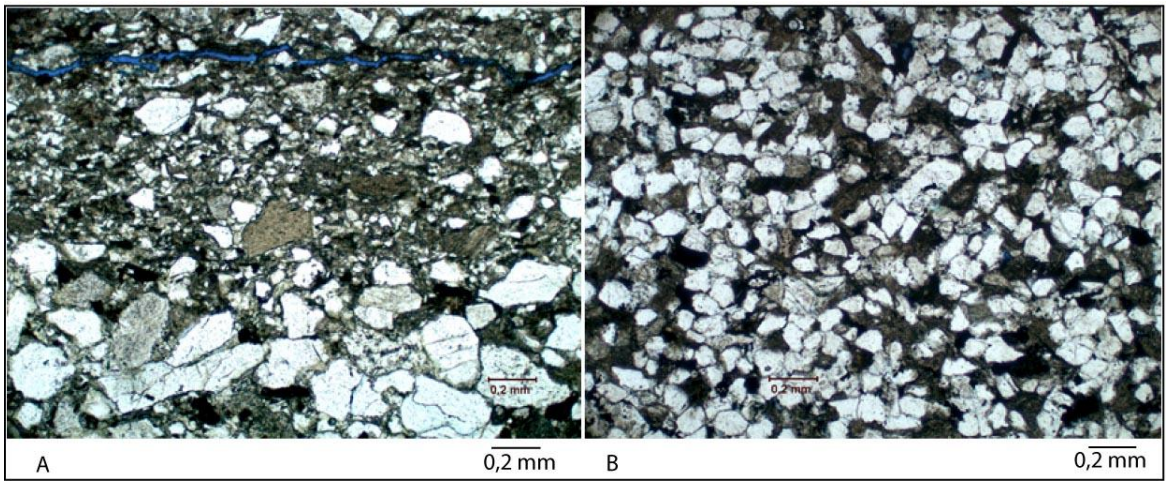

Figure 4 - 22: A) Upwards fining sequence, poorly sorted (Vestal 125). B) Well sorted sandstone (Vestal130).

Sand sized samples from Hollendardalen Fm. are normally sub-rounded to angular in shape (Figure 4 - 22-B). Grain contacts are mainly tangential and concavo-convex (Figure 4 - 22-B). Sorting varies from poor to well (Figure 4 - 22-A and B). Elongated mica grains tend to be bended between sand grains. Monocrystalline quartz is the dominant component with values up to 47,3 %. Quartz overgrowth is observed by SEM studies (Figure 4 - 23-A), but the majority of quartz grains do not show overgrowth. Organic content varies from 2,3 % to an excess of 10 % (Appendix 4), coal fragments are visible in Figure 4 - 22-B. In point counting analysis the quartz feldspar relationship is above 2 in all samples. Feldspar grains are normally partially altered to clay minerals. Sample 125/09 shows an upwards fining sequence in poorly sorted sandstone (facies iii.c) (Figure 4 - 22-A). Figure 4 - 23-A shows cross lamination, where the black grains are coal fragments that are oriented parallel to the foreset.

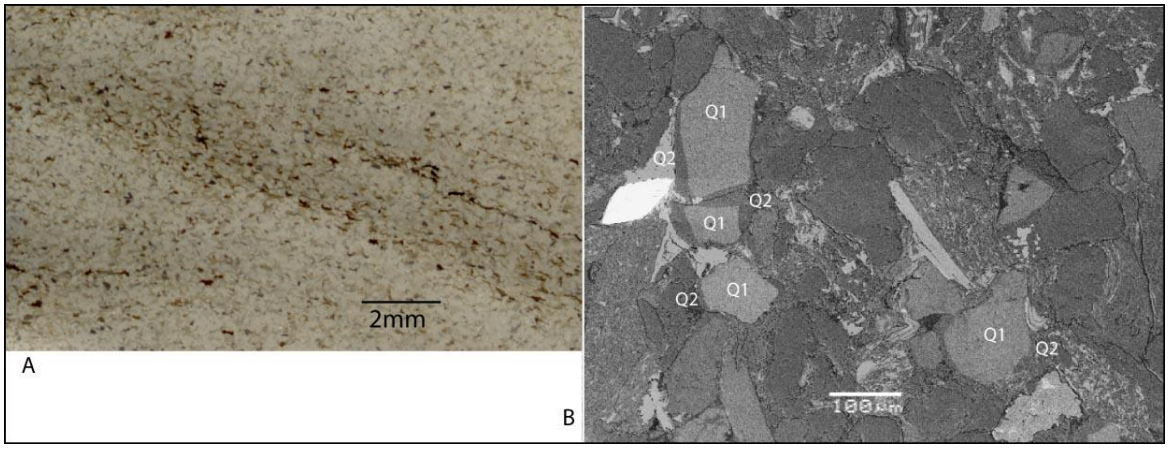

Figure 4 - 23: A) Cross lamination in ripples (Vestal 131, 8 m). B) Quartz overgrowth observed by SEM studies (Vestal 131, level 8 m). Q1 = primary quartz, Q2 = quartz overgrowth. Note concavo-convex contact in the upper left corner.

4.2.3 Vesuv mountain

At this locality (Figure 3 - 1) only Battfjellet Fm. is exposed. Samples were collected in a fine to medium grained sandstone.

Petrographic description

Two samples were collected, from the top (163/09) and the base (164/09) of the outcrop.

XRD results

The two samples differs in their quartz and clay content, sample 163/09 with a quartz content of 63,8 XRD% while 164/09 contain 52,6 XRD% (Figure 4 - 24, Appendix 3). 163/09 displays the lowest illite and mica content with 8,1 XRD%, 164/09 contains 17,7 XRD%. 163/09 has 25,9 XRD% feldspar content, subdivided into K-feldspar (2,5 XRD%) and plagioclase (23,4 XRD%) (Figure 4 - 24). 164/09 contains 24,6 XRD% feldspar, with K-feldspar (2,5 XRD%) and plagioclase (22 XRD%). 2,4 XRD% kaolinite is found in 164/09 and 5 XRD% in 163/09 (Figure 4 - 24).

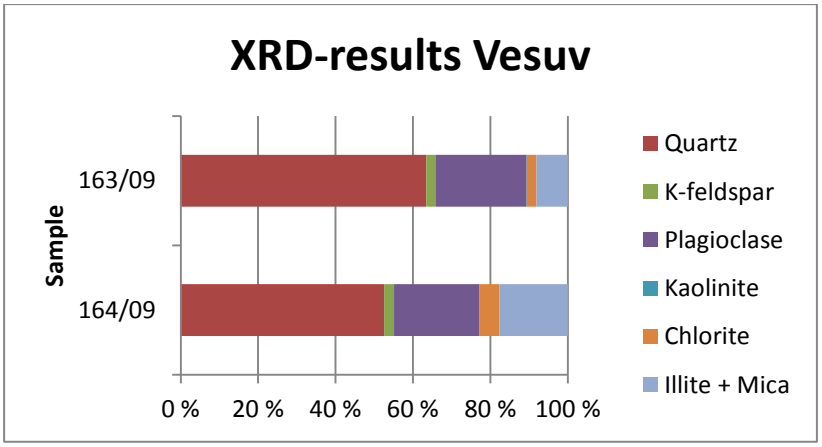

Figure 4 - 24: XRD-results Vesuv. 163/09 sampled at the top of the section, 164/09 at the base.

Thin section description

Both samples are grain supported sands where grains have angular to sub-rounded shape. Grain contacts are cancavo-convex and tangential, long contacts have been observed (Figure 4 - 25-A, B). In point counting analysis both samples contain more calcite minerals (up to 2,3 %) than observed in Hollendardalen Fm (Appendix 4). The sorting of sand grains is moderately well (Figure 4 - 25-A, B). Elongated grains as mica and coal fragments do not

show any preferred orientation, but some are bent between grains. Monocrystalline quartz is the largest component with amounts up to 50 %. Some polycrystalline quartz minerals are observed in amount up to 3,3 %. Polycrystalline quartz contains mainly more than 5 individual grains. Feldspar minerals show partially alteration to clay minerals. The quartz feldspar relation is above 3 in both samples.

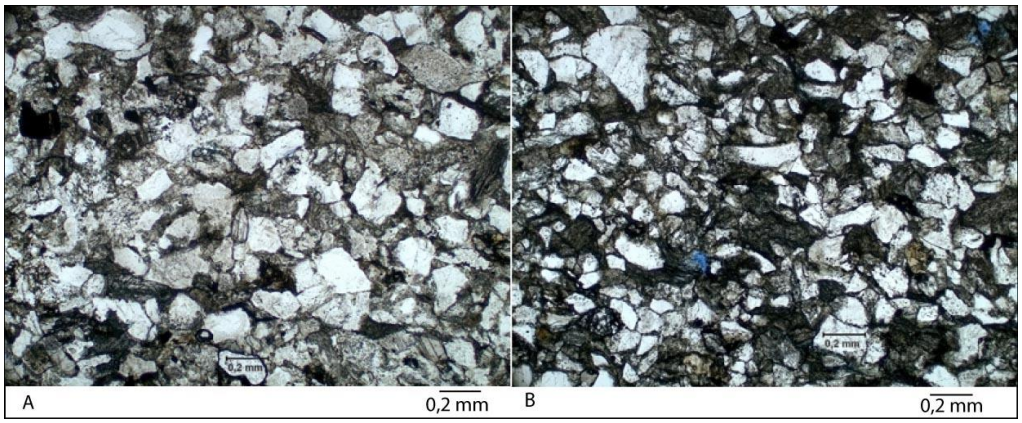

Figure 4 - 25: A) Sandstone from the top of the section (163/09). B) Sandstone from the base of the section (164/09).

4.2.4 Holmsenfjellet

Figure 4 - 26: Holmsenfjellet looking toward southwest, person for scale. Marstranderbreen Mb. Covered in scree material in the lower part of the image.

Sedimentological description

At the Holmsenfjellet section (Figure 3 - 1, Figure 4 - 27), 27 meters are recognized as Hollendardalen Fm. and the Marstranderbreen Mb. is 26 meters thick. Gilsonryggen Mb. and Battfjellet Fm. are not exposed.

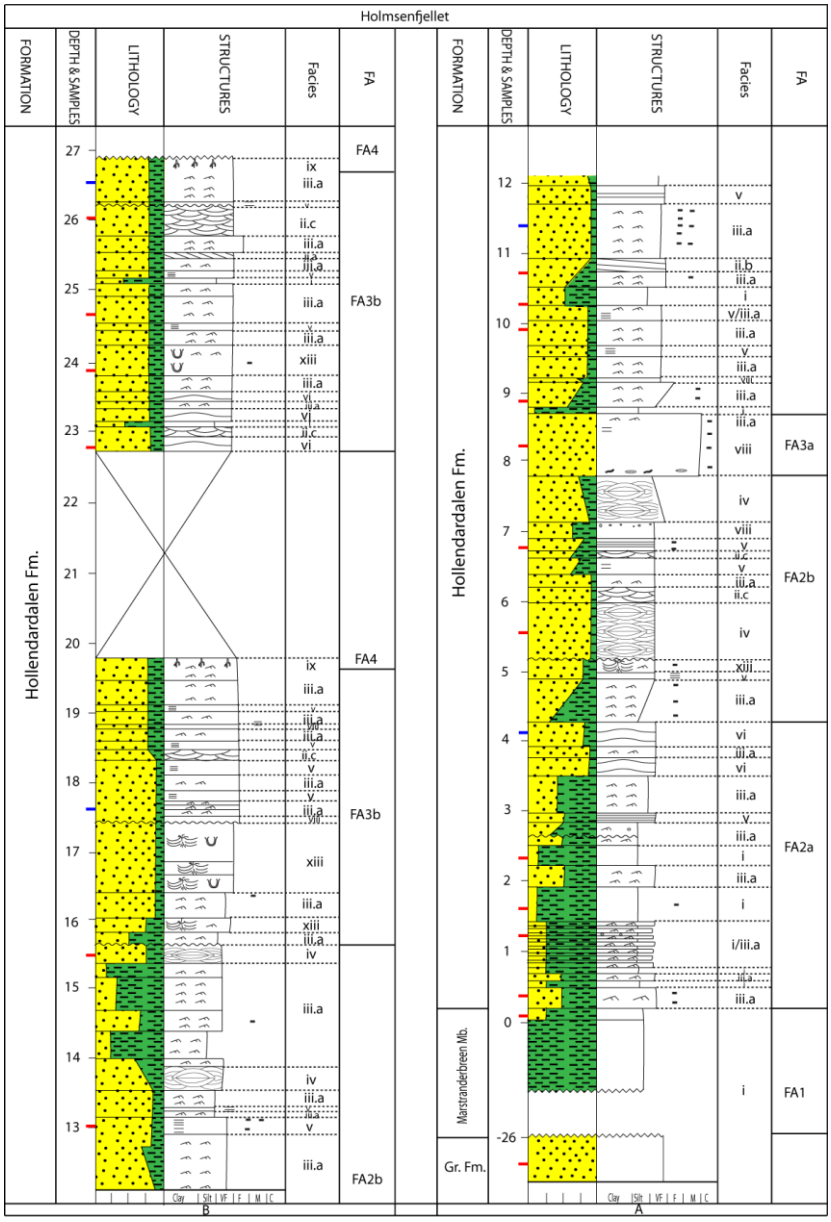

Figure 4 - 27: Log of the Holmsenfjellet section. A) Represent the interval between -26 m and 12 m. B) represent the interval between 12 m and 27 m. FA = facies associations. Red marks represent XRD and/ or thin section analyzed samples, blue marks are thin section, XRD and heavy mineral analyzed samples.

At the Holmsenfjellet section the Hollendardalen Fm. is subdivided into four upward coarsening units (0 m - 4,3 m, 4,3 m – 8,7 m, 8,7 m – 14 m and 14 m – 27,9 m). The lower unit (0 – 4,3 m) is a FA2a facies association consisting of shales of facies i interbedded by sandstones of facies iii.a (Figure 4 - 27). Above this FA2b and FA3a facies associations are present (4,3 m – 8,7 m),with grain sizes between very fine and medium. The FA2b facies association is dominated by hummocky (facies iv,) and trough (ii.c) cross-stratified sandstones (Figure 4 - 27). A middle upward coarsening unit is present between 8,7 m and 14 m and consists mainly of facies iii.a sandstones (Figure 4 - 27). The upper unit (14 m – 27,9 m) consists of two FA3b and two FA4 facies associations. Sandstones with root structures

(facies ix) represent the FA4 facies associations. The thickness of this facies association is unknown (Figure 4 - 27). Trough (facies ii.c, Table 4 – 1) and ripple laminated sandstones (facies iii.a) are main facies of the FA3b facies associations. Soft bed deformed sandstones (facies xiii) are also observed (Figure 4 - 27). Paleocurrent measurements on symmetrical ripples and cross-bedded sandstones show an infill direction from northwest (Figure 4 - 28).

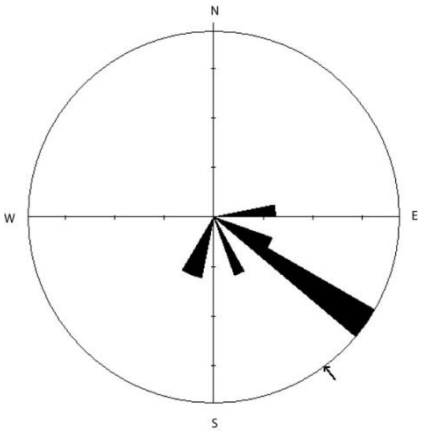

Figure 4 - 28: Paleocurrent measurements of asymmetrical ripples and cross-bedded sandstones. Plot based on measurements from Appendix 7.

Petrographic description

21 samples were analyzed, one sample (61/09) comes from Grumantbyen Fm. the remaining from Hollendardalen Fm. (Figure 4 - 29). 21 samples were prepared for thin section analysis, of these were 20 point counted; one sample was from Grumantbyen Fm., the remaining from Hollendardalen Fm. (Appendix 4), Battfjellet Fm. and Gilsonryggen Mb. are not exposed at Holmsenfjellet.

XRD results

Feldspar minerals are enriched in the analyzed samples from Grumantbyen Fm. with 61,2 XRD%, divided into plagioclase (40,8 XRD%) and K-feldspar (20,4 XRD%) (Figure 4 - 29). Quartz make up 31,3 XRD%. Illite and mica constitute 5,9 XRD%. Chlorite and kaolinite are present in minor amounts 1,1 XRD% and 0,6 XRD% respectively (Figure 4 - 29 and Appendix 3).

Quartz make up the largest constituents in studied Hollendardalen Fm. samples, with amounts varying from 39,6 XRD% to 70 XRD%. Feldspar minerals makes up maximum 28,5 XRD%, and can be subdivided into plagioclase (up to 22,2 XRD%) and K-feldspar (up to 16,1 XRD%

(Figure 4 - 29). Illite and mica amounts make up 21,5 XRD%. The kaolinite amount varies from 0 XRD% to 9,5 XRD%. Chlorite is present in amounts up to 12,1 XRD% (Figure 4 - 29).

The quartz/feldspar ratio in Grumantbyen Fm. is 0,5, while in Hollendardalen Fm. samples the ratio is 2. There is one exception in sample 52/09 with 0,7 (Figure 4 - 29).

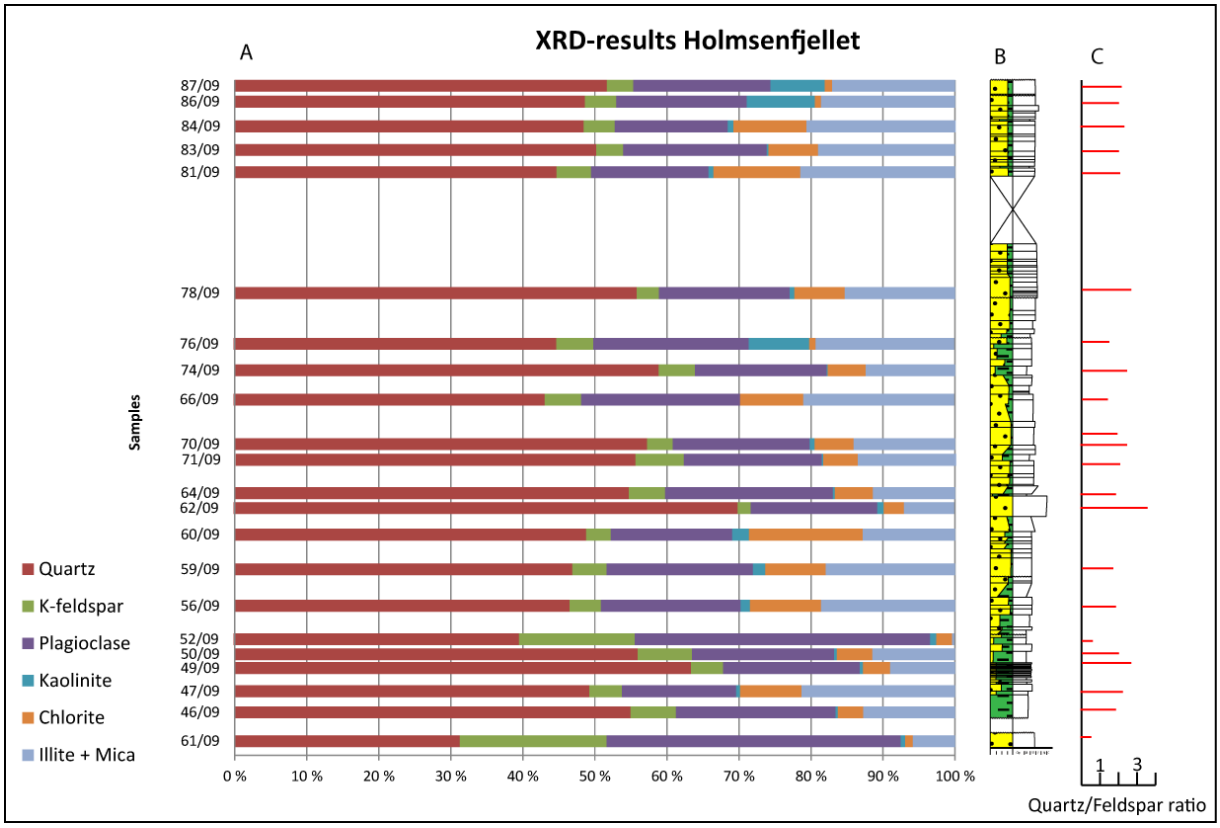

Figure 4 - 29: A) XRD-results from Holmsenfjellet. Sample 61/09 is from Grumantbyen Fm., other samples are from Hollendardalen Fm. Samples are presented stratigraphically. B) Simplified log. C) Quartz/feldspar ratio.

Thin section description

Studied sandstone samples consist of sub-rounded and angular grains. Grain contacts are concavo-convex and tangential, long contacts are observed (Figure 4 - 30-A and B). Sorting is normally moderately well, however poor sorting occurs. Elongated minerals do not show preferred orientation, but they some are bent between grains. Pore spacing is observed, but they are not connected. Samples with silt grain size show more bioturbation than samples of sand grain size. Partial feldspar alteration to clay sized minerals is more common in samples from Hollendardalen Fm. than in Grumantbyen Fm. samples. Monocrystalline quartz makes up the most common constituent in the Hollendardalen Fm. samples with an amount of 35 %

(Appendix 4). Polycrystalline quartz and chert are observed in amounts up to 2 % and 1 % respectively (Figure 4 - 30-A). Polycrystalline quartz grains are made of more than 5 individual grains. Quartz/feldspar ratio is above 1,5 in all analyzed samples. Coal fragments have angular shape and constitute up to 10% (Figure 4 - 30-A and Appendix 4), higher values are found in coal rich shales.

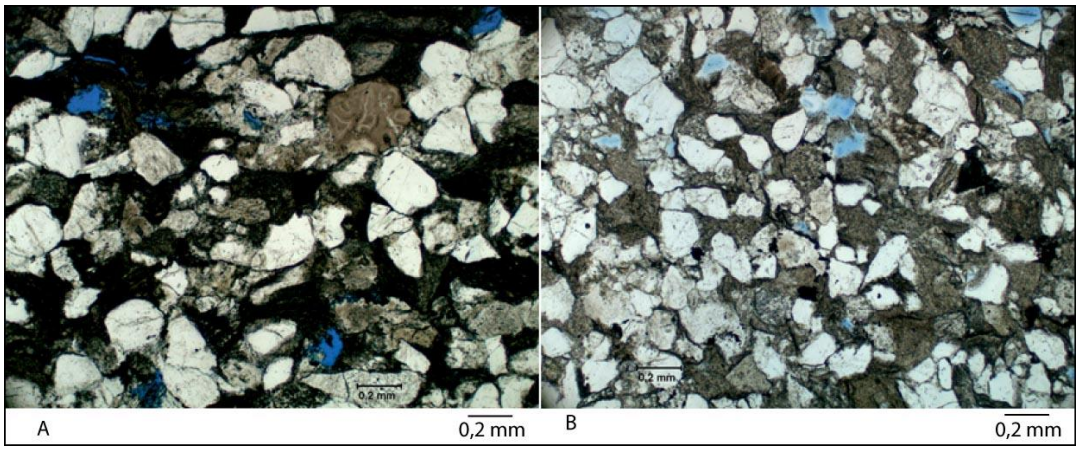

Figure 4 - 30: A) Moderately well sorted sandstone, note brown chert grain and organic material (Hol 62/09). B) Moderately well sorted sandstone (Hol 70/09).

4.2.5 Trodalen

Figure 4 - 31: Trodalen section, looking east. Outcrop continuous to right.

Sedimentological description

About 20 meters were logged in Trodalen (Figure 3 - 1 and Figure 4 - 32), Grumantbyen Fm., Marstranderbreen Mb., Hollendardalen Fm. and Gilsonryggen Mb. are exposed.

Bioturbation have destroyed all sedimentary structures in Grumantbyen Fm. It consists of a fine grained sandstone (Figure 4 - 32). Siltstones of Marstranderbreen Mb. overlie sandstones of Grumantbyen Fm. with a sharp contact. The Marstranderbreen Mb. unit is 23 meters thick (Figure 4 - 32).

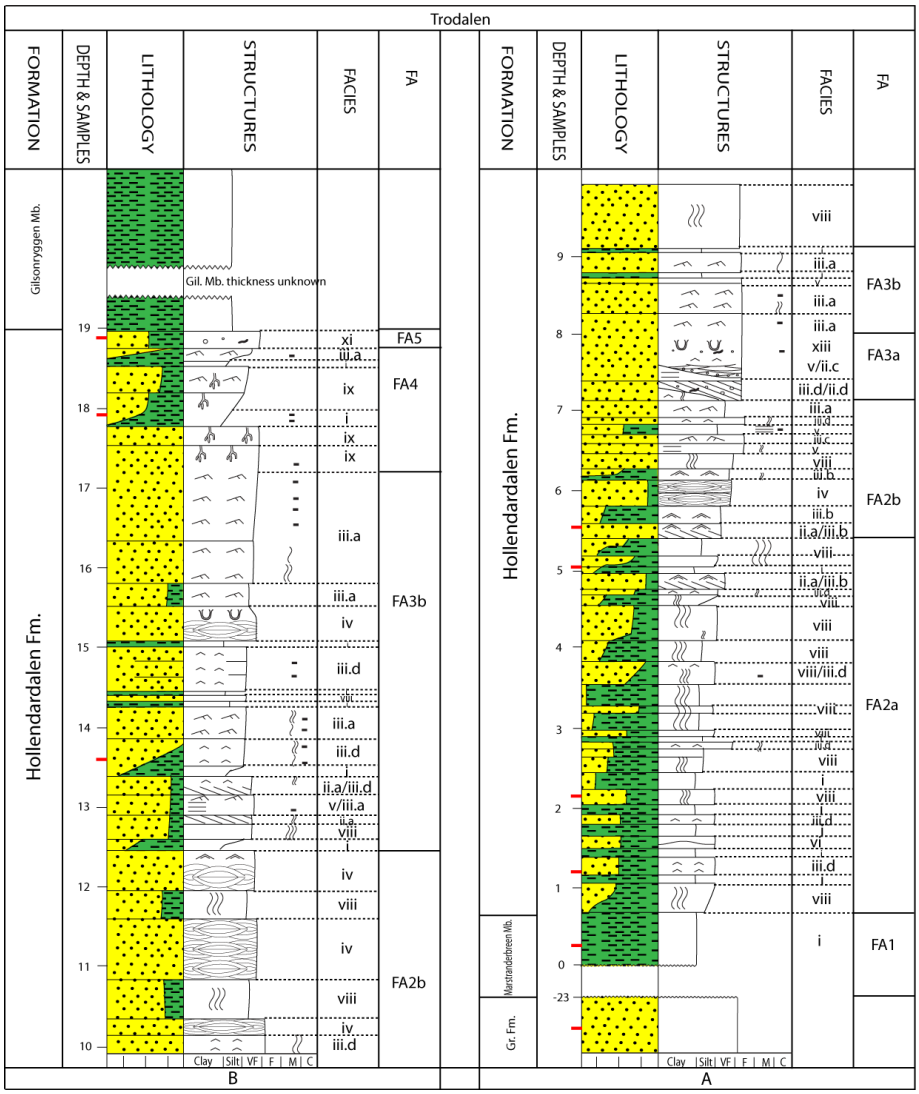

Figure 4 - 32: Trodalen section. A) Represent the interval between -23 m and 10 m. B) Represent the interval between 10 m and 19 m. Red marks are thin section and/or XRD analyzed samples, blue marks are thin section, XRD and heavy mineral analyzed samples. FA = facies associations.

The Hollendardalen Fm. consists of three main units; a lower upwards coarsening unit (0,6 m – 10,3 m), a middle upwards fining unit (10,3 m – 15 m) and an upper upwards coarsening unit (15 m – 17,8 m) (Figure 4 - 32). In addition two small upwards coarsening units of a FA4 facies association are observed between 17,8 m and 18,5 m (Figure 4 - 32). The lower unit (0,6 m – 10,3 m) begins with a FA2a facies association, this facies association is characterized by shales of facies i that are interbedded by bioturbated sandstones (facies viii). Above the FA2a facies association a FA2b facies association is present, this consists of hummocky cross-stratified sandstones (facies iv, Table 4 – 1) and ripple laminated sandstones (facies iii.a and iii.b) (Figure 4 - 32). A FA3a facies association with fine grain size containing facies ii.d, v and xii underlies ripple laminated sandstones (facies iii.a) of a FA3b facies association. The

middle upwards fining unit (10,3 m – 15 m) is divided into a lower FA2b and an upper FA3b facies association. The FA2b facies association is dominated by sandstones of facies viii and iv (Table 4 – 1), while the FA3b facies association consists primarily of sandstones of facies iii.a and iii.d (Figure 4 - 32). The upper upwards coarsening unit (15 m – 17,8 m) is dominated ripple laminated sandstones of facies iii.a and iii.d. Grain sizes lies between very fine and fine sand. The upper 20 cm of the Trodalen section is a FA5 facies association; this is the westernmost exposure of this facies association. Paleocurrent measurements on asymmetrical ripples show an infill direction generally from northwest (Figure 4 - 33-A). Measurements of symmetrical ripples crest show that they are striking northeast-southwest (Figure 4 - 33-B).

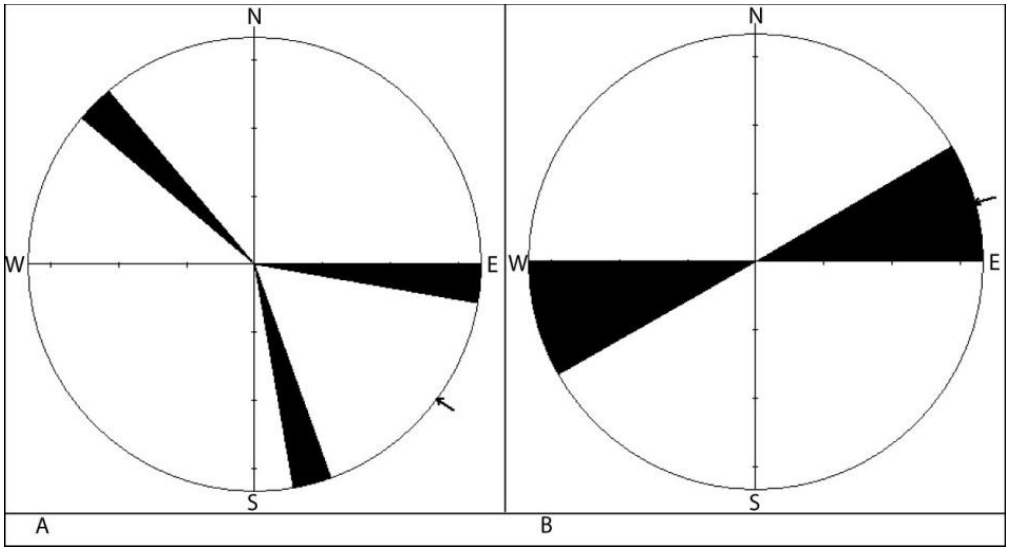

Figure 4 - 33: A) Paleocurrent measurement of asymmetrical ripples and cross-bedded sandstones, B) measurements of symmetrical ripple crests. Plot made from data in Appendix 7.

Petrographic description

Nine samples were analyzed by XRD (Figure 4 - 34). One sample (21/10) is from Grumantbyen Fm., while the other samples represent Hollendardalen Fm. (Figure 4 - 34). Five samples were point counted, one sample (21/10) comes from Grumantbyen, the remaining four samples are from Hollendardalen Fm. Gilsonryggen Mb. and Battfjellet Fm. are not exposed (Figure 4 - 34 and Appendix 4).

XRD results

Figure 4 - 34: A) XRD-results of Trodalen. Sample 21/10 is from Grumantbyen Fm. the remaining are from The Hollendardalen Fm. B) Simplified log. C) Quartz/feldspar ratio.

Feldspar minerals make up the main constituent in Grumantbyen Fm. with a total of 56,2 XRD%, whereby 45,2 XRD% is plagioclase and 11,1 XRD% is K-feldspar. Quartz constitutes 39,7 XRD%. Illite and mica constitutes 2,8 XRD%. Chlorite and kaolinite are only present in small amounts 0,8 XRD% and 0,5 XRD% respectively (Figure 4 - 34).

The samples analyzed from Hollendardalen Fm. consist primarily of quartz, from 49 XRD% to 69,8 XRD% (Figure 4 - 34). Feldspar content varies from 22,00 XRD% to 28,9 XRD%, divided into plagioclase (up to 23,56 XRD%) and K-feldspar (up to 11,1 XRD%). Illite and mica makes up 15,6 XRD%. Chlorite and kaolinite are present with amounts up 6 XRD% and 2,9 XRD% respectively (Figure 4 - 34). The quartz/feldspar ratio is above 2 for all Hollendardalen Fm. samples (Figure 4 - 34 and Appendix 5).

Thin section description

Samples of silt grain size are normally bioturbated, if not lamination is observed in thin section analysis. Sample 19/10, sandstone of facies xi, is bioturbated, poorly sorted and contains mud rip-up clasts. Sorting is normally moderately well to well (Figure 4 - 35-A) and grains have sub-rounded shape. Feldspar alteration to clay sized minerals is more common in

Grumantbyen Fm. samples than in Hollendardalen Fm. samples. Grain contacts are mainly concavo-convex. Monocrystalline quartz is the main compound, up to 36 % (Appendix 4). Polycrystalline quartz are found in amounts up to 2,5 %, they contain more than five individual grains. Heavy minerals are observed in point counting analysis and SEM studies (Figure 4 - 35-B). In SEM studies kaolinite is observed (Figure 4 - 35-B). Quartz overgrowth is observed, but is not common. Elongated grains do sometimes show preferred orientation parallel to bedding.

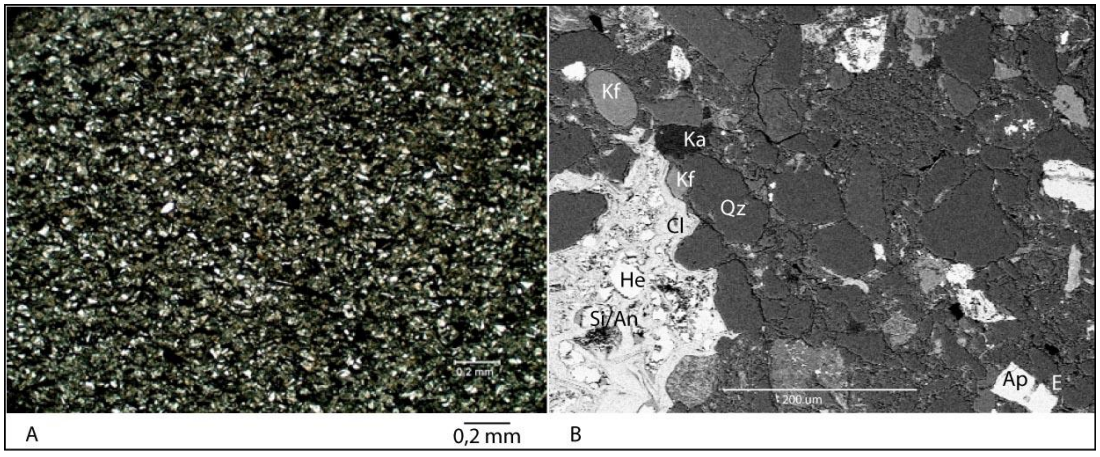

Figure 4 - 35: A) Moderate well sorted sandstone (2/10). B) SEM picture of sample 21/10. Kf = K-feldspar, Ka = kaolinite, Qz = quartz, Cl = chlorite, He = hematite, Si = siderite, An = ankerite, Ap = apatite.

4.2.6 Tillbergfjellet Vest

Figure 4 - 36 Tillbergfjellet Vest section, person for scale. Looking towards east.

Sedimentological description

16 m was logged from the Tillbergfjellet section (Figure 3 - 1, Figure 4 - 36 and Figure 4 - 38). Grumantbyen Fm., Marstranderbreen Mb., Hollendardalen Fm., Gilsonryggen Mb., and

Battfjellet Fm. are exposed. The Marstranderbreen Member measures 25,0 m and Hollendardalen Fm. measures 15,85 m (Figure 4 - 38).

Grumantbyen Fm. consists of bioturbated sandstones, where all sedimentary structures are destroyed (Figure 4 - 38). Above the Grumantbyen Fm. Marstranderbreen Mb. overlies with a sharp boundary, consisting of finely laminated siltstones (facies i, Table 4 – 1)

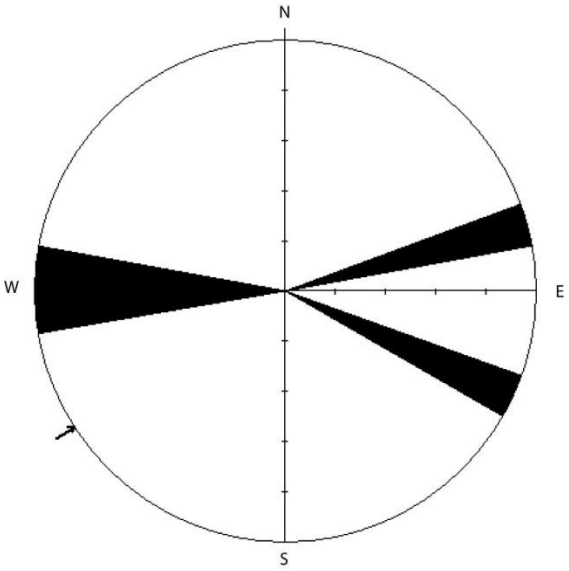

Figure 4 - 37: Palecurrent measurements of asymmetrical ripples and cross-bedded sandstones in Hollendardalen Fm. Plot made from measurements in Appendix 7.

Hollendardalen Fm. consists of three upwards coarsening units (0 m – 5,8 m, 5,8 m – 8,8 m and 8,8 m – 15,9 m) (Figure 4 - 38). The lower unit is a FA2a facies association consisting of bioturbated siltstones and sandstones of facies viii, interbedded by sandstones (facies iv and iii.d, Table 4 – 1) The middle upwards coarsening unit (5,8 m – 8,8 m) contains FA2b, FA3b and FA4 facies associations (Figure 4 - 38). Sandstones in the FA2b and FA3b facies association are of facies viii and iv, with grain sizes from very fine to fine. Unconsolidated coals (facies x) and ripple laminated sandstones (facies iii.a) characterize the FA4 facies association (Figure 4 - 38). The upper unit (8,8 m – 15,9 m) is coarsening upwards from silt to fine sand. It consists of FA3b, FA4 and FA5 facies associations. The FA3b facies association is dominated by ripple laminated sandstones (facies iii.a, Table 4 – 1) Only 20 cm of the FA4 facies association is exposed, the rest is covered by scree material (Figure 4 - 38). The top of the section is a FA5 facies association of facies xi sandstones. Paleocurrent measurements of ripples show an infill from west and east (Figure 4 - 37).

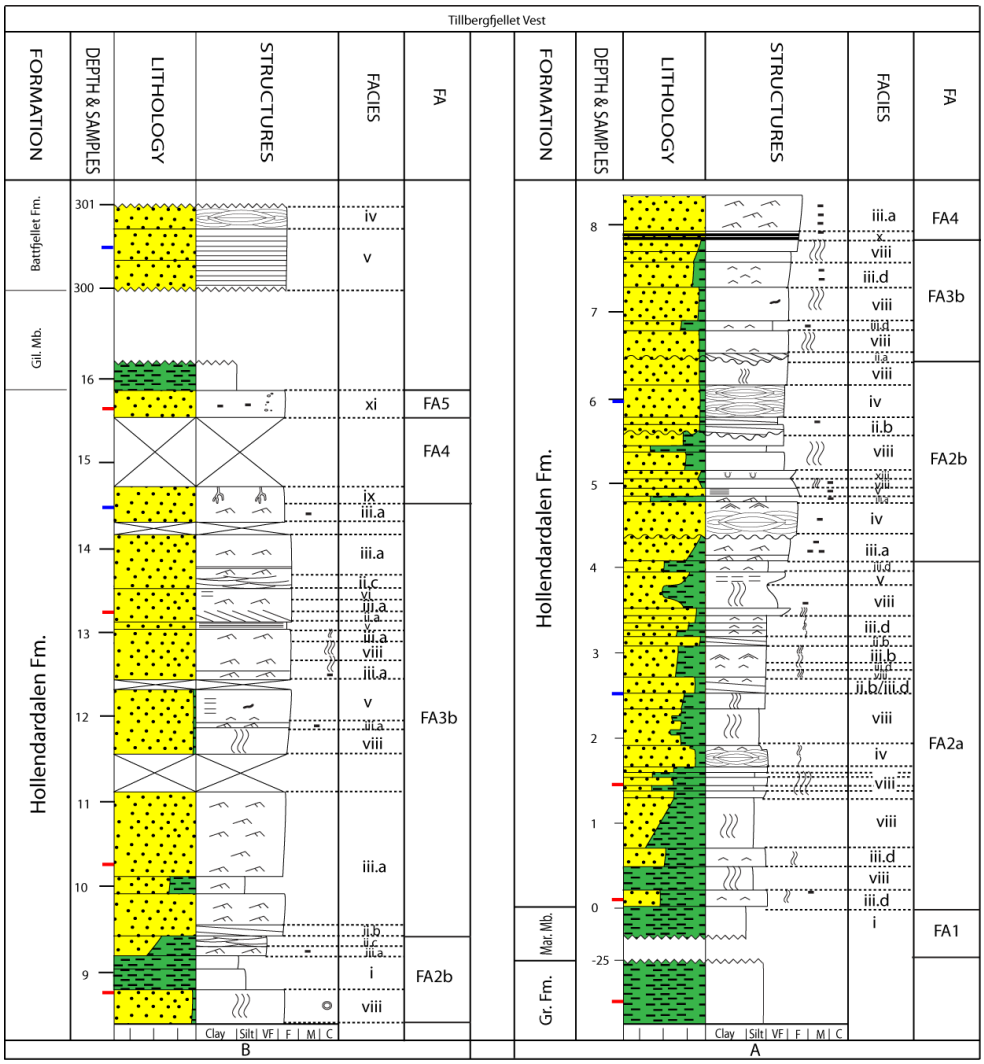

Figure 4 - 38: Log of Tillbergfjellet Vest section. A)Represent the interval between -25 m and 8,3 m. B) Represent the interval between 8,3 m and 15,8 m and Battfjellet Fm. FA = facies associations. Red marks are thin section and/or XRD analyzed samples, blue are thin section, XRD and heavy mineral analyzed samples.

Petrographic description

Eleven Tillbergfjellet Vest samples were analyzed by XRD (Figure 4 - 39). One sample (1/10) represents Grumantbyen Fm., while TillBatt 1/10 is from Battfjellet Fm., and the remaining nine samples are from Hollendardalen Fm. Eight samples were point counted. Six of these were from Hollendardalen Fm., one from Grumantbyen Fm. one from and Battfjellet Fm.

XRD results

Feldspar minerals make up the largest mineral fraction in Grumantbyen Fm. with 55,7 XRD%, consisting of plagioclase (41,1 XRD%) and K-feldspar (14,5 XRD%). Quartz

constitute 42,4 XRD%. Other minerals present in minor amounts are illite and mica (1,5 XRD%), kaolinite (0,1 XRD%) and chlorite (0,3 XRD%) (Figure 4 - 39). The quartz/feldspar ratio is 0.8.

Nine samples from Hollendardalen Fm. were analyzed. Quartz make up the largest mineral contribution with amounts up to 84,5 XRD% (Figure 4 - 39). Feldspar minerals constitute up to 27,1 XRD%, divided into plagioclase (up to 20,5 XRD%) and K-feldspar (up to 6,6 XRD%). Illite and mica contribute with amounts up to 19 XRD% (Figure 4 - 39). Kaolinite and chlorite are present with 4,1 XRD% and 3,9 XRD% respectively. The quartz/feldspar ratio varies from 2 to 6, in an upwards increasing trend (Figure 4 - 39 and Appendix 5).

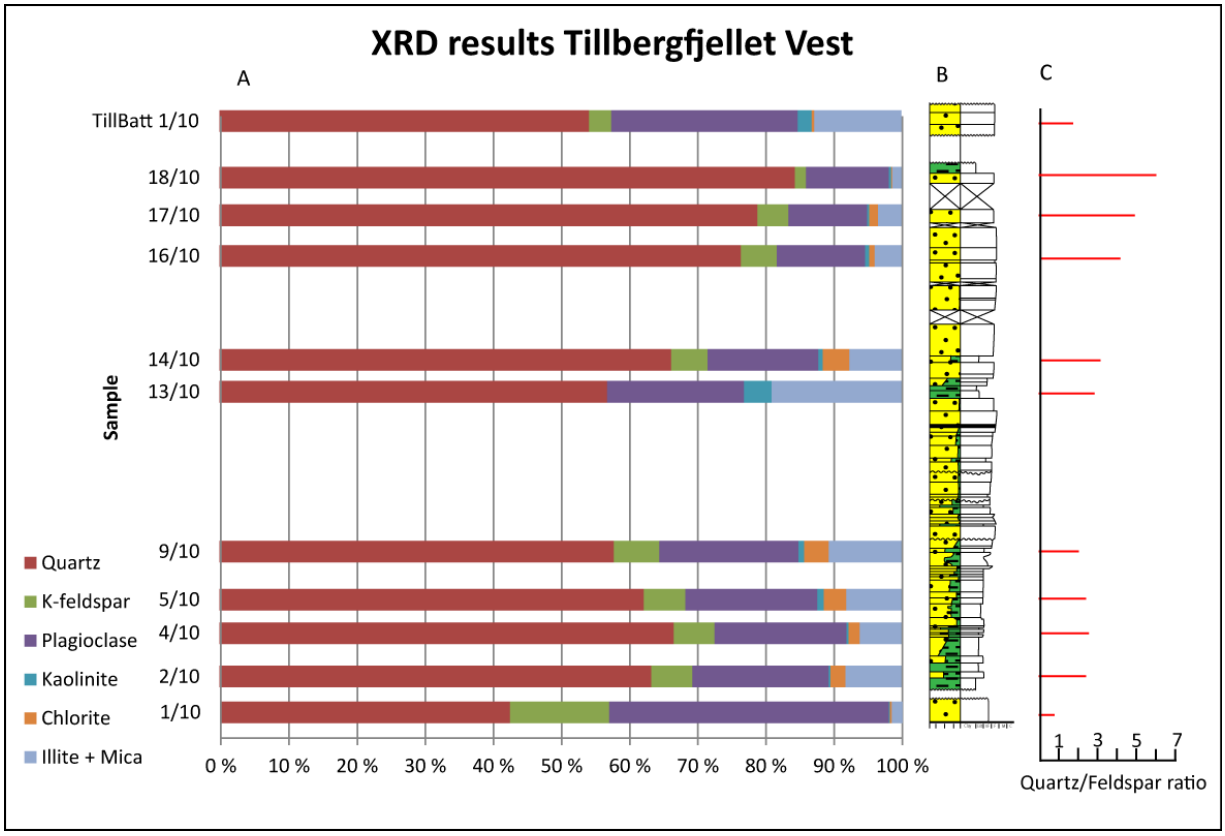

Figure 4 - 39: XRD results Tillbergfjellet Vest. 1/10 = Grumantbyen Fm., TillBatt 1/10 = Battfjellet Fm., remaining samples are from Hollendardalen Fm.

One sample (TillBatt 1/10) from Battfjellet Fm. was analyzed (Figure 4 - 39). Quartz make out the largest contribution with 54,2 XRD%. Feldspar minerals contribute with 32,6 XRD%, separated into plagioclase (27,4 XRD%) and K-feldspar (3,2 XRD%) (Figure 4 - 39). The illite and mica content make up 12,7 XRD%. Chlorite and kaolinite are present in amounts of

0,4 XRD% and 2,1 XRD% respectively. The quartz/feldspar ratio is 1,8 (Figure 4 - 39 and Appendix 5).

Thin section description

Sample 1/10 represents Grumantbyen Fm. This is bioturbated sandstone where all sedimentary structures are destroyed (Figure 4 - 40-A). Glauconite make up 1,5 % of minerals (Figure 4 - 40-A). Feldspar quartz ratio is 0,8 (Appendix 5).

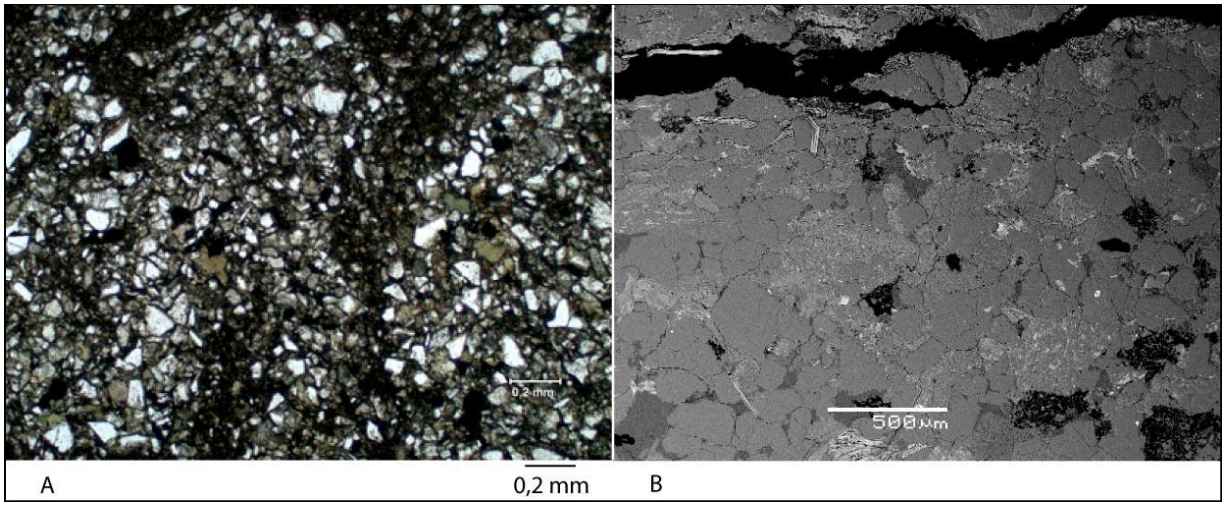

Figure 4 - 40: A) Sample 1/10 from Grumantbyen Fm. Note bioturbation and dark green glauconite minerals. B) Note bent mica flake in the upper part and small framboidal pyrite minerals (Sample 18/10).

Samples from Hollendardalen Fm. and Battfjellet Fm. are similar in mineral composition. Sandstones are grain supported with concavo-convex and tangential contacts. Elongated minerals, mainly mica, are bent between other grains (Figure 4 - 40-B). Monocrystalline quartz is the main mineral component up to 45 % (Appendix 4). Grains are angular to sub-rounded in shape and sorting varies from poor to moderately well. Polycrystalline quartz consist of more than five individual grains and are found in amounts up to 2,8 %. Shales and siltstones show a higher degree of bioturbation than sandstones. Feldspar minerals are partially altered to clay minerals, albite is observed in SEM studies. The quartz/feldspar ratio is above 2 in all samples from Hollendardalen Fm. and Battfjellet Fm. (Appendix 4). Small framboidal pyrite minerals are observed by SEM analysis (Figure 4 - 40-A).

4.2.7 Gangdalen Sør

Gangdalen Sør is located in the southern part of Gangdalen (Figure 3 - 1).

Figure 4 - 41: Gangdalen Sør. The upper sandstone that stands out is Hollerndardalen Formation, sandstones that stand out in the lower left corner is the Grumantbyen Formation. Looking toward north.

Sedimentological description

Grumantbyen Fm., Marstranderbreen Mb., Hollendardalen Fm. and Gilsonryggen Mb. are exposed (Figure 4 - 41 and Figure 4 - 42). Marstranderbreen Member measures 6 m and Hollendardalen Formation 14,5 m.

Hollendardalen Fm. consists of two upwards coarsening units (2,8 m – 10,2 m and 10,2 m – 14,7 m) (Figure 4 - 42). The lower unit contains a lower FA2a and an upper FA2b facies association. Shales of facies i that are interbedded by sandstones of facies ii.b and viii (Table 4 – 1) characterize the FA2a facies association (Figure 4 - 42). The rest of the section is a FA2b facies association. The lower upwards coarsening unit it is dominated by hummocky cross-stratified sandstones (facies iv, Table 4 – 1) The upper unit (10,2 m – 14,7 m) is slightly upwards coarsening in the very fine grain size. It consists of bioturbated sandstones of facies viii, the silt content in this unit is larger than in the lower unit (Figure 4 - 42).

The Gilsonryggen Mb is about 320 meters thick, Battfjellet Fm. overlies the Gilsonryggen Mb. with a sharp boundary. It consists of fine-grained sandstones of facies iii.a and v.

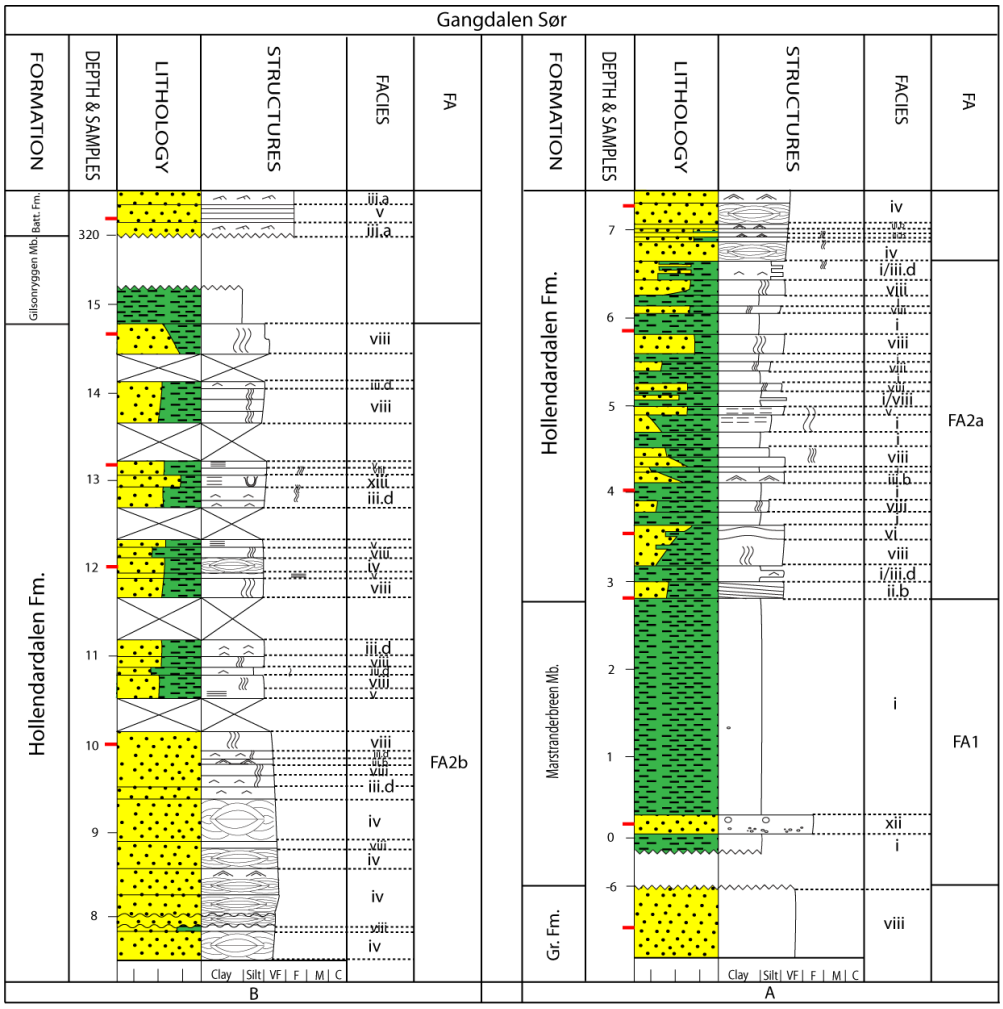

Figure 4 - 42: Log of the Gangdalen Sør section. A) Represents the interval from -6 m to 7,5 m. B) Represent the interval between 7,5 m and 15,2m and the Battfjellet Formation. FA = facies associations. Red marks represent XRD and/or thin section analyzed samples, while blue are XRD, thin section and heavy mineral analyzed samples.

Petrographic description

Twelve samples were analyzed by XRD and six were prepared for thin section analysis. One sample was cut in the Grumantbyen Fm., one from Battfjellet Fm. and the remaining ten samples are from Hollendardalen Fm. (Figure 4 - 43 and Appendix 3). Six samples were point counted, sample 1/10 comes from Grumantbyen Fm. sample 16/10 comes from Battfjellet Fm., the remaining four samples are from Hollendardalen Fm. (Figure 4 - 43).

XRD results

In sample 1/10 from Grumantbyen Fm., feldspar minerals make up the largest fraction (48,6 XRD%), divided into plagioclase (35, XRD%) and K-feldspar (13,6 XRD%) (Figure 4 - 43).

Quartz make up 48,5 XRD%. This gives a quartz/feldspar ratio of 1. Other minerals present in small amounts are illite and mica (1,5 XRD%), kaolinite (0,6 XRD%) and chlorite (0,9 XRD%) (Figure 4 - 43).

Ten samples from Hollendardalen Fm. were analyzed. Quartz is the most common mineral with amounts up to 76 XRD% (Figure 4 - 43). Feldspar minerals make up 38,2 XRD%; subdivided into plagioclase (up to 29,9 XRD%) and K-feldspar (up to 8,9 XRD%). Illite and mica constitute up to 14 XRD%. Other minerals present in minor amounts are kaolinite and chlorite with amounts up to 4,9 XRD% and 3,1 XRD% respectively (Figure 4 - 43). The quartz/feldspar ratio increases upwards in the section from 1.3 to above 3 (Figure 4 - 43 and Appendix 3).

One sample (16/10) was analyzed from Battfjellet Fm. (Figure 4 - 43 and Appendix 3). Quartz is the main component with 67 XRD%. The feldspar group constitutes 23,2 XRD%; subdivided on plagioclase (19,6 XRD%) and K-feldspar (3,6 XRD%). This yields a quartz/feldspar ratio of 2,9. Illite and mica constitute 6,7 XRD%. Chlorite and kaolinite are present in amounts of 2,7 XRD% and 0,4 XRD% respectively.

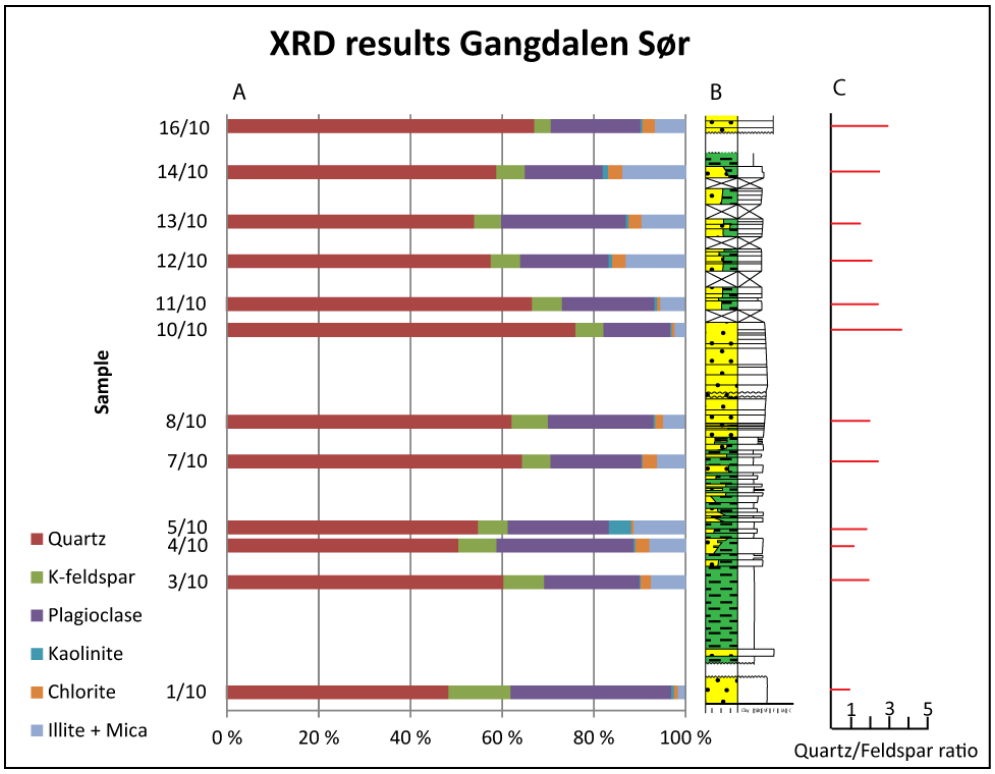

Figure 4 - 43: A) XRD results Gangdalen Sør, 1/10 = Grumantbyen Fm., 16/10 = Battfjellet Fm., the remaining samples are from the Hollendardalen Formation. B) Simplified log. C) Quartz/feldspar ratio.

Thin section description

In sample 1/10 from Grumantbyen Fm. grains are angular to sub-rounded shaped and moderately well sorted. Bioturbation is observed in thin section studies. Feldspar minerals are the most common with 32,3 % (Appendix 4). Glauconite is observed in thin section and SEM analysis (Figure 4 - 44-A).

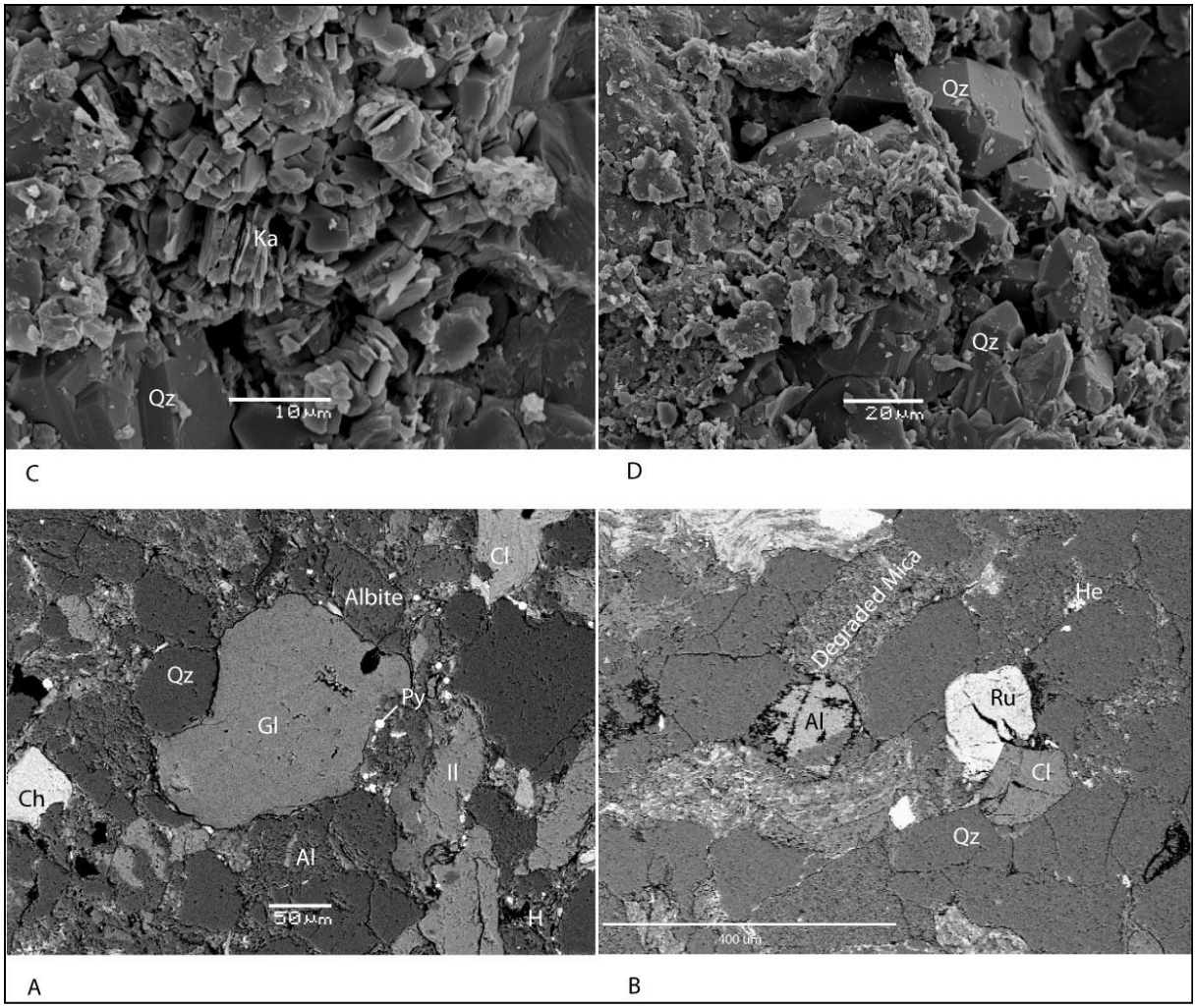

Figure 4 - 44: A) Large glauconite mineral (Gl), fraomboidal pyrite (Py), Chlorite (Cl) and albite (Al) in sample 1/10 from the Grumantbyen Fm. B) Partially altered albite (Al), degraded mica and rutile (Ru), Chlorite (Cl), Hematite (He). (sample 16/10 from Battfjellet Fm.) C) Diagenetic kaolinite (sample 16/10). D) Quartz cementation (sample 16/10).

Hollendardalen Fm. samples in the upper part of the section (10 m – 14,5 m) (Figure 4 - 42) are normally poorly sorted, whiles samples below are moderately well sorted. Grains are angular to sub-rounded in shape with mainly concavo-convex contacts. Monocrystalline quartz is the most abundant mineral (44,8 %); polycrystalline quartz (2,8 %) and chert (3,8 %) are observed (Appendix 4) Lamination occurs in studied thin sections, elongated grain

(mainly mica and coal fragments) show preferred orientation parallel to lamination. Bent micas and mud rip-up clasts are observed.

Battfjellet Fm. is represented by one sample, and is similar to Hollendardalen Fm. samples. Altered albite and degraded micas are observed in SEM analysis (Figure 4 - 44-A and B). Quartz cementation and diagenetic kaolinite are present between grains (Figure 4 - 44-C and D). This also occurs in samples from Hollendardalen Fm.

4.2.8 Tverrdalen

Figure 4 - 45: Tverrdalen section, person for scale. Marstranderbreen Mb. covered by scree in the lower part.

Sedimentological description

Grumantbyen Fm., Marstranderbreen Mb. and Hollendardalen Fm. are exposed (Figure 3 - 1, Figure 4 - 45and Figure 4 - 46). Marstranderbreen Mb. measures 8 m and Hollendardalen Fm. measures 4,9 m (Figure 4 - 46). The Tverrdalen section is the easternmost of the logged sections.

Sandstones in the Grumantbyen Fm. are highly bioturbated and all sedimentary structures are destroyed (facies viii Table 4 – 1), (Figure 4 - 46).

Two upwards coarsening units (0 m – 3,2 m and 3,2 m – 4,8 m) are observed in the Tverrdalen section (Figure 4 - 46). The lower unit (0 m – 3,2 m) consists of FA2a and FA2b facies association. The FA2a facies association is characterized by bioturbated sandstones (facies viii, Table 4 – 1), interbedded by ripple laminated sandstones (facies iii.b and iii.d) (Figure 4 - 46). Sandstones with parallel bedding dominate the FA2b facies association.

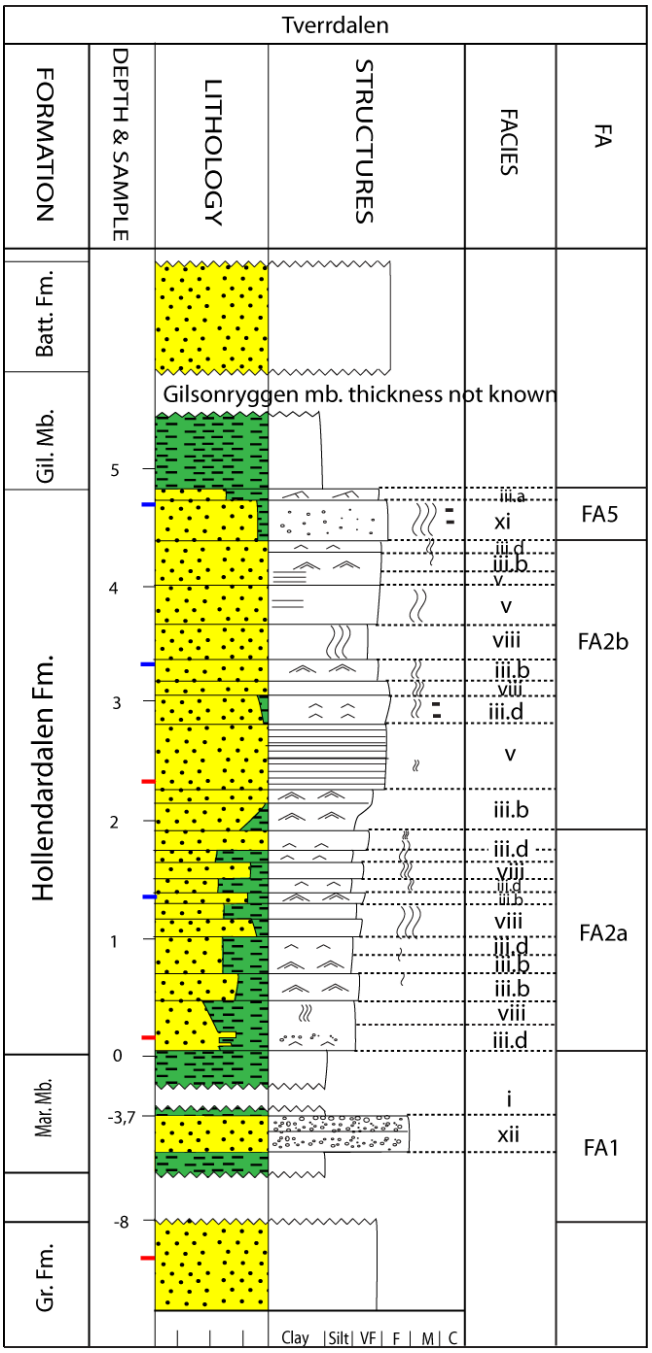

Figure 4 - 46: Log of Tverrdalen section. FA = facies associations. Red marks in "Depth & Sample" column are samples analyzed by XRD and/or thin section, blue markings are samples analyzed by XRD, thin section and heavy mineral.

FA2b and FA5 facies associations make up the upper upwards coarsening unit (3,2 m – 4,8 m). The FA2b facies association consists of parallel-bedded sandstones (facies v) and ripple laminated sandstones (facies iii.b) (Figure 4 - 46). The topmost sandstone is poorly sorted sandstone of facies xi and FA5 facies association. Measurements of symmetrical ripple show that the ripple crest is striking northwest-southeast, this indicate a sediment infill from either northeast or southwest. Asymmetrical ripples were not observed at this section.

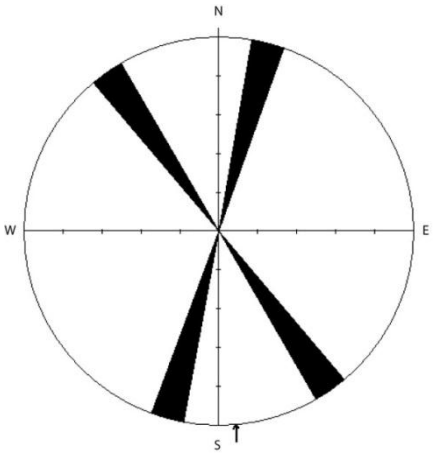

Figure 4 - 47: Measurements of symmetrical ripple crests. Plot made from data in Appendix 7.

Petrographic description

Seven samples were analyzed by XRD (Figure 4 - 48 and Appendix 3). Five samples were point counted (Figure 4 - 48). One sample comes from Grumantbyen Fm., one from Gilsonryggen Mb. whilst the remaining samples are from Hollendardalen Fm. The Gilsonryggen sample was not point counted.

XRD results

Feldspar minerals make up the largest fraction of the Grumantbyen Fm with 54,1 XRD% subdivided into plagioclase (36,5 XRD%) and K-feldspar (17,5 XRD%) (Figure 4 - 48). Quartz constitute 42,5 XRD%. Other minerals present are illite and mica (2,4 XRD%), chlorite (0,7 XRD%) and kaolinite (0,4 XRD%) (Figure 4 - 48). The quartz/feldspar ratio is 0,8 (Appendix 3).

Quartz makes up the largest constituent of the analyzed samples from Hollendardalen Fm. with amounts up to 75,1 XRD% (Figure 4 - 48). The feldspar content can be subdivided into plagioclase (up to 28 XRD%) and K-feldspar (up to 16,7 XRD%) with a total of 45 XRD%. Illite and mica constitute up to 9,6 XRD%. Chlorite and kaolinite are present in amounts up to 2,3 XRD% and 0,66 XRD% respectively (Figure 4 - 48). The quartz/feldspar ratio increases upwards from 1,5 to 3,6 (Appendix 5).

Sample 11/10 from Gilsonryggen Mb. contains quartz as the main constituent with 55 XRD% (Figure 4 - 48). Plagioclase makes up the largest part of the feldspar minerals with 30 XRD%, while K-feldspar is 7,8 XRD%. Illite and mica contribute with 5,5 XRD%. Chlorite and kaolinite constitute 0,9 XRD% and 0,5 XRD% respectively (Figure 4 - 48). The

quartz/feldspar ratio equals 1,4, a decrease from the underlying Hollendardalen Fm. (Appendix 5).

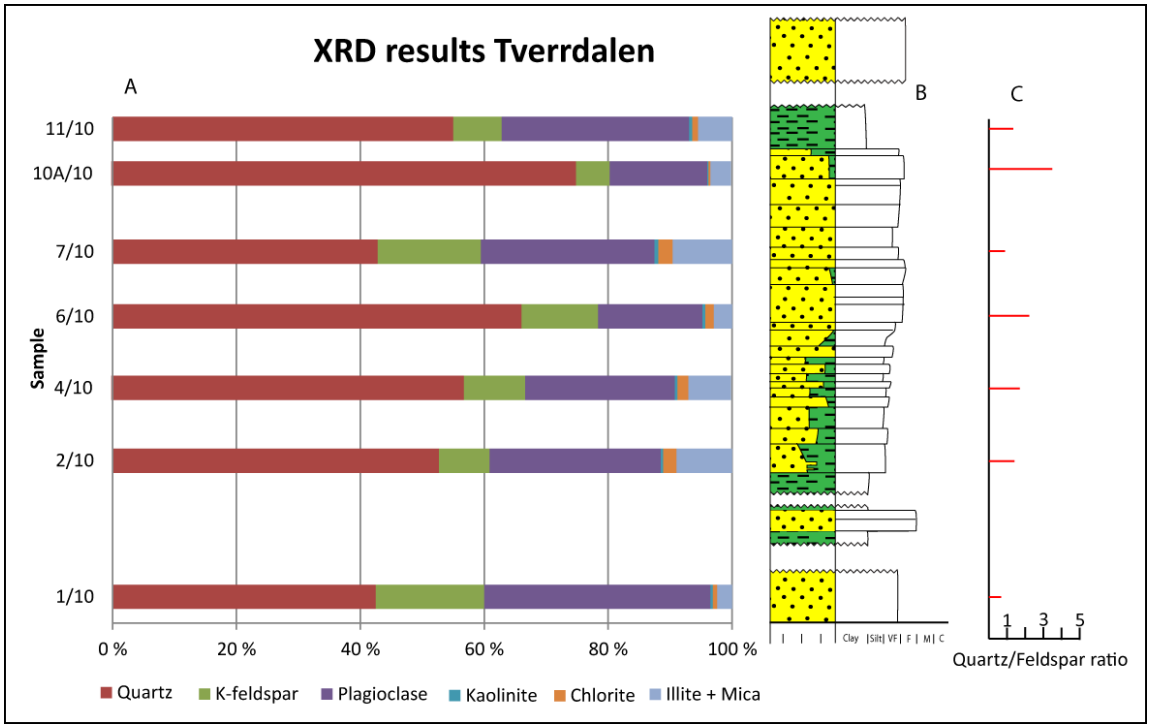

Figure 4 - 48: XRD results Tverrdalen. Sample 6881 = Grumantbyen Fm., Samples 6882 – 6887 Hollendardalen Fm.

Thin section description

Sample 1/10 from the Grumantbyen Fm. is a moderately well sorted sandstone with angular to sub-rounded grains. It contains 1,5 % glauconite (Figure 4 - 49-A), which is higher than what is observed in Hollendardalen and Battfjellet formations. Bending of mica flakes is common in all analyzed samples. Quartz/feldspar ratio is 0,6 (Appendix 5).

Hollendardalen Fm. sandstones are moderate well sorted and have sub-rounded grains. Poorly sorted samples are observed (Figure 4 - 49-B). Grain contacts are concavo-convex. Monocrystalline quartz is the main fraction in the Hollendardalen Fm. (49 %) samples, and both polycrystalline quartz (up to 2 %) and chert (up to 1,5 %) are observed. Partial feldspar alteration is common, and the quartz/feldspar ratio is above 2 in all samples from Hollendardalen and Battfjellet formations. Coal fragments are normally observed in amounts up to 7 % (Appendix 4).

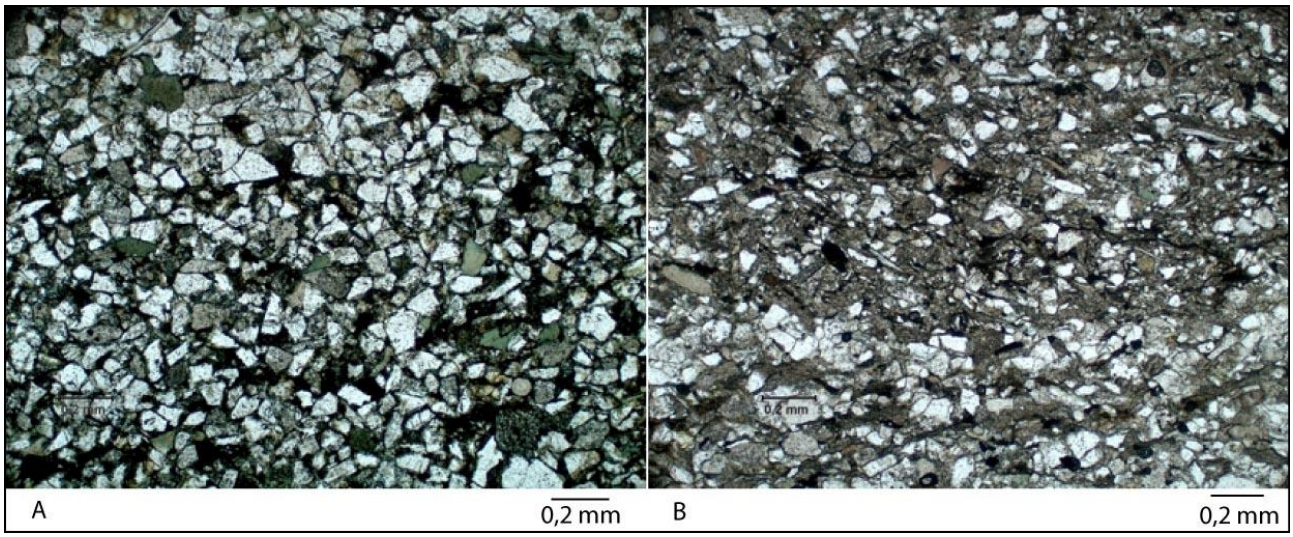

Figure 4 - 49: A) Mark green glauconite minerals, sample 1/10 from Grumantbyen Fm. B) Poorly sorted sample 4/10.

4.3 Rock-Eval pyrolysis

21 samples were analyzed by Rock-Eval pyrolysis. All samples are from Hollendardalen Fm., except from one sample (Tverrdalen 11/10) which is from Gilsonryggen Mb. Clay and silt grain sized samples were used for the Rock-Eval pyrolysis. The pyrolysis procedure is described in 3.11 along with calculation of the hydrogen index (HI) and oxygen index (OI). Four parameters were measured during pyrolysis S1 (thermally distilled free hydrocarbons), S2 (mg HC/g rock) and S3 (mg CO_2/g rock) and T_{max}. S1 values are generally below 0,5, S2 values are below 2,17 (normally less than 1), and S3 have measured values below 1 (Table 4 - 3). T_{max} values range between 438 ˚C and 448 ˚C, with normal values around 442 ˚C.

Figure 4 - 50 shows the hydrogen index plotted against the oxygen index in a modified van Krevelen diagram. All analyzed samples gather in the kerogen type three area (Figure 4 - 50).

Hydrogen index (HI) and production index (PI) were calculated for all analyzed samples. HI values are normally below 83 HC/g C_{org}, with some exceptions of samples with values up to 96,9 (Table 4 - 3).

Table 4 - 3: Results of Rock-Eval analysis. Hol. Fm. = Hollendardalen Formation, Gil. Mb. = Gilsonryggen Member. Tmax = temperature at maximum S2 pyrolysis, HI = Hydrogen index, PI = production index.

Outcrop/Core	Sample	Formation	S1	S2	S3	TOC	T_{max}	HI	PI
Oppkuvbekken	88/09	Hol. Fm.	0,21	1,04	0,49	1,07	441	96,92	0,17
Vestalbekken	109/09	Hol. Fm.	0,14	0,87	0,38	1,05	437	83,25	0,14
	4/10	Hol. Fm.	0,12	0,67	0,85	1,03	442	65,18	0,15
Holmsenfjellet	46/09	Hol. Fm.	0,27	1,53	0,89	1,67	441	91,78	0,15
	50/09	Hol. Fm.	0,12	0,55	0,81	0,87	442	62,94	0,18
	64/09	Hol. Fm.	0,15	0,70	0,77	1,00	438	69,93	0,18
Trodalen	1/10	Hol. Fm.	0,07	0,17	0,71	0,60	439	28,54	0,29
	3/10	Hol. Fm.	0,13	0,51	1,08	0,77	445	66,00	0,20
	6/10	Hol. Fm.	0,07	0,30	0,44	0,49	443	61,74	0,19
	17/10	Hol. Fm.	0,19	1,26	0,62	1,81	448	69,57	0,13
Tillbergfjellet Vest	2/10	Hol. Fm.	0,14	0,81	0,47	1,07	442	75,98	0,15
	4/10	Hol. Fm.	0,18	0,84	0,48	1,11	441	75,88	0,18
	13/10	Hol. Fm.	0,04	0,03	1,16	0,29	449	10,32	0,57
Gangdalen Sør	3/10	Hol. Fm.	0,20	1,26	0,60	1,68	441	75,04	0,14
	5/10	Hol. Fm.	0,13	0,62	0,85	0,94	441	66,28	0,17
	7/10	Hol. Fm.	0,40	2,17	0,60	2,09	443	103,73	0,16
	11/10	Hol. Fm.	0,22	1,46	0,45	1,78	442	81,84	0,13
Tverrdalen	11/10	Gil. Mb.	0,14	1,40	1,00	2,70	441	51,93	0,09
BH 8/06	16,8	Hol. Fm.	0,15	1,29	0,68	1,77	434	73,09	0,10
	15,85	Hol. Fm.	0,28	2,41	0,68	2,71	439	88,90	0,10
	15,3	Hol. Fm.	0,20	1,62	0,61	1,94	438	83,46	0,11

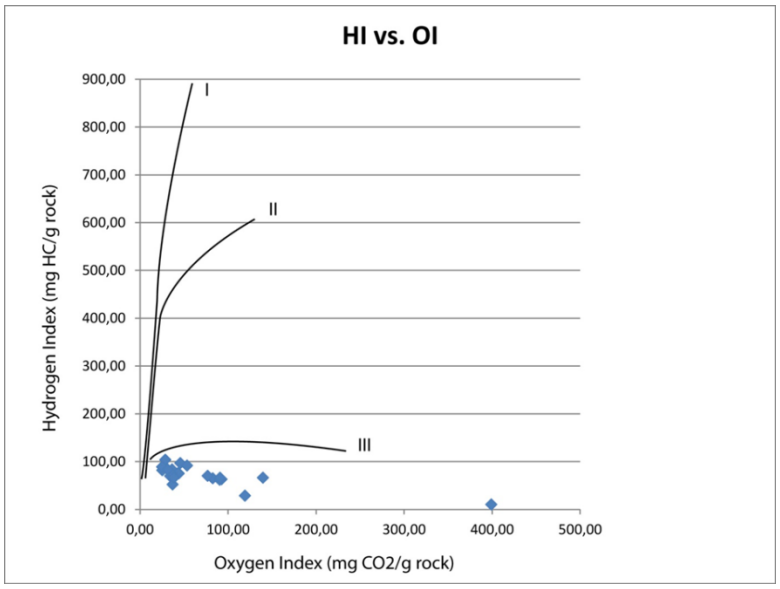

Figure 4 - 50: Rock-Eval results in a modified Van Krevelen diagram. All samples gather below the kerogen type three line.

4.4 Heavy mineral analysis

23 samples from eight outcrops were analyzed for heavy mineral composition. Samples were taken from Grumantbyen, Hollendardalen and Battfjellet formations. Unfortunately not all samples could be analyzed due to restricted grain size of very fine. Therefore only two samples from Battfjellet Fm. were analyzed.

Table 4 - 4: Modified heavy mineral data set from Appendix 2. Ap = apatite, Ca = calcic amphibole, Cp = clinopyroxene, Ep = epidote, Ct = chloritoid, Gt = garnet, Ru = rutile, To = tourmaline, Zr = zircon, ATi = apatite:titanite index, GZi = garnet:zircon index, RuZi = rutile:zircon index.

Sample	Ap	Ca	Cp	Ep	Ct	Gt	Ru	To	Zr	ATi	GZi	RuZi
Battfjellet Fm.												
VESUV 163/09	23,5				52,0	R	4,5	4,5	14,0	84,0	2,4	19,7
VESUV 164/09	9,5				82,5	0,5	1,5	1,5	4,5	88,0	2,9	21,9
GANGS 16/10	39,5				22,0	R	6,0	7,0	23,0	85,0	2,0	17,4
TILLBLAT 1/10	34,5				48,5	R	2,0	9,0	4,5	84,0	4,8	33,8
Hollendardalen Fm.												
VES 113/09	37,0				3,0	17,0	4,0	14,5	19,0	72,0	48,3	20,3
VES 129/09	66,0				11,5	2,0	2,0	13,5	4,0	83,0	29,4	37,9
VESLAL 131/09	37,0				1,0	9,0	9,0	10,5	29,0	75,0	24,0	24,0
OPPK 94/09	21,5				1,0	16,5	4,5	5,5	37,5	75,0	32,2	13,0
OPPK 100/09	37,0				2,0	19,5	6,0	17,5	15,0	68,0	55,0	23,7
OPPK 105/09	39,5				48,5	1,0	0,5	5,5	4,5	86,5	32,4	17,9
OPPK 107/09	62,0				16,0	R	1,5	17,0	1,0	79,5	4,8	47,4
HOL 56/09	41,5				2,0	8,0	4,0	15,0	24,0	74,5	17,4	16,0
HOL 69/09	41,0				6,5	9,0	6,5	8,5	22,5	83,0	20,3	18,7
HOL 78/09	40,0				12,5	1,5	3,0	13,0	26,0	76,0	7,4	11,5
HOL 87/09	38,0				9,5	2,5	6,5	20,0	17,5	68,0	12,1	25,3
TVERR 4/10	49,5				1,0	12,0	5,0	12,0	14,5	75,0	45,4	21,9
TVERR 7/10	49,5				6,0	9,0	4,0	15,0	12,5	77,0	42,7	30,8
TVERR 10A/10	42,0				1,5	7,0	7,5	20,0	19,0	68,5	18,4	26,5
TILV 5/10	35,0				1,0	19,5	7,5	12,0	22,0	77,0	45,7	21,3
TILV 9/10	58,5				0,5	3,0	5,5	22,0	6,0	75,5	41,1	35,9
TILV 17/10	38,5				1,0	7,0	5,5	15,0	27,0	72,5	20,9	19,7
Grumantbyen Fm.												
VESTAL 138/09	16,4	2,6	1,3	1,3	5,3	42,1	1,3	11,8	15,2	58,1	73,6	8,0
HOL 61/09	29,0	R	R	R	7,5	28,0	1,5	15,0	14,0	73,5	67,5	15,4

Variations in the heavy mineral suits in the three abovementioned formations are observed. Grumantbyen Fm. is characterized by high garnet abundance (28 – 42 %), and traces of calcic amphibole, clinopyroxene and epidote (Table 4 - 4). Hollendardalen Fm. contains a variety of heavy minerals where no specific heavy mineral is dominating. Chloritoid amounts in

Battfjellet Fm. are much greater than in the other analyzed formations with amounts from 48,5 to 82,5 % (Table 4 - 4).

Differences in heavy mineral indexes are also observed. Figure 4 - 51 displays a ternary plot of the apatite:tourmaline index (ATi), garnet:zircon index (GZi) and rutile:zircon index (RuZi). Procedure for calculating heavy mineral indexes is presented in 3.10.

Andy Morton (Morton 2010, personal communication) conducted the analysis suggested using rutile:zircon index rather than TiO_2 minerals:zircon index (RZi) for provenance studies, due to presence of anatase and brookite in RZi which can be diagenetic product. Grumantbyen Fm. samples gather closer to the ATi-GZi line than the other formations (Figure 4 - 51). Analyzed samples from Battfjellet Fm. plots close to the ATi-RuZi line, while samples from Hollendardalen Fm. gather intermediate between the two other analyzed formations (Figure 4 - 51).

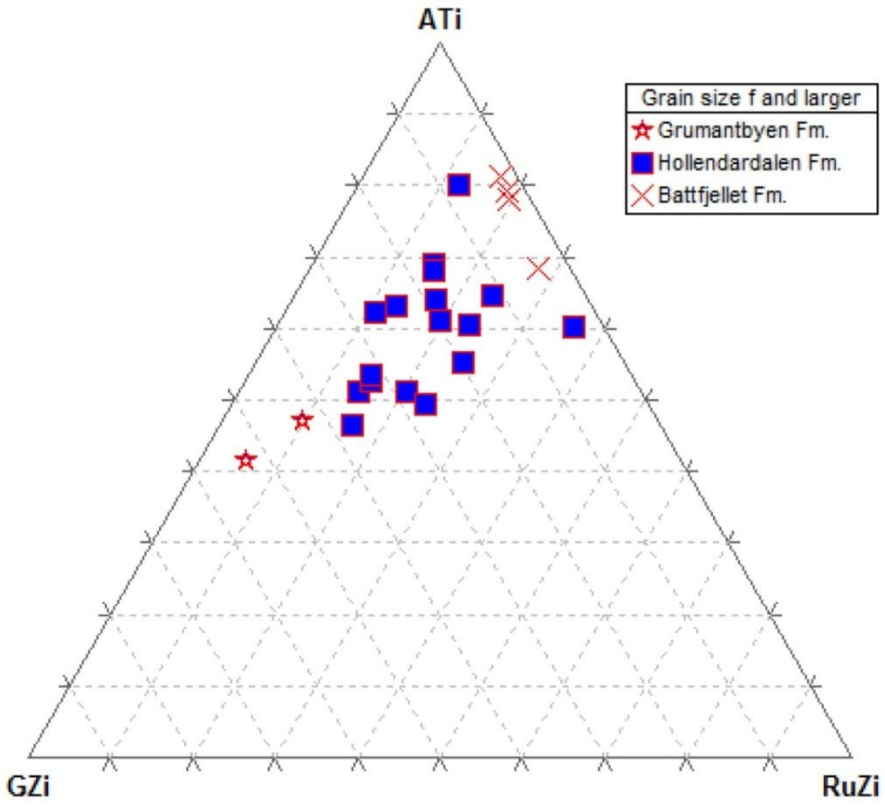

Figure 4 - 51: Ternary plot with ATi, GZi and RuZi. Red star = Grumantbyen Fm., blue box = Hollendardalen Fm. and red cross = Battfjellet Fm. Values from Appendix 2.

.

5 Discussion

5.1 Log correlation and facies associations

The development of the Central Basin is divided into two major tectonic phases. In the first (early-mid Paleocene) phase the Central Basin developed as a rift basin in an extension setting, with sediments brought from the east (Steel et al. 1985). The first phase ends with the sandstones of Grumantbyen Fm. In the second phase, (late Paleocene – early Eocene), sediments where brought in from the west as a result of a wrench regime with upheaval of the western margin and formation of the West Spitsbergen Orogen (Harland 1969, Steel et al. 1985). Hollendardalen Fm. represents the first sandstones of the second tectonic phase (Steel et al. 1985). It should be noted that Bruhn and Steel (2003) argued that the Central Basin could have developed as a foreland basin analogue under in a compressional regime.

Seven logged sections from Vestalbekken in the northwest to Tverrdalen in the southeast (Figure 3 - 1) were correlated based on the five facies associations described in chapter 4.1.2 (Figure 5 - 1). Hollendardalen Fm. displays a clear eastern thinning, from 21,5 meters at Oppkuvbekken section to 4,8 meters at Tverrdalen outcrop (Figure 5 - 1). Hollendardalen Fm. can be divided into lower and upper upwards coarsening parasequences. The two upwards coarsening parasequences are observed at all logged sections from west to east (Figure 5 - 1).

FA1

The FA1 facies association is dominated by siltstones of facies i (Table 4 – 1, Figure 4 - 9), and include the shales of Marstranderbreen Mb. Except from weak lamination no sedimentary structures are observed, which indicates a distal position and deposition below storm wave base where sediments fall out of suspension (Reading 1996). A setting of prodelta sedimentation is proposed for the FA1 facies association. This is consistent with the lack of sedimentary structures produced by wave and tidal processes and prevailing fine grained sedimentation observed by field studies. A prodelta setting fits well with the overlying facies associations discussed below.

The base of the pebble rich sandstone (facies xiii) within the FA1 facies association does not show an erosive boundary. Lacking an erosive base, transportation by gravity flows is

unlikely. Dalland (1977) described this sandstone as ice rafted debris, however this requires temperatures below zero, which is not in accordance with climatic studies (Schweitzer 1980, Sluijs et al. 2006). Transportation by kelp or driftwood also proposed by Dalland (1977), is a more likely explanation.

The FA1 facies association is thinning progressively towards the east, from 41 m at Vestalbekken section to 8 m at Tverrdalen section (Figure 5 - 1). A good correlation of this facies association was made from the westernmost logged section (Oppkuvbekken) to the easternmost outcrop (Tverrdalen) (Figure 5 - 1). How this facies association develops further eastwards is an unanswered question. The overlying sandstones of Hollendardalen Fm. might directly overlie Grumantbyen Fm. further east, or it might pinch out and disappear without ever being in contact with Grumantbyen Fm. This is an important question to address, because, if Hollendardalen Fm. directly overly Grumantbyen Fm. it will affect the regional stratigraphy. This study does not have sufficient data to give an answer and further studies are therefore necessary.

FA2

The FA2 facies association is subdivided into three facies associations (a, b and c) (Table 4 - 2).

The FA2a facies association is characterized by siltstones of facies i or viii that are interbedded by sandstones of facies iii.a, iii.b, iii.d, iv or viii (Table 4 – 1). These sandstones are the first that appear in the Hollendardalen Fm. (e.g. Figure 4 - 11 or Figure 4 - 32). Sandstone beds have a sharp contact against the underlying siltstones (Figure 4 - 9-B and Figure 4 - 10-A). Siltstones are probably deposited as background sedimentation while sandstone beds might be turbidites. Turbidic currents are formed when sediments oversteepen and are liquefied. Liquefied sediments then move downslope and sediments fall out of suspension as the current strength decreases. Oversteepening of sediments can occur in periods of increased sedimentation, often related to flood events (Harris et al. 2004). These turbidic currents form the Bouma-sequence (Lowe 1976, Bouma 2004, Harris et al. 2004). A complete Bouma-sequence is normally not observed in field studies (Shanmugam 1997, Bouma 2004), and was not in this study either. The appearance of sandstone beds containing asymmetrical ripples formed by a unidirectional current (Allen 1966) within the silty unit are likely formed by turbidic current deposits. With increased stratigraphic height within the

FA2a facies association, sandstone beds tend to be thicker, closer spaced and have increased sand content (e.g. Figure 4 - 11 or Figure 4 - 38). Wave induced sedimentary structures such as hummocky cross stratification (Dumas and Arnott 2006) are observed (Figure 4 - 20). These points lead to a probable depositional setting in the transitional zone between the prodelta and lower delta front. This depositional environment explains both the turbidites and the wave generated sedimentary structures.

The FA2a facies association is observed in the lower upwards coarsening parasequence which overlies the FA1 facies association at all studied sections (Figure 5 - 1). It displays a regressive development of the system with coarser grained sediments, increased sand content and closer spacing of sandstone beds.

The FA2b facies association differs from the FA2a facies association, with coarser sediments dominated by wave generated structures like hummocky cross-stratification (Dumas and Arnott 2006) and symmetrical ripple lamination (Komar 1974). The FA2b facies association is normally upwards coarsening, indicating a regression and shallower water depths. Presence of hummocky cross-stratification indicates that sediments are deposited immediately above the storm wave base (Dumas and Arnott 2006). Parallel bedded or laminated sandstones of facies v are also observed in several of the studied sections (Figure 4 - 27). With relation to over- and underlying facies associations and observed sedimentary structures, a depositional setting of wave dominated delta front is suggested for the FA2b facies association. Bhattacharya and Giosan (2003) describe wave influenced delta front sediments that are similar to our observations.

In the lower upwards coarsening parasequence the FA2b facies association succeeds the FA2a facies association at all studied sections (Figure 5 - 1). With its coarser grain sizes deposited above storm wave base it indicates a continued regressive development from the underlying FA2a facies association.

The FA2b facies association is also found at the base of the second upwards coarsening parasequence at all studied sections (Figure 5 - 1). In western and central parts of the studied area it succeeds the FA4 facies association (Oppkuvbekken, Vestalbekken and Tillbergfjellet Vest) or FA3b facies association (Holmsenfjellet and Trodalen) (Figure 4 - 27, Figure 4 - 32 and Fig. 3-1). In eastern parts of the basin (Gangdalen Sør and Tverrdalen) the FA2b facies association continues for the remainder of the logged section. However, a thin (30 cm) FA5

facies association overlies the FA2b facies association at Tverrdalen where it marks the upper exposure of Hollendardalen Fm. (Figure 5 - 1, Figure 4 - 6-B and Figure 4 - 46).

The FA2c facies association is only found at the Vestalbekken section (Fig 3-1, Figure 4 - 20). It is an upwards coarsening unit dominated by flaser-bedded sandstones (facies vii) (Table 4 – 1, Figure 4 - 8). Flaser-bedding is produced under tidal processes where current strength varies (Reineck and Wunderlich 1968). The FA2c facies association is located above a FA2a facies association and below an FA3 facies association (Figure 5 - 1, Figure 4 - 20). Considering this sequence together with the observed flaser-bedding, deposition on a tidal influenced delta front is proposed.

FA3

The FA3 facies association is divided into two subfacies associations (a and b) (Table 4 - 2).

Facies association FA3a (Figure 4 - 10-C) is observed in the lower upwards coarsening parasequence in western and central parts of the basin (Oppkuvbekken, Vestalbekken, Holmsenfjellet and Trodalen outcrops) (Figure 5 - 1). It overlies the FA2b facies association, except from Oppkuvbekken where it overlies FA2c facies association (Figure 4 - 11). The base of the facies association is erosive at all logged outcrops (Figure 5 - 1, Table 4 - 2).

The FA3a facies association is a fine to coarse grained sandstone with cross-bedded sandstones where foresets are planar or sigmoidal (facies ii.d) (Table 4 – 1, Figure 4 - 10-C). Sandstones of facies v with planar bedding and lamination are also observed. Occasionally reactivation surfaces of the foresets and variable foreset bed thicknesses of sandstone facies ii.d are observed. Individual beds are separated by erosive boundaries with rip-up mud clasts, pebble sized grains and pockets of fine sand. These structures and the parallel bedding of facies v are often associated with channels (Olariu and Bhattacharya 2006). Given the relation to over- and underlying facies associations (Figure 5 - 1) and observed facies, a sedimentary setting of distributary mouth bar sediments and channels is proposed. Olariu and Bhattacharya (2006) describe a similar setting. Reactivation surfaces of foresets and variable foreset bed thicknesses are probably caused by tide water effects (Kreisa and Moila 1986).

The FA3b (Figure 4 - 10-E) facies association is slightly upwards coarsening, indicating a regressive development. It is dominated by trough cross-stratified sandstones (facies ii.c) and cross-bedded sandstones. Several soft sediment deformed units (facies xiii) (Table 4 – 1) are

observed indicating rapid sedimentation (Lowe 1976). Sandstones in this facies contain only minor amounts of silt (Figure 4 - 38). Combined flow ripples (facies iii.c) are normally present, and both single- and double mud-drapes have been observed in the logged sections. Combined flow ripples (facies iii.c) and mud drapes are normally associated with tidal environments (Visser 1980, Yokokawa et al. 1995), while the observed hummocky cross-stratification is related to wave activity (Greenwood and Sherman 1986, Dumas and Arnott 2006). The variety of facies observed indicates that the depositional environment is not dominated by either wave or tidal processes. The FA3b facies association displays high sedimentation rate, indicated by soft sediment deformation, and low silt content. Together with the relation to over- and underlying facies associations, the soft sediments deformed units supports the interpretation of the FA3b facies association as distributary mouth bar sediments. Distributary mouth bar sediments are formed where rivers meet a standing body of water and sediments fall out of suspension (Wright et al. 1973, Wright 1977). Wave and tidal action winnow and transport finer grained sediments basinward leaving clean and well sorted sandstone (Wright et al. 1973).

The FA3b facies association occurs in the lower and the upper parasequence in the western and central parts of the studied area (Figure 5 - 1). It marks the upper boundary of the first upwards coarsening parasequence at Holmsenfjellet and Trodalen sections, while at Oppkuvbekken, Vestalbekken and Tillbergfjellet Vest it underlies FA4 facies association (Figure 5 - 1). In the upper upwards coarsening parasequence the FA3b facies association is present at Holmsenfjellet, Trodalen and Tillbergfjellet Vest outcrops, found between underlying FA2b and overlying FA4 facies associations (Figure 5 - 1).

FA4

This facies association range over a variety of facies, from continental deposits represented by sandstones with root horizons (facies ix) and coal layers (facies x), to marine sandstones abundant in shells (facies xiv), flaser bedding (facies vii), and ripple laminated sandstones (facies iii.a and iii.d) (Table 4 – 1). Upwards coarsening units are commonly associated with this facies association (Figure 4 - 11, Table 4 - 2). Based on the variety of observed facies and stratigraphic position sediments of the FA4 facies association is proposed to be deposited within a delta plain. Because of lack of interpreted channels, sediments were probably deposited in interdistributary bay areas (Reading 1996). Interdistributary bays might be

partially or fully protected from marine processes (Elliott 1974, Bhattacharya and Giosan 2003). Observed facies show influence of marine processes (flaser bedding, facies vii) and current related facies (asymmetrical ripples of facies iii.a). This indicates that some parts of the FA4 facies association has been influenced by marine processes. Vegetated areas normally occur in interdistributary areas (Elliott 1974). The observed root horizons of the FA4 facies association are probably result of these vegetated areas.

The FA4 facies association is observed in both the lower and upper upwards coarsening parasequence. FA4 thicknesses in the upper parasequence are greater than those in the lower parasequence (Figure 5 - 1). It is present at Oppkuvbekken, Vestalbekken and Tillbergfjellet logged sections in the lower parasequence, where it marks the upper boundary of the parasequence. In the upper parasequence it is observed in the central and western parts of the studied area (Figure 5 - 1), where it marks the upper boundary of Hollendardalen Fm, however, at Tillbergfjellet Vest section it underlies a thin (30 cm) FA5 facies association.

FA5

The FA5 (Figure 4 - 10) facies association is observed at three logged sections (Trodalen, Tillbergfjellet Vest and Tverrdalen) (Figure 5 - 1). Where it is present it marks the upper boundary of Hollendardalen Fm. towards the shales of Gilsonryggen Mb. (e.g. Figure 4 - 46). It consists of one facies of poorly sorted sandstone, abundant in pebble sized grains, coal and shell fragments (facies xi) (Table 4 – 1). Gilsonryggen Mb. overlies the Hollendardalen Fm. with a sharp boundary, a significant transgression must have occurred from Hollendardalen Fm. to Gilsonryggen Mb. With relation to the overlying shales of Gilsonryggen Mb. and the appearance of the facies xi sandstone, the FA5 facies association is proposed to be a transgressive lag deposit. Lag deposits often develop during transgression, commonly characterized by conglomeratic, glauconitic or fossiliferous beds with abundant shell and coal fragments (Kidwell 1989, Cattaneo and Steel 2003, Meloche 2010). Lag deposits are formed by shoreline ravinement and wave reworking during transgression. It overlies overlie shallow or more proximal facies (Meloche 2010) The FA5 facies association indicates a rapid transgression from the sandstone in Hollendardalen Fm. to the overlying shales of Gilsonryggen Mb.

Holmsenfjellet, a special case

The upper part (22,8 m – 26,8 m) of Holmsenfjellet section differs from the other logged sections (Figure 5 - 1). A third parasequence is observed, separated from the underlying upper upwards coarsening parasequence by 3 m of scree material. It can be a third parasequence or an up-faulted part of the upper parasequence. The sedimentary column of this unit (22,8 m – 26,8 m) and the upper part of the upper parasequence are similar to each other (Figure 4 - 27). If it is an up-faulted part, a reversed fault with an excess of 7,0 m of throw is necessary. Dalland (1979) did structural geological work in the Central Basin, however he did not identify any fault zones in the discussed area. Slickensides or other features related to faults were not observed at the section (Fleuty 1975, Petit 1987). A third parasequence does not fit with the development the rest of Hollendardalen Fm. (Figure 5 - 1), therefore the preferred explanation is that the upper part of Holmsenfjellet section is an up-faulted part of the upper upwards coarsening parasequence. This is supported by work done by Hanevik (2011, master thesis UiB). Further studies are necessary to better support this explanation.

Paleocurrent measurements

Paleocurrent measurements display changing infill directions from western to eastern logged sections. Ripple and cross-bedded sandstones are used for paleo-current measurements. Western and central logged sections are dominated by paleocurrent-measurements of a northwest direction (Figure 4 - 19, Figure 4 - 28 and Figure 4 - 33). In eastern outcrops (Gangdalen Sør and Tverrdalen) measurements are based on wave ripples. Current ripples are few in these areas, probably due to a distal position of the sediments (Figure 5 - 1). Measurements in these eastern areas show that the paleo-shoreline was oriented northwest-southeast (Figure 4 - 47). This indicates that sediments in eastern outcrops receive sediments from a northeasterly source relative to northwest in western sections. It should be noted that paleocurrent measurements are few, and may not give statistically valid results. These observations are consistent with work done by Hanevik (2011, master thesis UiB). His work is based on a larger dataset collect from 18 logged sections in the same studied area.

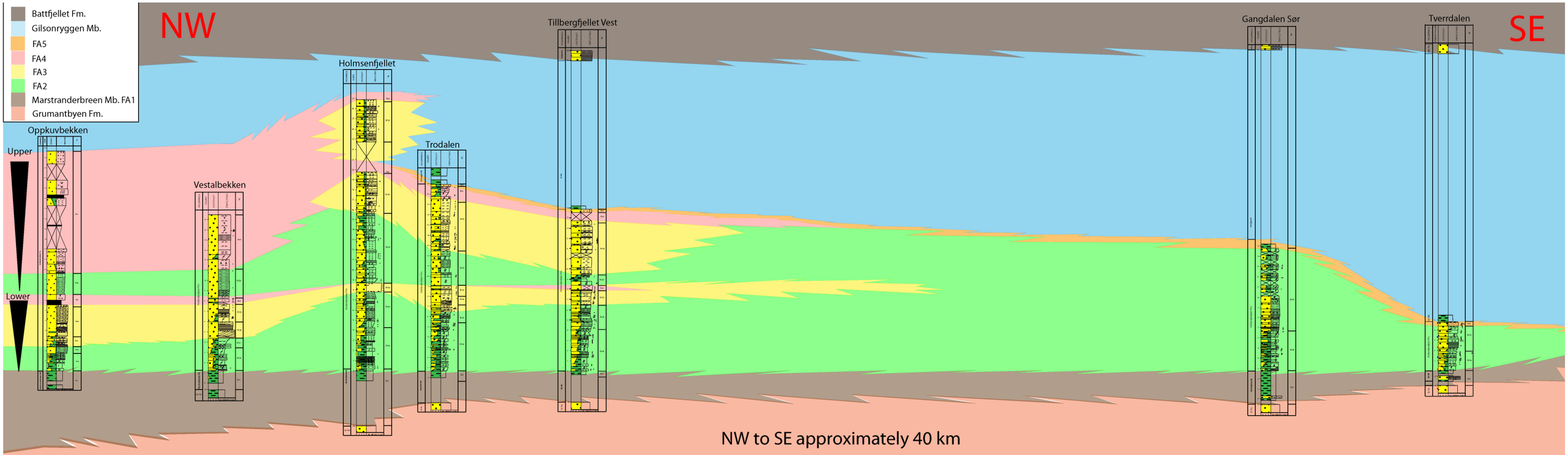

Figure 5 - 1: Log correlation and facies associations. Transect approximately W to E. Exaggerated vertical scale compared to horizontal.

5.2 Petrography

The mineral composition of sediments is generally a result of parent rock mineralogy, climate, transporting agents (type and transporting time) and diagenesis. Weathering processes are generally divided into two main groups; mechanical and chemical. The most active of these processes depends on several factors, such as climate, precipitation and relief. Mechanical weathering is the process by which rocks are disintegrated into smaller fragments without significant change in their chemical or mineralogical composition. Chemical weathering occurs in three overall processes; weathering of source rocks, transportation in fluvial systems and sediment recycling (Nesbitt et al. 1997).

From thin section analysis matrix content, clay sized mineral content varies between 15 % and 50 % (point counting of thin sections chapter 4.2 and Appendix 4). This is probably a mixture of illite and chlorite, which are identified in XRD-analysis, and silt/clay sized quartz and feldspar minerals. By thin section analysis it is apparent that feldspar minerals are significantly more abundant than rock fragments. Using the classification scheme proposed by Pettijohn (1954) samples from Grumantbyen, Hollendardalen and Battfjellet formations are classified as feldspathic graywacke. The matrix content (15 % - 50 %, as described above) in samples from Grumantbyen, Hollendardalen and Battfjellet formations together with sub-rounded and angular grain shape and moderate to poor sorting all point to immature sediments (Folk 1974).

Rock-Eval pyrolysis and TOC/TC were conducted on samples from Grumantbyen, Hollendardalen and Battfjellet formations. TOC values are normally under 0,5 % (Appendix 1). S1 (thermally distilled free hydrocarbons) measurements are below 1, while S2 (mg HC/g rock) measurements are generally below 1 (Table 4 - 3). These values are consistent for poor source rocks (Peters 1986). Plotting hydrogen index against oxygen index in a modified Van Krevelen diagram, all samples gather in the kerogen three area (Figure 4 - 50). Samples that plot in the kerogen three area are derived from higher land plants which indicate a continent close position for the analyzed samples. This is in accordance with the interpreted depositional environment discussed in chapter 5.1. Estimated T_{max} values range between 437 ˚C and 449 ˚C, with normal values are around 441 ˚C. The production index (PI) calculations are normally around 0,15 (Table 4 - 3). Using measurements based empirical data obtained by Peters and Cassa (1994) these T_{max} values are equivalent to Ro values between 0,6-0,65.

These Ro values are similar with vitrinite studies conducted by Throndsen (1982). T_{max} and PI values indicate analyzed samples have reached the "top oil window".

The characteristic shape of diagenetic kaolinite has been observed in SEM analysis (Figure 4 - 44-C) (Lanson 2002). XRD results show that kaolinite is present in sandstones of Grumantbyen, Hollendardalen and Battfjellet formations, but only in minor amounts (normally less than 0,5 XRD%) (Appendix 3). Feldspar minerals dissolve and kaolinite precipitates from pore fluids at temperatures between 20˚C - 100˚C. This process demands removal of Na^+ and K^+ by meteoric water (Lanson 2002). The formation is further restricted to tropical and subtropical climates with abundant rainfall and acidic pore water (Potter et al. 1980). Feldspar is abundant in all samples, so low kaolinite amounts cannot be explained by lack of feldspar minerals. It can be explained by lack of meteoric flushing due to low porosity and permeability, or climatic conditions not favoring kaolinite precipitation. Pore space is observed in thin section analysis, but it is scarce and pores are not interconnected. Porosity and permeability before burial were probably better than what is observed in thin sections. Pore space might have been lost due to compaction after deposition. Signs of mechanical compaction are clear by concavo-convex and long contacts of sand grains (Houseknecht 1987) (Figure 4 - 17-A and Figure 4 - 23-B) and bending of mica flakes between sand grains (Figure 4 - 15-A and Figure 4 - 17-A). Chemical weathering of minerals has occurred, observed by partial alteration of feldspars (Figure 4 - 40-B). This indicates that some pore fluids have been present. Hollendardalen Fm. shows continental deposits in the FA4 facies association (Table 4 - 2), therefore meteoric water should have been present. Sluijs et al. (2006) proposes an increased temperature in the Paleocene-Eocene in the Arctic Oceans ending with the Paleocene Eocene Thermal Maximum (PETM) at roughly 55 Ma. The PETM was a short period of about 200,000 years of rapid warming and increased precipitation (Röhl et al. 2000, Sluijs et al. 2008). After the PETM the climate returned to cooler and dryer climate (Sluijs et al. 2006). Riber (2009) pinpointed the PETM position within the shales of Gilsonryggen Mb. by an increase of kaolinite amounts. A stratigraphically upward increase and thereafter a decrease in kaolinite amounts was observed (Dypvik et al. 2011). Therefore it is likely that the low kaolinite amounts observed in Grumantbyen, Hollendardalen and Battfjellet formations are a result of a climate too cold and too dry to favor kaolinite formation.

From XRD analysis, illite is the most abundant of the clay minerals. Illite has also been observed by thin section and SEM studies (Figure 4 - 17-A, B, Figure 4 - 44-A), though it is hard to deduce the origin of the illite minerals. In sandstones diagenetic illite mainly forms by illitization of kaolinite (Lanson 2002). The reaction requires presence of K-feldspar, which is abundant in analyzed sandstones samples (Appendix 3). Throndsen (1982) used vitrinite reflectance to estimate burial depths in the Central Basin, inferring a burial depth of 1700 m for Grumantbyen Fm. This is not deep enough to form authigenic illite, as the reaction occurs between 3500 and 4000 meters with temperatures of 130 – 140 ˚C (Bjørlykke 1998, Lanson 2002). Based on burial and temperature requirements for diagenetic illite formation, the observed illite minerals probably have detrital origin.

Chlorite is observed in thin section analysis and SEM studies (Figure 4 - 17-A, Figure 4 - 44-A, B). XRD analysis confirms the presence of chlorite in values of 1 XRD% to 21 XRD% (Appendix 3). In thin section and SEM analysis chlorite appears to have a detrital origin. Diagenetic chlorite might form as coating on quartz or have rosette mineral growth (Grigsby 2001). These forms have not been observed by SEM studies. The high abundance of detrital illite and chlorite relative to diagenetic kaolinite indicate that mechanical weathering in the hinterland is the main source for clay minerals. The reason for this can either be cold and dry climate that do not favor chemical weathering, or rapid upheaval and erosion of the hinterland. The amount of time (residence time) material is exposed to environments where chemical weathering occurs is important for the degree of chemical weathering. During rapid erosion and high sedimentation rate the residence time of sediments is short which might be a reason for the low amount of diagenetic minerals observed.

In Grumantbyen Fm. glauconite is observed in thin section analysis with amounts up to 1,5 % (Thin section description in chapter 4.2.6) (Figure 4 - 40-A), while in Hollendardalen and Battfjellet formations amounts are normally 0 – 1 %. Occurrence of glauconite is confirmed by SEM studies (Figure 4 - 44-A). Glauconite forms in specific environments of agitated and shallow marine settings with oxidizing conditions (McRae 1972). These waters are also characterized by slow sedimentation rates (Chafetz and Reid 2000). In modern oceans glauconite has been reported to form at water depths greater than 50 meters (Chafetz and Reid 2000). Based on the relatively high abundance of Glauconite a shallow water depositional environment is likely for Grumantbyen Fm., in accordance with earlier studies of Grumantbyen Fm. (Müller and Spielhagen 1990).

Quartz cementation forms by dissolution of amorphous silica at temperatures between 60˚C and 80˚C and by pressure dissolution of quartz at temperatures between 100˚C and 150˚C. The reaction demands diffusive transport of silica (Bjørkum 1996). Quartz cementation has been observed by SEM analysis, where it develops as quartz overgrowth (Figure 4 - 23, Figure 4 - 44-D). Quartz cementation fills pore space and reduces porosity and permeability in the sandstone. Amount of quartz overgrowth and cementation is low which might be due to insufficient burial depth or too poor porosity and permeability, which halt diffusive transport and subsequent precipitation. As mentioned above Throndsen (1982) estimated the burial depth of Grumantbyen Fm. to be 1700 meters, which might not be deep enough to reach conditions favoring quartz dissolution. Bjørlykke and Egeberg (1993) state that sandstones in the North Sea buried at less than 2,5 – 3,0 km have very little quartz cement.

Carbonate minerals have not been observed by XRD analysis, and few calcite grains have been identified in thin section and SEM analysis. The observed calcite grains are rounded and seem to have a detrital origin. Calcite precipitates from dissolution of aragonite and low Mg-calcite at temperatures from 20ºC - 50ºC and 60ºC-70ºC respectively (Bjørlykke 1998). Conditions favoring calcite cementation have probably been obtained in the studied area, as mentioned a burial depth of Grumantbyen Fm has been estimated to be 1700 m. The lack of carbonate minerals can be explained by a source rock deficient in carbonate.

Only minor amounts of pyrite have been observed in thin sections in the studied area (Figure 4 - 44-A). XRD analysis does not show presence of pyrite in the studied samples. Pyrite develops under anoxic conditions and shallow burial where detrital iron reacts with H_2S producing pyrite (Berner 1984). H_2S is produced by bacteria that use organic matter as reducing agent and energy source (Berner 1984). Opaque minerals are observed in thin section analysis, most of which is organic material (e.g. Figure 4 - 15-A). Given abundance of organic material, the lack of pyrite can be explained by oxygenated bottom conditions.

Provenance

By comparing proximal parts (west) and distal parts (east) in Hollendardalen Fm. there are observed differences in feldspar mineralogy. Samples that have been compared have the same grain size. Assuming that a parent rock in the west is the only sediment source, the total feldspar/total clay ratio would be expected to decrease from proximal to distal areas (west to east) (Figure 5 - 1). This is because feldspar weathering increases with greater transportation

distance and clay sized minerals are more likely to be transported to distal parts of the basin. But, there is observed an increase in the total feldspar/total clay ratio from proximal to distal areas (Figure 5 - 2). Change in diagenetic conditions in proximal and distal areas could explain the observed differences. However, thin section studies and SEM analysis show feldspar weathering to clay minerals in all sections (Figure 4 - 44-B), however the extent of this is difficult to quantify. By comparing the K-feldspar/plagioclase ratio it is observed that it increases from 0,08 to 0,51 from western to eastern areas (very fine grain size) (Figure 5 - 3). Difference in K-feldspar and plagioclase weathering rates are too low to explain the observed K-feldspar/plagioclase ratio (Nesbitt et al. 1996). Thus, the increased K-feldspar/plagioclase ratio indicates a more K-feldspar-rich source rock for the distal, relative to the proximal sediments. Paleocurrent measurements indicate transportation of material from northwest in western and central parts of the basin. However, measurements based on wave ripples in eastern sections (Gangdalen Sør and Tverrdalen) (Figure 4 - 47) show that the paleo-shoreline had a northwest-southeast orientation. It is likely that the eastern logged sections areas received sediments from northeast which were enriched in K-feldspar relative to plagioclase.

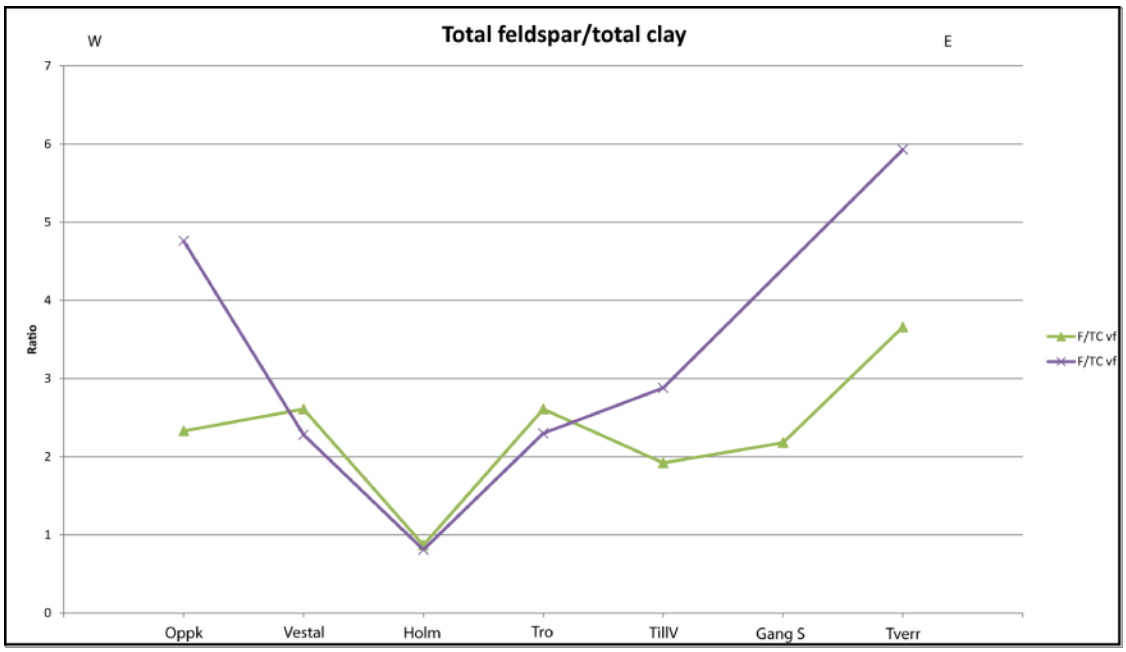

Figure 5 - 2: Plot of total feldspar/total clay from XRD samples, west on left side.

There are several mineralogical differences between Grumantbyen, Hollendardalen and Battfjellet formations. The most obvious from XRD studies is the difference in quartz/feldspar ratio. Grumantbyen Fm. is associated with a ratio below 1, while

Hollendardalen and Battfjellet formations have a ratio that normally ranges between 2 and 3 (Appendix 5).

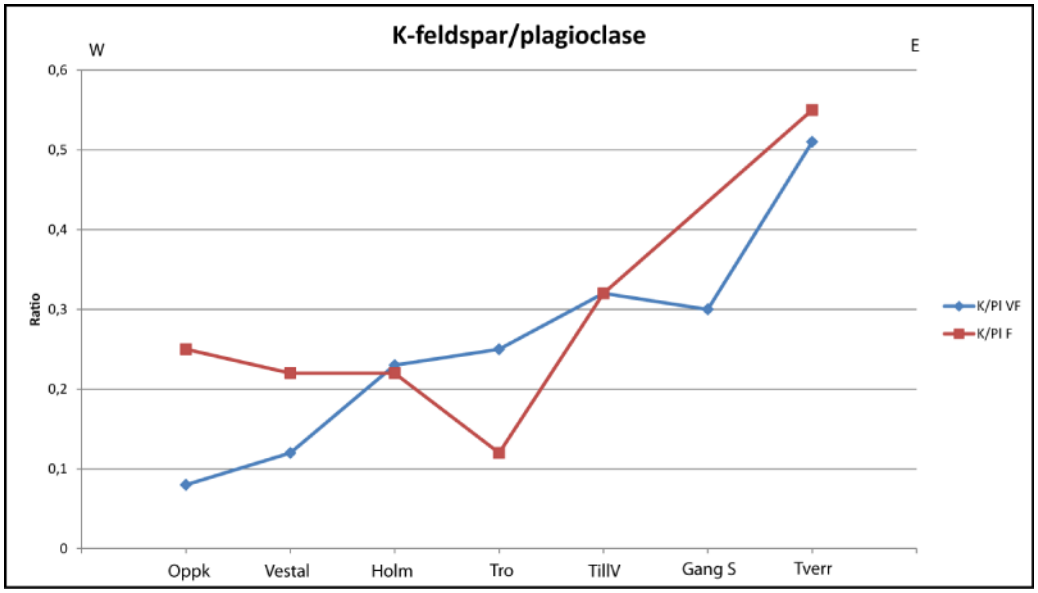

Figure 5 - 3: Plot of K-feldspar/plagioclase from XRD-results. Increasing ratio towards east.

Heavy mineral assemblage in the three above mentioned formations are not similar. The assemblages can give information of type of parent rock and changes in provenance (Morton and Hallsworth 1994). Parent rocks of the studied sediments are probably a mix of several lithologies, but some main lithologies might be singled out. These are discussed below. A point to note is that in almost all samples studied, regardless of formation, chert is observed in thin section analysis. Chert clasts observed might be from the Kapp Starostin Formation and related to "The Permian Chert Event" (Szaniawski and Malkowski 1979, Worsley 2008).

Grumantbyen Fm. is characterized by higher garnet amounts (28 – 42 %) than observed in the other formations (Table 4 - 4). It also contains minor traces of calcic amphibole, clinopyroxene and epidote which are not present in the other studied formations (Table 4 - 4). These heavy minerals are common for metamorphic rocks (Morton 1991). A parent rock of metamorphic origin is therefore likely for Grumantbyen Fm. The heavy mineral assemblage of Hollendardalen Fm. contains a variety of heavy minerals, which no specific minerals dominating (Table 4 - 4). This variety in heavy mineral composition is characteristic for the studied Hollendardalen Fm. samples. Putting constraints on the source rock of Hollendardalen Fm. is not easy based on these data. A metamorphic parent rock is possible, but a mix of source rock lithologies is also possible, indicated by the presence of chert clasts. Battfjellet

Fm. contains a significant amount of chloritoid (48,5 – 82,5 %), which make up the bulk heavy mineral assemblage in this formation (Table 4 - 4). Chloritoid is a mineral associated with metapelites (Ghent et al. 1987). Data from Vilberg (2011, master thesis NTNU) support a parent rock of metamorphic origin based on thin section analyses conducted on Battfjellet Fm. Atkinson (1956) identified chloritoid in Barents, Scotia and Kerr groups of the Hecla Hoek Fm. Therefore Hecla Hoek Fm. acts as a source rock candidate for Battfjellet Fm. Lack of monazite, a common mineral in granites and granitic pegmatites, exclude granites as a parent rock (Morton and Hallsworth 1994). Further studies comparing the chloritoid minerals and heavy mineral suits of Hecla Hoek Fm. and Battfjellet Fm. are needed to give a definite conclusion.

By comparing ATi, GZi and RuZi indices it is observed that Grumantbyen, Hollendardalen and Battfjellet formations do not group together (Figure 4 - 51). Studied samples from Grumantbyen Fm. group closer to the ATi-GZi line, and closer to the GZi corner than the other studied formations (Figure 4 - 51). Battfjellet Fm. samples group close to the ATi-RuZi line and with somewhat higher ATi amounts (Figure 4 - 51), while samples from Hollendardalen group between Grumantbyen Fm. and Battfjellet Fm. samples. The observed differences in heavy mineral assemblage and heavy mineral indices between the formations can be explained either by unroofing of the parent rock or a change in regional provenance (Morton and Hallsworth 1994). A likely theory is a change in regional provenance from the underlying Grumantbyen Fm. and Hollendardalen Fm. This is supported by earlier studies indicating a change from an eastern infill direction for Grumantbyen Fm. to a more westerly infill direction for the overlying formations (Kellogg 1975, Steel et al. 1985, Helland-Hansen 1990). Field measurements give indications for a northwest infill direction for western localities and northeast for eastern localities, as discussed above. Change in quartz/feldspar ratio and the different heavy mineral assemblages in Grumantbyen and Hollendardalen formations also indicate a change of source rock mineralogy from Grumantbyen Fm. to Hollendardalen Fm. Heavy mineral assemblages of these two formations indicate a change in parent rock mineralogy. However, since both have a westerly source, unroofing of the parent rock may explain the observed heavy mineral differences. The number of analyzed samples per formation is low, Grumantbyen Fm. is represented by two samples, while Battfjellet Fm. is represented by four samples. This may be too low to give statistically valid results. Hollendardalen Fm. is well covered by 17 samples (Table 4 - 4). Further studies are needed to put better constraints on the provenance of these formations.

6 Conclusion

The formation of the Central Basin can be divided into two phases. The first phase (early-mid Paleocene) of an extensional regime sediments were brought in from the east. In the second phase (late Paleocene – early Eocene) sediments were brought in from the west, from the rising West Spitsbergen Orogen, this occurred in a wrench regime related to a dextral slip along the De Geer line (Steel et al. 1985). However Bruhn and Steel (2003) argue that the central basin developed as a foreland basin analogue where sediments were brought in from the east by a peripheral bulge.

Hollendardalen Fm. shows an upwards shallowing trend and is divided into two upwards coarsening parasequences, which can be recognized throughout the studied area (Fig. 6-1-B). The thickest sedimentary accumulations are found in the west, and the formation is progressively thinning towards the east. Sedimentary structures and lithological stacking indicate a depositional environment of wave and tide dominated delta. The lower upwards coarsening parasequence is coarsening up from a FA1 facies association of prodelta sediments into delta front sediments of the FA2 facies association (Figure 6 - 1-B). In the western and central parts of the studied section the lower upwards coarsening parasequence ends with distributary mouth bar sediments of the FA3 facies association underlain by delta plain sediments of the FA4 facies association. In the eastern parts of the basin the FA2 facies association is continuing for the remaining of the logged section, only underlying by a thin transgressive lag deposit of the FA5 facies association, which marks the upper boundary towards the Gilsonryggen Mb. The upper upwards coarsening parasequence resemble the lower upwards coarsening parasequence by coarsening up from delta front sediment (FA2) into distributary mouth bar sediments (FA3) and ends with delta plain sediments (FA4) (Figure 6 - 1-B).

The K-feldspar/plagioclase ratio increase from 0,08 in the west to 0,51 in the east. This indicates that there is s source rock enriched in K-feldspar relative to plagioclase that is feeding the eastern parts of the basin. K-feldspar and plagioclase have different weathering rates, but it is probably not high enough to explain the observed difference. The total feldspar/total clay ratio is also increasing towards distal parts of the basin (towards east) which support a change in source rock mineralogy. It is expected to decrease towards distal parts of the basin due to increased feldspar weathering and that clay sized material are more

likely to be transported to more distal parts of the basin. Paleocurrent measurements indicate that there is change in infill direction from west to east in the basin, western areas show infill from northwest, while astern parts show an infill from northeast (Figure 6 - 1-A). This indicates that the source rock enriched in K-feldspar relative to plagioclase is probably located in the north.

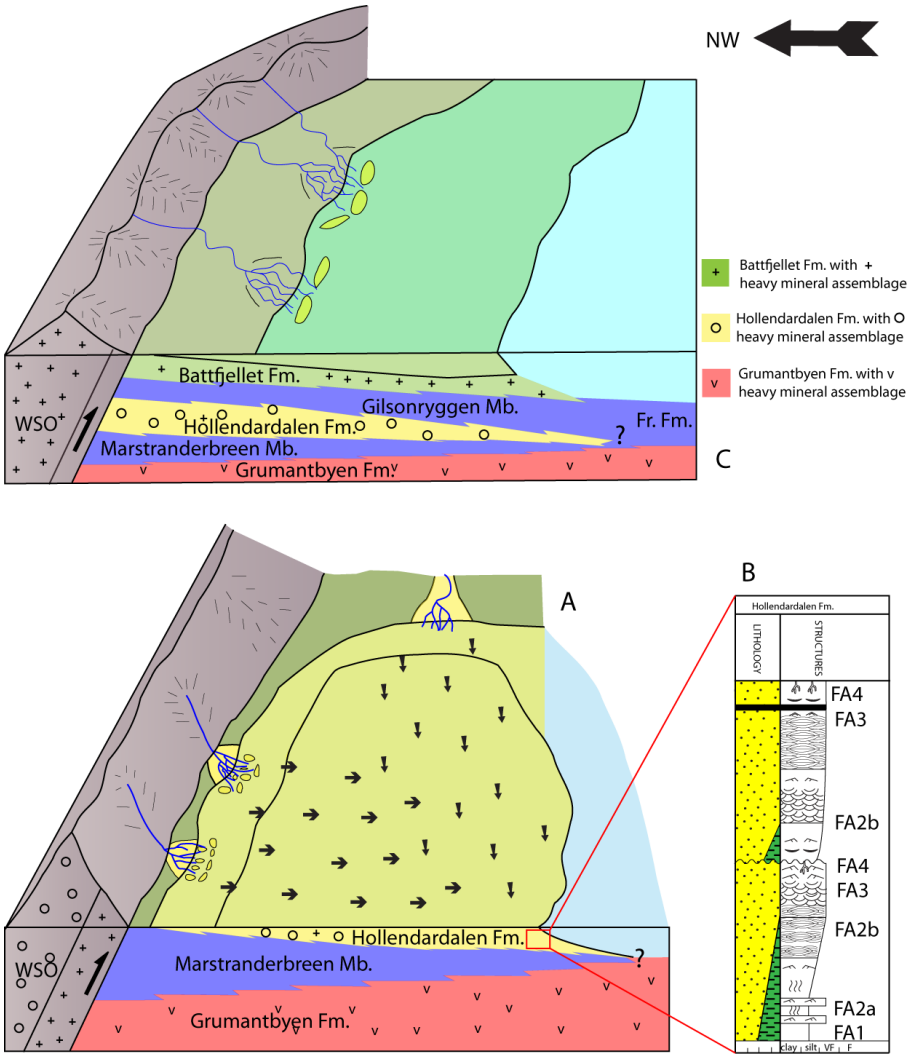

Figure 6 - 1: Illustrative drawing of the Central Basin. A) Sediment infill of Hollendardalen Fm., from northwest and northeast. B) General log of Hollendardalen Fm. C) Heavy mineral assemblage of Grumantbyen, Hollendardalen and Battfjellet formations.

Heavy mineral assemblages in the three studied formations (Grumantbyen, Hollendardalen and Battfjellet formations) are not similar (Figure 6 - 1-C). This indicates that there are different source rock lithologies that are feeding the three formations. There is a change in regional provenance from Grumantbyen Fm. to Hollendardalen Fm. which is accompanied by a change in source rock lithology. This is not only based on heavy mineral assemblages, but

also quartz/feldspar ratio that is normally below 1 in Grumantbyen Fm. and above 2 in Hollendardalen Fm. Hollendardalen Fm. and Battfjellet Fm. are probably sourced from the West Spitsbergen Orogen (Figure 6 - 1-C).

References

Allen, J.R.L. 1966. On bed forms and paleocurrents. *Sedimentology* 6, 153-190.

Atkinson, D. 1956. The occurrence of chloritoid in the Hecla Hoek formation of Prince Charles Foreland, Spitsbergen. *Geological Magazine* 93, 63-71.

Berner, R.A. 1984. Sedimentary pyrite formation: an update. *Geochimica et Cosmochimica Acta* 48, 605-615.

Bhattacharya, J.P. and Giosan, L. 2003. Wave influenced deltas: geomorphological implications for facies reconstruction. *Sedimentology* 50, 187-210.

Bjørkum, P.A. 1996. How important is pressure in causing dissolution of quartz in sandstones? *Journal of Sedimentary Research* 66, 147.

Bjørlykke, K. 1998. Clay mineral diagenesis in sedimentary basins-a key to the prediction of rock properties. Examples from the North Sea Basin. *Clay Minerals* 33, 15-34.

Bjørlykke, K. and Egeberg, P. 1993. Quartz cementation in sedimentary basins. *AAPG Bulletin* 77, 1538-1538.

Bouma, A.H. 2004. Key controls on the characteristics of turbidite systems. *Geological Society, London, Special Publications* 222, 9.

Bragg, W.H. and Bragg, W.L. 1913. The reflection of X-rays by crystals. *Proceedings of the Royal Society of London Series a-Containing Papers of a Mathematical and Physical Character* 88, 428-438.

Bruhn, R. and Steel, R. 2003. High-resolution sequence stratigraphy of a clastic foredeep succession (Paleocene, Spitsbergen): An example of peripheral-bulge-controlled depositional architecture. *Journal of Sedimentary Research* 73, 745-755.

Cattaneo, A. and Steel, R.J. 2003. Transgressive deposits: a review of their variability. *Earth-Science Reviews* 62, 187-228.

Chafetz, H. and Reid, A. 2000. Syndepositional shallow-water precipitation of glauconitic minerals. *Sedimentary Geology* 136, 29-42.

Dalland, A. 1977. Erratic clasts in the Lower Tertiary deposits of Svalbard–evidence of transport by winter ice. *Norsk Polarinstitutt Årbok* 1976, 151–166.

Dalland, A. 1979. Structural geology and petroleum potential of Nordenskiold Land, Svalbard, 30-20.

Dallmann, W.K., Midbøe, P.S., Nøttvedt, A. and Steel, R.J. 1999. Tertiary lithostratigraphy. *In* Dallmann, W.K. (ed). *Lithostragraphic Lexicon of Svalbard*: Norsk Polarinstitutt, 215-263.

Dumas, S. and Arnott, R. 2006. Origin of hummocky and swaley cross-stratification—The controlling influence of unidirectional current strength and aggradation rate. *Geology* 34, 1073.

Dypvik, H., Riber, L., Burca, F., Ruther, D., Jargvoll, D., Nagy, J. and Jochmann, M. 2011. The Paleocene-Eocene thermal maximum (PETM) in Svalbard-clay mineral and geochemical signals. *Palaeogeography, Palaeoclimatology, Palaeoecology*.

Elliott, T. 1974. Interdistributary bay sequences and their genesis. *Sedimentology* 21, 611-622.

Fleuty, M. 1975. Slickensides and slickenlines. *Geological Magazine* 112, 319-322.

Folk, R. 1974. Petrology of Sedimentary Rocks: Austin, Texas, Hemphill Pub. *Co, 182p*.

Folk, R.L. 1954. The distinction between grain size and mineral composition in sedimentary-rock nomenclature. *The Journal of Geology* 62, 344-359.

Frey, R.W. and Pemberton, S.G. 1985. Biogenic structures in outcrops and cores; I, Approaches to ichnology. *Bulletin of Canadian Petroleum Geology* 33, 72.

Ghent, E.D., Stout, M.Z., Black, P. and Brothers, R. 1987. Chloritoid bearing rocks associated with blueschists and eclogites, northern New Caledonia. *Journal of Metamorphic Geology* 5, 239-254.

Greenwood, B. and Sherman, D.J. 1986. Hummocky cross stratification in the surf zone: flow parameters and bedding genesis. *Sedimentology* 33, 33-45.

Grigsby, J.D. 2001. Origin and growth mechanism of authigenic chlorite in sandstones of the lower Vicksburg Formation, south Texas. *Journal of Sedimentary Research* 71, 27.

Hanevik, E.P. 2011. *Sedimentology and sandbody geometry of the Hollendardalen Formation (in press)*. Master thesis, University of Bergen.

Harland, W. 1969. Contribution of Spitsbergen to understanding of tectonic evolution of North Atlantic region. *North Atlantic Geology and Continental Drift: American Association of Petroleum Geologists, Memoir* 12, 817-851.

Harris, P.T., Hughes, M.G., Baker, E.K., Dalrymple, R.W. and Keene, J.B. 2004. Sediment transport in distributary channels and its export to the pro-deltaic environment in a tidally dominated delta: Fly River, Papua New Guinea. *Continental shelf research* 24, 2431-2454.

Helland-Hansen, W. 1990. Sedimentation in Paleogene foreland basin, Spitsbergen. *AAPG Bull* 74, 260–272.

Helland-Hansen, W. 2010. Facies and stacking patterns of shelf deltas within the Palaeogene Battfjellet Formation, Nordenskiöld Land, Svalbard: implications for subsurface reservoir prediction. *Sedimentology* 57, 190-208.

Houseknecht, D.W. 1987. Assessing the relative importance of compaction processes and cementation to reduction of porosity in sandstones. *AAPG Bulletin* 71, 633-642.

Jakobsson, M., Macnab, R., Mayer, L., Anderson, R., Edwards, M., Hatzky, J., Schenke, H. and Johnson, P. 2010. *An improved bathymetric portrayal of the Arctic Ocean: Implications for ocean modeling and geological, geophysical and oceanographic analyses, Geophysical Research Letters* 2008 [Accsessed: 19.04.10 2010].

Kellogg, H.E. 1975. Tertiary stratigraphy and tectonism in svalbard and continental-drift. *Aapg Bulletin-American Association of Petroleum Geologists* 59, 465-485.

Kidwell, S.M. 1989. Stratigraphic Condensation of Marine Transgressive Records: Origin of Major Shell Deposits in the Miocene of Maryland. *The Journal of Geology* 97, 1-24.

Komar, P.D. 1974. Oscillatory ripple marks and the evaluation of ancient wave conditions and environments. *Journal of Sedimentary Research* 44, 169.

Kreisa, R. and Moila, R. 1986. Sigmoidal tidal bundles and other tide-generated sedimentary structures of the Curtis Formation, Utah. *Bulletin of the geological Society of America* 97, 381.

Lanson, B. 2002. Authigenic kaolin and illitic minerals during burial diagenesis of sandstones: a review. *Clay Minerals* 37, 22.

Livsic, J. 1992. Tectonic history of Tertiary sedimentation of Svalbard. *Norsk Geologisk Tidsskrift* 72, 121-127.

Lowe, D.R. 1976. Subaqueous liquefied and fluidized sediment flows and their deposits. *Sedimentology* 23, 285-308.

Lowell, J. 1972. Spitsbergen Tertiary orogenic belt and the Spitsbergen fracture zone. *Geological Society of America Bulletin* 83, 3091.

McRae, S. 1972. Glauconite. *Earth-Science Reviews* 8, 397-440.

Meloche, D. 2010. Challenge The Paradigm Part 2: Submarine Gravel Deposits in the WCSB-Wave Ravinement Lags or Current Traction Carpets?

Moore, D.M. and Reynolds, R.C. 1989. *X-ray diffraction and the identification and analysis of clay minerals*, Oxford: Oxford University Press. XVI, 332 s. pp.

Morton, A. and Hurst, A. 1995. Correlation of sandstones using heavy minerals; an example from the Statfjord Formation of the Snorre Field, northern North Sea. *Geological Society Special Publications* 89, 3-22.

Morton, A.C. 1991. Geochemical studies of detrital heavy minerals and their application to provenance research. *Geological Society, London, Special Publications* 57, 31.

Morton, A.C. and Hallsworth, C. 1994. Identifying provenance-specific features of detrital heavy mineral assemblages in sandstones. *Sedimentary Geology* 90, 241-256.

Morton, A.C. and Hallsworth, C.R. 1999. Processes controlling the composition of heavy mineral assemblages in sandstones. *Sedimentary Geology* 124, 3-29.

Müller, D. and Spielhagen, R. 1990. Evolution of the Central Tertiary Basin of Spitsbergen: towards a synthesis of sediment and plate tectonic history. *Palaeogeography, Palaeoclimatology, Palaeoecology* 80, 153-172.

Nagy, J. 2005. Delta-influenced foraminiferal facies and sequence stratigraphy of Paleocene deposits in Spitsbergen. *Palaeogeography, Palaeoclimatology, Palaeoecology* 222, 161-179.

Naoroz, M. 2010. Intern prosedyre for TOC-analyse, Inst. for Geofag. Oslo.

Nathorst, A. 1910. Beitrage zur Geologie der Baren-Insel. *Spitzbergens und des*.

Nesbitt, H., Young, G., McLennan, S. and Keays, R. 1996. Effects of chemical weathering and sorting on the petrogenesis of siliciclastic sediments, with implications for provenance studies. *The Journal of Geology* 104, 525-542.

Nesbitt, H.W., Fedo, C.M. and Young, G.M. 1997. Quartz and Feldspar Stability, Steady and Non-steady-State Weathering, and Petrogenesis of Siliciclastic Sands and Muds. *The Journal of Geology* 105, 173-192.

Olariu, C. and Bhattacharya, J.P. 2006. Terminal distributary channels and delta front architecture of river-dominated delta systems. *Journal of Sedimentary Research* 76, 212.

Peters, K.E. 1986. Guidelines for evaluating petroleum source rock using programmed pyrolysis. *AAPG Bull* 70, 318-329.

Peters, K.E. and Cassa, M.R. 1994. Applied source rock geochemistry. *Memoirs-American association ofpetroleum geologists*, 93-93.

Petit, J. 1987. Criteria for the sense of movement on fault surfaces in brittle rocks. *Journal of Structural Geology* 9, 597-608.

Petschick, R. 2004. MacDiff 4.2. 5. *Powder diffraction software Available from: http://servermac geologie uni-frank-furt de/Staff/Homepages/Petschick/RainerE html*.

Pettijohn, F. 1954. Classification of sandstones. *The Journal of Geology* 62, 360-365.

Potter, P.E., Maynard, J.B. and Pryor, W.A. 1980. *Sedimentology of shale: study guide and reference source*, New York: Springer. x,306 s., pl. pp.

Reading, H.G. 1996. *Sedimentary environments: processes, facies and stratigraphy*: Wiley-Blackwell.

Reineck, H.E. and Wunderlich, F. 1968. Classification and origin of flaser and lenticular bedding. *Sedimentology* 11, 99-104.

Riber, L. 2009. *Paleogene depositional conditions and climatic changes of the Frysjaodden Formation in central Spitsbergen (sedimentology and mineralogy)*, University of Oslo.

Röhl, U., Bralower, T., Norris, R. and Wefer, G. 2000. New chronology for the late Paleocene thermal maximum and its environmental implications. *Geology* 28, 927.

Schweitzer, H.J. 1980. Environment and climate in the early Tertiary of Spitsbergen. *Palaeogeography, Palaeoclimatology, Palaeoecology* 30, 297-311.

Shanmugam, G. 1997. The Bouma sequence and the turbidite mind set. *Earth-Science Reviews* 42, 201-229.

Sluijs, A., Röhl, U., Schouten, S., Brumsack, H.J., Sangiorgi, F., Damsté, J.S.S. and Brinkhuis, H. 2008. Arctic late Paleocene–early Eocene paleoenvironments with special emphasis on the Paleocene-Eocene thermal maximum (Lomonosov Ridge, Integrated Ocean Drilling Program Expedition 302). *Paleoceanography* 23, PA1S11.

Sluijs, A., Schouten, S., Pagani, M., Woltering, M., Brinkhuis, H., DamstÃ, J.S.S., Dickens, G.R., Huber, M., Reichart, G.J. and Stein, R. 2006. Subtropical Arctic Ocean temperatures during the Palaeocene/Eocene thermal maximum. *Nature* 441, 610-613.

Steel, R., Dalland, A., Kalgraff, K. and Larsen, V. 1981. The Central Tertiary Basin of Spitsbergen: sedimentary development of a sheared margin basin. *Geology of the North Atlantic Borderland: Canadian Society of Petroleum Geologists, Memoir* 7, 647-664.

Steel, R., Gjelberg, J., Helland-Hansen, W., Kleinspehn, K., Nøttvedt, A. and Rye-Larsen, M. 1985. The Tertiary strike-slip basins and orogenic belt of Spitsbergen. 339-359.

Sykes, R. and Snowdon, L.R. 2002. Guidelines for assessing the petroleum potential of coaly source rocks using Rock-Eval pyrolysis. *Organic Geochemistry* 33, 1441-1455.

Szaniawski, H. and Malkowski, K. 1979. Conodonts from the Kapp Starostin Formation (Permian) of Spitsbergen. *Acta Palaeontologica Polonica* 24, 231-264.

Talwani, M. and Eldholm, O. 1977. Evolution of norwegian greenland sea. *Geological Society of America Bulletin* 88, 969-999.

Throndsen, T. 1982. Vitrinite reflectance studies of coals and dispersed organic matter in tertiary deposits in the advent-dalen area, svalbard. *Polar Research* 1982, 77-91.

Vilberg, A. 2011. *Petrography and diagenesis in sedimentray facies within Paleogene formations, Nathorstland, Svalbard (in press).* Norges teknisk-naturvitenskapelige universitet, NTNU.

Visser, M. 1980. Neap-spring cycles reflected in Holocene subtidal large-scale bedform deposits: a preliminary note. *Geology* 8, 543.

Welton, J.E. 1984. *SEM petrology atlas*, Tulsa, Okla.: American Association of Petroleum Geologists. III, 237 s. pp.

Wentworth, C.K. 1922. A scale of grade and class terms for clastic sediments. *The Journal of Geology* 30, 377-392.

Worsley, D. 2008. The post-Caledonian development of Svalbard and the western Barents Sea. *Polar Research* 27, 298-317.

Wright, L. 1977. Sediment transport and deposition at river mouths: a synthesis. *Bulletin of the geological Society of America* 88, 857.

Wright, L., Coleman, J.M., Programs, U.S.O.o.N.R.G. and Institute, L.S.U.C.S. 1973. Variations in morphology of major river deltas as functions of ocean wave and river discharge regimes.

Yokokawa, M., Masuda, F. and Endo, N. 1995. Sand particle movement on migrating combined-flow ripples. *Journal of Sedimentary Research* 65, 40.

Appendix

Appendix 1

Appendix 1: Results of TOC/TC data. Hol. Fm. = Hollendardalen Formation, Gru. Fm. = Grumantbyen Formation, Batt. Fm. = Battfjellet Formation, Mar. Mb. = Marstranderbreen Member, Gil. Mb. = Gilsonryggen Member. TC = total carbon, TOC = total organic carbon,

Outcrop/Core	Sample	Formation	TC (%)	TOC (%)	Outcrop/Core	Sample	Formation	TC (%)	TOC (%)
Oppkuvbekken	88/09	Hol. Fm.	1,26	1,22		71/09	Hol. Fm.	2,39	2,32
	108/09	Hol. Fm.	0,92	0,89		70/09	Hol. Fm.	0,15	0,11
	100/09	Hol. Fm.	0,18	0,09		66/09	Hol. Fm.	0,39	0,36
	105/09	Hol. Fm.	0,14	0,11		74/09	Hol. Fm.	0,53	0,48
	107/09	Hol. Fm.	0,15	0,11		76/09	Hol. Fm.	0,11	0,09
Vestalbekken	138/09	Gru. Fm.	1,3	0,78		78/09	Hol. Fm.	0,09	0,09
	109/09	Hol. Fm.	1,18	1,1		81/09	Hol. Fm.	0,21	0,18
	113/09	Hol. Fm.	0,72	0,65		83/09	Hol. Fm.	0,41	0,4
	114/09	Hol. Fm.	0,98	0,91		84/09	Hol. Fm.	0,43	0,41
	124/09	Hol. Fm.	12,46	12,1		86/09	Hol. Fm.	0,13	0,13
	129/09	Hol. Fm.	0,19	0,11		87/09	Hol. Fm.	0,21	0,14
	04/10	Hol. Fm.	1,07	1,03		61/09	Gru. Fm.	0,55	0,53
Vesuv	163/09	Batt. Fm.	0,45	0,07	Trodalen	3/10	Hol. Fm.	0,95	0,77
	164/09	Batt. Fm.	0,37	0,11		4/10	Hol. Fm.	0,66	0,6
Holmsenfjellet	46/09	Hol. Fm.	1,86	1,67		6/10	Hol. Fm.	0,49	0,49
	47/09	Hol. Fm.	0,46	0,18		17/10	Hol. Fm.	1,84	1,81
	49/09	Hol. Fm.	0,32	0,28	Tilbergfjellet Vest	2/10	Hol. Fm.	1,08	1,07
	50/09	Hol. Fm.	0,92	0,87		4/10	Hol. Fm.	1,13	1,11
	52/09	Hol. Fm.	0,64	0,58		13/10	Hol. Fm.	0,37	0,29
	56/09	Hol. Fm.	0,14	0,1	Gangdalen Sør	3/10	Mar. Mb.	1,72	1,68
	59/09	Hol. Fm.	0,26	0,08		5/10	Hol. Fm.	0,97	0,94
	60/09	Hol. Fm.	1,3	1,28		7/10	Hol. Fm.	2,13	2,09
	62/09	Hol. Fm.	0,31	0,11		11/10	Hol. Fm.	1,83	1,78
	64/09	Hol. Fm.	0,85	0,8	Tverrdalen	11/10	Gil. Mb.	2,75	2,7

Appendix 2

Appendix 2: Results of heavy mineral results. Hol. Fm. = Hollendardalen Formation, Gru. Fm. = Grumantbyen Formation, Batt. Fm. = Battfjellet Formation. ATi = apatite:tourmaline index, GZi = garnet:zircon index, RZi = TiO2 minerals:zircon index, RuZi = rutile:zircon index, MZi = monazite:zircon index, CZi = chrome spinel:zircon index.

Oppkuvbekken	**Sample**	**Formation**	**ATi**	**GZi**	**RZi**	**RuZi**	**MZi**	**CZi**
	94/09	Hol. Fm.	75,0	32,2	18,4	13,0	12,0	2,4
	100/09	Hol. Fm.	68,0	55,0	32,2	23,7	7,9	0,9
	105/09	Hol. Fm.	86,5	32,4	30,3	17,9	4,2	4,2
	107/09	Hol. Fm.	79,5	4,8	55,4	47,4	1,0	13,0
Vestalbekken	138/09	Gru. Fm.	58,1	73,6	17,9	8,0	4,2	0,0
	113/09	Hol. Fm.	72,0	48,3	27,3	20,3	9,8	4,8
	129/09	Hol. Fm.	83,0	29,4	47,1	37,9	2,7	7,7
	131/09	Hol. Fm.	75,0	24,0	33,3	24,0	7,8	2,0
Vesuv	163/09	Batt. Fm.	84,0	2,4	24,5	19,7	1,0	1,5
	164/09	Batt. Fm.	88,0	2,9	23,7	21,9	0,0	0,0
Holmsenfjellet	56/09	Hol. Fm.	74,5	17,4	22,5	16,0	5,7	2,9
	69/09	Hol. Fm.	83,0	20,3	23,4	18,7	7,0	1,6
	78/09	Hol. Fm.	76,0	7,4	13,4	11,5	4,3	6,1
	87/09	Hol. Fm.	68,0	12,1	31,0	25,3	3,3	5,2
	61/09	Gru. Fm.	73,5	67,5	30,5	15,4	5,6	1,5
Tillbergfjellet Vest	5/10	Hol. Fm.	77,0	45,7	25,7	21,3	12,7	1,0
	9/10	Hol. Fm.	75,5	41,1	44,5	35,9	4,3	1,5
	17/10	Hol. Fm.	72,5	20,9	24,8	19,7	8,3	3,4
Tillbergfjellet Battfjellet	1/10	Batt. Fm.	84,0	4,8	35,5	33,8	2,0	5,7
Gangdalen Sør	16/10	Batt. Fm.	85,0	2,0	18,7	17,4	2,9	2,0
Tverrdalen	4/10	Hol. Fm.	75,0	45,4	30,6	21,9	6,5	7,4
	7/10	Hol. Fm.	77,0	42,7	38,8	30,8	3,2	10,9
	10A/10	Hol. Fm.	68,5	18,4	32,1	26,5	6,1	2,4

Appendix 3

Appendix 3: Results of XRD analysis. Hol. Fm. = Hollendardalen Formation, Gru. Fm. = Grumantbyen Formation, Batt. Fm. = Battfjellet Formation, Gil. Mb. = Gilsonryggen Member, Mar. Mb. = Marstrenderbreen Member.

Outcrop/Core	Sample	Formation	Quartz	K-feldspar	Plagioclase	Kaolinite	Chlorite	Illite + Mica
Oppkuvbekken	88/09	Hol. Fm.	59,9 %	5,6 %	23,9 %	0,6 %	2,4 %	7,6 %
	94/09	Hol. Fm.	75,1 %	4,9 %	15,1 %	0,4 %	1,1 %	3,4 %
	108/09	Hol. Fm.	59,8 %	6,1 %	19,9 %	0,9 %	5,3 %	8,1 %
	98/09	Hol. Fm.	77,5 %	2,3 %	14,1 %	1,0 %	2,0 %	3,0 %
	100/09	Hol. Fm.	78,9 %	4,2 %	13,9 %	0,2 %	0,5 %	2,4 %
	102/09	Hol. Fm.	76,7 %	2,2 %	17,0 %	0,4 %	0,7 %	3,1 %
	105/09	Hol. Fm.	59,0 %	0,0 %	27,0 %	0,0 %	4,3 %	9,7 %
	107/09	Hol. Fm.	70,8 %	3,8 %	19,7 %	0,2 %	1,1 %	4,4 %
Vestalbekken	109/09	Hol. Fm.	55,5 %	7,2 %	21,7 %	0,6 %	3,9 %	11,1 %
	112/09	Hol. Fm.	64,2 %	6,3 %	20,6 %	0,5 %	2,1 %	6,3 %
	113/09	Hol. Fm.	75,1 %	0,0 %	19,9 %	0,2 %	0,7 %	4,1 %
	114/09	Hol. Fm.	69,0 %	4,4 %	19,1 %	0,3 %	1,9 %	5,4 %
	116/09	Hol. Fm.	77,4 %	2,5 %	15,5 %	0,5 %	1,0 %	3,2 %
	124/09	Hol. Fm.	66,2 %	5,8 %	19,3 %	0,0 %	0,0 %	8,6 %
	125/09	Hol. Fm.	73,1 %	4,0 %	16,0 %	0,4 %	1,3 %	5,3 %
	126/09	Hol. Fm.	72,4 %	4,2 %	16,7 %	0,4 %	1,8 %	4,6 %
	129/09	Hol. Fm.	70,5 %	4,1 %	20,8 %	0,2 %	1,0 %	3,5 %
	130/09	Hol. Fm.	81,7 %	3,3 %	10,4 %	0,3 %	1,5 %	2,8 %
	4/10	Hol. Fm.	54,2 %	6,7 %	18,3 %	0,2 %	8,8 %	11,8 %
	6/10	Hol. Fm.	77,1 %	2,9 %	15,6 %	0,1 %	1,4 %	3,0 %
	7/10	Hol. Fm.	68,4 %	3,5 %	17,5 %	0,4 %	3,2 %	7,0 %
	138/09	Gru. Fm.	40,5 %	10,9 %	44,1 %	0,3 %	0,5 %	3,8 %
Vesuv	164/09	Batt. Fm.	52,6 %	2,5 %	22,0 %	0,1 %	5,0 %	17,7 %
	163/09	Batt. Fm.	63,5 %	2,5 %	23,4 %	0,1 %	2,4 %	8,1 %
Holmsenfjellet	46/09	Hol. Fm.	54,9 %	6,3 %	22,2 %	0,3 %	3,6 %	12,7 %
	47/09	Hol. Fm.	49,2 %	4,5 %	15,9 %	0,6 %	8,5 %	21,3 %
	49/09	Hol. Fm.	63,4 %	4,5 %	19,0 %	0,5 %	3,8 %	9,0 %
	50/09	Hol. Fm.	55,9 %	7,6 %	19,7 %	0,4 %	5,0 %	11,5 %
	52/09	Hol. Fm.	39,6 %	16,1 %	41,0 %	0,9 %	2,2 %	0,3 %
	56/09	Hol. Fm.	46,5 %	4,4 %	19,4 %	1,3 %	9,9 %	18,6 %
	59/09	Hol. Fm.	46,9 %	4,8 %	20,3 %	1,7 %	8,4 %	18,0 %
	60/09	Hol. Fm.	47,5 %	3,8 %	19,9 %	0,8 %	6,8 %	21,2 %
	62/09	Hol. Fm.	70,0 %	1,8 %	17,6 %	0,9 %	2,8 %	7,0 %
	64/09	Hol. Fm.	54,7 %	5,0 %	23,3 %	0,3 %	5,3 %	11,4 %
	71/09	Hol. Fm.	55,5 %	6,7 %	19,2 %	0,2 %	4,8 %	13,6 %
	70/09	Hol. Fm.	57,3 %	3,6 %	19,0 %	0,7 %	5,4 %	14,1 %

	66/09	Hol. Fm.	43,2 %	5,1 %	22,1 %	0,0 %	8,8 %	20,9 %
	74/09	Hol. Fm.	58,9 %	5,0 %	18,3 %	0,1 %	5,3 %	12,4 %
	76/09	Hol. Fm.	44,8 %	5,2 %	21,6 %	8,4 %	0,9 %	19,2 %
	78/09	Hol. Fm.	55,8 %	3,1 %	18,2 %	0,6 %	7,0 %	15,3 %
	81/09	Hol. Fm.	44,7%	4,8 %	16,3 %	0,7 %	12,1 %	21,5 %
	83/09	Hol. Fm.	50,2 %	3,8 %	19,9 %	0,2 %	6,9 %	19,0 %
	84/09	Hol. Fm.	48,4 %	4,3 %	15,7 %	0,8 %	10,2 %	20,7 %
	86/09	Hol. Fm.	48,6 %	4,3 %	18,1 %	9,57 %	0,8 %	18,6 %
	87/09	Hol. Fm.	51,7 %	3,7 %	19,0 %	7,5 %	1,0 %	17,1 %
	61/09	Gru. Fm.	31,3 %	20,3 %	40,8 %	0,6 %	1,1 %	5,9 %
Trodalen	1/10	Hol. Fm.	61,7 %	4,7 %	23,5 %	0,1 %	0,8 %	9,3 %
	2/10	Hol. Fm.	57,3 %	5,5 %	19,8 %	0,4 %	4,1 %	12,9 %
	3/10	Hol. Fm.	57,2 %	7,3 %	19,7 %	0,3 %	4,4 %	11,1 %
	6/10	Hol. Fm.	49,0 %	10,3 %	18,6 %	0,5 %	6,0 %	15,6 %
	7/10	Hol. Fm.	69,8 %	4,3 %	18,0 %	0,2 %	2,2 %	5,6 %
	14/10	Hol. Fm.	64,7 %	5,3 %	19,8 %	2,9 %	0,3 %	6,9 %
	17/10	Hol. Fm.	62,7 %	0,0 %	22,0 %	0,0 %	2,3 %	13,0 %
	19/10	Hol. Fm.	61,8 %	2,9 %	23,8 %	1,8 %	1,7 %	8,0 %
	21/10	Gru. Fm.	39,7 %	11,1 %	45,2 %	0,5 %	0,8 %	2,8 %
Tillbergfjellet Vest	1/10	Gru. Fm.	42,4 %	14,5 %	41,1 %	0,1 %	0,3 %	1,5 %
	2/10	Hol. Fm.	63,4 %	6,0 %	20,0 %	0,3 %	2,2 %	8,2 %
	4/10	Hol. Fm.	66,6 %	6,0 %	19,3 %	0,3 %	1,7 %	6,1 %
	5/10	Hol. Fm.	62,2 %	6,1 %	19,4 %	0,9 %	3,3 %	8,1 %
	9/10	Hol. Fm.	57,9 %	6,6 %	20,5 %	0,9 %	3,6 %	10,6 %
	13/10	Hol. Fm.	56,9 %	0,0 %	20,1 %	4,1 %	0,0 %	19,0 %
	14/10	Hol. Fm.	66,2 %	5,4 %	16,3 %	0,6 %	3,9 %	7,6 %
	16/10	Hol. Fm.	76,5 %	5,3 %	12,9 %	0,6 %	0,8 %	3,9 %
	17/10	Hol. Fm.	78,9 %	4,6 %	11,5 %	0,3 %	1,3 %	3,4 %
	18/10	Hol. Fm.	84,5 %	1,6 %	12,1 %	0,3 %	0,32 %	1,3 %
Tillbergfjellet Battfjellet	1/10	Batt. Fm.	54,2 %	3,2 %	27,4 %	2,1 %	0,4 %	12,7 %
Gangdalen Sør	3/10	Hol. Fm.	60,2 %	8,9 %	20,7 %	0,3 %	2,2 %	7,7 %
	4/10	Hol. Fm.	50,3 %	8,4 %	29,9 %	0,4 %	3,1 %	8,1 %
	5/10	Hol. Fm.	54,7 %	6,5 %	22,0 %	4,9 %	0,5 %	11,3 %
	7/10	Hol. Fm.	64,3 %	6,2 %	19,8 %	0,2 %	3,1 %	6,2 %
	8/10	Hol. Fm.	62,3 %	7,9 %	23,0 %	0,4 %	1,7 %	4,7 %
	10/10	Hol. Fm.	76,0 %	6,1 %	14,5 %	0,4 %	0,6 %	2,4 %
	11/10	Hol. Fm.	66,7 %	6,6 %	20,2 %	0,6 %	0,7 %	5,3 %
	12/10	Hol. Fm.	57,5 %	6,5 %	19,3 %	0,8 %	2,9 %	13,1 %
	13/10	Hol. Fm.	53,9 %	5,9 %	27,2 %	0,6 %	2,8 %	9,6 %
	14/10	Hol. Fm.	58,6 %	6,2 %	17,0 %	1,1 %	3,1 %	14,0 %
	1/10	Gru. Fm.	48,5 %	13,6 %	35,0 %	0,6 %	0,9 %	1,5 %

	18/10	Batt. Fm.	67,0 %	3,6 %	19,6 %	0,4 %	2,7 %	6,7 %
Tverrdalen	2/10	Hol. Fm.	52,7 %	8,2 %	27,6 %	0,4 %	2,2 %	8,9 %
	4/10	Hol. Fm.	57,0 %	9,9 %	24,1 %	0,4 %	1,8 %	6,8 %
	6/10	Hol. Fm.	66,1 %	12,3 %	16,9 %	0,4 %	1,4 %	2,9 %
	7/10	Hol. Fm.	42,8 %	16,7 %	28,0 %	0,7 %	2,3 %	9,6 %
	10A/10	Hol. Fm.	75,1 %	5,4 %	15,7 %	0,2 %	0,3 %	3,3 %
	11/10	Gil. Mb.	55,0 %	7,8 %	30,2 %	0,5 %	0,9 %	5,5 %
	1/10	Gru. Fm.	42,5 %	17,5 %	36,5 %	0,4 %	0,7 %	2,4 %

Appendix 4

Appendix 4: The results of point counting of thin sections. Qm = Quartz monocrystalline, Qp = Quartz polycrystalline, Opq = Opaque, Fs = Feldspar, Bt = Biotite, Pc = Plagioclase, WM = White mica, Chl = chlorite, Gl = Glauconite, HM = Heavy mineral, Com = Comment, Hol Fm. = Hollendardalen Formation, Gru. Fm. = Grumantbyen Formation, Batt. Fm. = Battfjellet Formation. NC = Not counted. Samples noted as "not counted" are thin sections either too fine grained or too badly prepared to be counted.

Outcrop/core:	Fm	Sample	Qm	Qp	Opq	Chert	Fs	Bt	Pc	Clay	Illite	WM	Chl	Gl	HM	Other	Com
Oppkuvbekken	Hol. Fm.	88/09															NC
	Hol. Fm.	94/09	40,3 %	4,0 %	7,5 %	1,3 %	10,8 %	5,8 %	0,0 %	4,5 %	21,8 %	3,3 %	0,8 %	0,3 %	0,0 %	0,0 %	
	Hol. Fm.	108/09															NC
	Hol. Fm.	100/09	45,9 %	2,0 %	2,7 %	1,2 %	11,2 %	2,2 %	0,0 %	4,2 %	26,4 %	3,7 %	0,0 %	0,2 %	0,0 %	0,0 %	
	Hol. Fm.	105/09	31,3 %	2,7 %	6,2 %	1,0 %	5,2 %	4,2 %	0,7 %	1,0 %	33,5 %	13,2 %	0,5 %	0,5 %	0,0 %	0,0 %	
	Hol. Fm.	107/09	43,6 %	2,2 %	4,3 %	1,0 %	11,1 %	2,2 %	1,0 %	3,1 %	23,6 %	7,7 %	0,2 %	0,0 %	0,0 %	0,0 %	
Vestalbekken	Gru. Fm.	138/09															NC
	Hol. Fm.	110/09	44,3 %	0,5 %	10,3 %	0,5 %	18,5 %	0,3 %	0,0 %	3,5 %	20,5 %	1,3 %	0,5 %	0,0 %	0,0 %	0,0 %	
	Hol. Fm.	113/09	35,2 %	0,2 %	6,7 %	0,0 %	9,5 %	0,7 %	0,0 %	3,0 %	40,9 %	3,0 %	0,7 %	0,0 %	0,0 %	0,0 %	
	Hol. Fm.	114/09	23,3 %	0,0 %	16,8 %	0,0 %	8,5 %	2,3 %	0,0 %	0,5 %	46,3 %	2,0 %	0,3 %	0,3 %	0,0 %	0,0 %	
	Hol. Fm.	120/09															NC
	Hol. Fm.	124/09															NC
	Hol. Fm.	125/09	38,8 %	0,8 %	3,8 %	0,3 %	14,8 %	1,5 %	0,0 %	3,0 %	34,8 %	2,0 %	0,5 %	0,0 %	0,0 %	0,0 %	
	Hol. Fm.	129/09	34,8 %	0,5 %	10,8 %	0,0 %	8,5 %	1,5 %	0,0 %	1,5 %	40,5 %	1,8 %	0,3 %	0,0 %	0,0 %	0,0 %	
	Hol. Fm.	130/09	47,0 %	0,2 %	8,0 %	0,0 %	16,2 %	1,2 %	0,0 %	1,0 %	24,4 %	1,0 %	0,5 %	0,0 %	0,5 %	0,0 %	
	Hol. Fm.	131/09	41,6 %	2,5 %	5,0 %	0,5 %	11,3 %	0,0 %	0,0 %	1,3 %	36,3 %	1,5 %	0,0 %	0,0 %	0,0 %	0,0 %	
	Hol. Fm.	7/10	39,4 %	2,8 %	3,0 %	0,5 %	10,1 %	1,5 %	0,0 %	7,5 %	33,7 %	1,0 %	0,5 %	0,0 %	0,0 %	0,0 %	
	Hol. Fm.	6/10	33,6 %	2,5 %	2,3 %	0,0 %	14,0 %	2,0 %	0,3 %	4,8 %	36,1 %	3,8 %	0,0 %	0,8 %	0,0 %	0,0 %	
Vesuv	Batt. Fm.	163/09	50,0 %	2,3 %	3,0 %	0,0 %	0,8 %	16,8 %	0,3 %	1,0 %	20,8 %	3,0 %	0,0 %	0,0 %	0,0 %	2,3 %	
	Batt. Fm.	164/09	40,0 %	3,3 %	1,5 %	0,0 %	1,3 %	13,5 %	0,0 %	0,8 %	35,0 %	2,5 %	0,3 %	0,0 %	0,0 %	2,0 %	
Holmsenfjellet	Hol. Fm.	46/09	8,8 %	0,0 %	18,6 %	0,0 %	5,6 %	0,0 %	0,0 %	35,5 %	30,4 %	1,0 %	0,0 %	0,0 %	0,0 %	0,0 %	

	Hol. Fm.	47/09	23,9 %	0,5 %	12,7 %	0,0 %	10,7 %	0,0 %	0,0 %	3,7 %	47,1 %	1,2 %	0,0 %	0,0 %	0,0 %	0,0 %	
	Hol. Fm.	49/09	21,9 %	0,0 %	11,2 %	0,0 %	13,2 %	0,0 %	0,0 %	15,2 %	37,9 %	0,5 %	0,0 %	0,0 %	0,0 %	0,0 %	
	Hol. Fm.	52/09	11,9 %	0,0 %	26,4 %	0,0 %	4,0 %	0,0 %	0,0 %	3,2 %	54,2 %	0,2 %	0,0 %	0,0 %	0,0 %	0,0 %	
	Hol. Fm.	56/09	38,3 %	1,0 %	4,5 %	0,0 %	14,3 %	0,5 %	0,0 %	5,0 %	35,8 %	0,8 %	0,0 %	0,0 %	0,0 %	0,0 %	
	Hol. Fm.	59/09	36,6 %	1,5 %	6,2 %	0,7 %	8,7 %	1,2 %	0,2 %	4,0 %	39,6 %	0,5 %	0,7 %	0,0 %	0,0 %	0,0 %	
	Hol. Fm.	60/09	16,3 %	0,5 %	27,2 %	0,2 %	12,1 %	0,5 %	0,0 %	9,1 %	33,8 %	0,2 %	0,0 %	0,0 %	0,0 %	0,0 %	
	Hol. Fm.	62/09	34,8 %	2,8 %	6,5 %	1,0 %	15,3 %	1,0 %	0,0 %	5,3 %	32,8 %	0,5 %	0,3 %	0,0 %	0,0 %	0,0 %	
	Hol. Fm.	64/09	23,9 %	0,5 %	12,7 %	0,0 %	10,7 %	0,0 %	0,0 %	3,7 %	47,1 %	1,2 %	0,0 %	0,0 %	0,0 %	0,0 %	
	Hol. Fm.	71/09	14,5 %	0,0 %	45,9 %	0,0 %	9,1 %	0,0 %	0,0 %	1,2 %	29,2 %	0,0 %	0,0 %	0,0 %	0,0 %	0,0 %	
	Hol. Fm.	70/09	30,4 %	1,7 %	7,7 %	0,2 %	20,5 %	0,2 %	0,0 %	5,7 %	32,3 %	1,0 %	0,0 %	0,0 %	0,2 %	0,0 %	
	Hol. Fm.	66/09	36,3 %	0,0 %	8,4 %	0,0 %	16,3 %	0,0 %	0,0 %	2,5 %	35,1 %	1,0 %	0,5 %	0,0 %	0,0 %	0,0 %	
	Hol. Fm.	74/09	19,3 %	0,0 %	13,5 %	0,0 %	16,0 %	0,3 %	0,3 %	4,5 %	45,3 %	1,0 %	0,0 %	0,0 %	0,0 %	0,0 %	
	Hol. Fm.	76/09	30,6 %	0,0 %	7,0 %	0,5 %	15,2 %	0,7 %	0,0 %	0,5 %	43,3 %	1,5 %	0,5 %	0,0 %	0,2 %	0,0 %	
	Hol. Fm.	78/09	40,0 %	0,5 %	4,9 %	0,0 %	17,9 %	0,5 %	0,0 %	0,5 %	34,3 %	1,2 %	0,0 %	0,2 %	0,0 %	0,0 %	
	Hol. Fm.	81/09	0,5 %	0,5 %	9,0 %	0,2 %	21,4 %	1,5 %	0,0 %	4,0 %	37,9 %	0,7 %	0,0 %	0,2 %	0,2 %	0,0 %	
	Hol. Fm.	83/09	25,7 %	0,0 %	18,9 %	0,2 %	16,7 %	0,7 %	0,0 %	2,1 %	34,4 %	1,2 %	0,0 %	0,0 %	0,0 %	0,0 %	
	Hol. Fm.	84/09	27,5 %	1,4 %	9,4 %	0,7 %	21,0 %	1,0 %	0,0 %	6,0 %	31,6 %	1,4 %	0,0 %	0,0 %	0,0 %	0,0 %	
	Hol. Fm.	86/09	36,7 %	0,7 %	5,0 %	0,2 %	16,9 %	0,7 %	0,0 %	4,2 %	34,0 %	1,0 %	0,5 %	0,0 %	0,0 %	0,0 %	
	Hol. Fm.	87/09	34,8 %	2,0 %	6,3 %	0,8 %	14,5 %	1,0 %	0,0 %	2,3 %	37,0 %	1,3 %	0,3 %	0,0 %	0,0 %	0,0 %	
	Gru. Fm.	61/09	23,3 %	0,3 %	9,5 %	0,5 %	0,0 %	35,0 %	0,0 %	0,8 %	29,5 %	0,8 %	0,0 %	0,5 %	0,0 %	0,0 %	
Trodalen	Hol. Fm.	2/10															NC
	Hol. Fm.	7/10	25,0 %	0,5 %	14,5 %	0,0 %	6,5 %	4,5 %	0,0 %	0,0 %	44,0 %	4,8 %	0,3 %	0,0 %	0,0 %	0,0 %	
	Hol. Fm.	10/10	37,1 %	2,5 %	4,5 %	0,5 %	5,0 %	3,7 %	0,2 %	4,0 %	40,0 %	2,2 %	0,2 %	0,0 %	0,0 %	0,0 %	
	Hol. Fm.	14/10	18,3 %	0,5 %	23,0 %	0,0 %	6,3 %	1,0 %	0,0 %	3,3 %	42,3 %	5,5 %	0,0 %	0,0 %	0,0 %	0,0 %	
	Hol. Fm.	19/10	36,0 %	0,3 %	11,8 %	0,0 %	13,3 %	2,5 %	0,0 %	6,3 %	24,5 %	5,0 %	0,3 %	0,0 %	0,3 %	0,0 %	
	Gru. Fm.	21/10	26,8 %	1,0 %	5,0 %	0,0 %	1,0 %	34,5 %	0,8 %	2,0 %	23,5 %	3,0 %	0,3 %	2,0 %	0,3 %	0,0 %	
Tillbergfjellet Vest	Hol. Fm.	5/10	28,4 %	0,2 %	13,0 %	0,7 %	12,0 %	1,7 %	0,0 %	1,0 %	35,9 %	6,5 %	0,5 %	0,0 %	0,0 %	0,0 %	
	Hol. Fm.	9/10	24,4 %	1,2 %	9,5 %	0,2 %	18,0 %	1,2 %	0,0 %	3,5 %	36,4 %	5,2 %	0,2 %	0,0 %	0,0 %	0,0 %	

	Hol. Fm.	14/10	38,5 %	2,3 %	4,0 %	0,0 %	12,3 %	1,3 %	0,0 %	6,0 %	33,5 %	2,0 %	0,0 %	0,0 %	0,3 %	0,0 %	
	Hol. Fm.	16/10	43,3 %	1,0 %	1,8 %	0,0 %	17,0 %	3,0 %	0,0 %	3,0 %	27,0 %	3,8 %	0,3 %	0,0 %	0,0 %	0,0 %	
	Hol. Fm.	17/10	45,0 %	0,5 %	4,5 %	0,5 %	14,0 %	0,8 %	0,0 %	1,8 %	32,0 %	0,8 %	0,0 %	0,0 %	0,3 %	0,0 %	
	Hol. Fm.	18/10	39,3 %	2,4 %	6,6 %	1,2 %	14,3 %	1,5 %	0,0 %	3,9 %	26,9 %	3,9 %	0,0 %	0,0 %	0,0 %	0,0 %	
	Gru. Fm.	1/10	23,4 %	0,2 %	4,5 %	0,0 %	1,0 %	30,8 %	0,0 %	1,0 %	33,3 %	4,0 %	0,2 %	1,5 %	0,0 %	0,0 %	
Tillbergfjellet Battfjellet	Batt. Fm.	1/10	40,8 %	2,8 %	6,5 %	0,0 %	1,0 %	20,5 %	0,0 %	2,0 %	15,8 %	9,5 %	0,5 %	0,0 %	0,8 %	0,0 %	
Gangdalen Sør	Gru. Fm.	1/10	24,0 %	0,5 %	9,3 %	0,8	32,3%	1,0 %	0,0	2,6 %	28,0 %	0,3 %	0,8 %	0,5 %	0,0 %	0,0 %	
	Hol. Fm.	4/10															NC
	Hol. Fm.	8/10	31,3 %	1,0 %	12,3 %	2,3 %	8,0 %	3,5 %	0,0 %	0,3 %	35,3 %	5,3 %	1,0 %	0,0 %	0,0 %	0,0 %	
	Hol. Fm.	10/10	44,8 %	2,8 %	3,3 %	3,8 %	13,5 %	4,0 %	0,0 %	2,0 %	22,0 %	2,0 %	0,8 %	1,3 %	0,0 %	0,0 %	
	Hol. Fm.	12/10	23,0 %	0,2 %	17,5 %	0,0 %	17,3 %	1,0 %	0,0 %	2,2 %	32,1 %	5,2 %	0,7 %	0,7 %	0,0 %	0,0 %	
	Hol. Fm.	13/10	24,8 %	0,3 %	14,0 %	0,0 %	12,8 %	0,8 %	0,0 %	1,5 %	40,3 %	4,8 %	1,0 %	0,0 %	0,0 %	0,0 %	
	Hol. Fm.	14/10															NC
	Batt. Fm.	16/10	41,9 %	2,0 %	4,2 %	1,2 %	2,0 %	18,0 %	0,0 %	3,5 %	17,2 %	8,7 %	0,7 %	0,2 %	0,2 %	0,5 %	
Tverrdalen	Gru. Fm.	1/10	26,5%	0,8%	5,75%	0,8%	44,5%	1,3%	0,0%	2,8%	15,8%	0,5%	0,0%	1,5%	0,0%	0,0%	
	Hol. Fm.	2/10															NC
	Hol. Fm.	4/10	34,4 %	1,2 %	5,7 %	1,5 %	14,6 %	3,0 %	0,5 %	2,7 %	31,7 %	3,7 %	0,7 %	0,2 %	0,0 %	0,0 %	
	Hol. Fm.	6/110	39,8 %	2,0 %	7,8 %	1,0 %	11,0 %	4,3 %	0,0 %	5,0 %	25,8 %	2,8 %	0,3 %	0,5 %	0,0 %	0,0 %	
	Hol. Fm.	7/10	23,8 %	0,2 %	19,6 %	0,0 %	10,4 %	1,5 %	0,0 %	1,7 %	40,0 %	2,2 %	0,5 %	0,0 %	0,0 %	0,0 %	
	Hol. Fm.	10A/10	49,0 %	2,3 %	5,0 %	1,5 %	15,3 %	2,0 %	0,0 %	0,3 %	23,3 %	0,8 %	0,8 %	0,0 %	0,0 %	0,0 %	

Appendix 5

Appendix 5: The calculated quartz/feldspar ratios, based on thin section (TS) and XRD analysis.

Outcrop/borehole	Formation	Sample	XRD-number	Height (m)	XRD-ratio	TS-ratio
Oppkuvbekken	Hol. Fm.		6648	0,40	2,03	
	Hol. Fm.	94/09	6653	1,70	3,76	4,12
	Hol. Fm.		6649	3,20	2,31	
	Hol. Fm.		6654	3,40	4,73	
	Hol. Fm.	100/09	6650	4,90	4,36	4,27
	Hol. Fm.		6655	6,40	4,00	
	Hol. Fm.	105/09	6651	8,50	2,19	5,71
	Hol. Fm.	107/09	6652	9,80	3,01	3,80
Vestalbekken	Gru. Fm.	138/09	6659		0,74	
	Hol. Fm.	109/09	6656	0,20	1,92	
	Hol. Fm.	110/09		0,45		2,42
	Hol. Fm.	112/09	6662	1,30	2,39	
	Hol. Fm.	113/09	6660	1,70	3,78	3,74
	Hol. Fm.	114/09	6657	2,30	2,94	2,74
	Hol. Fm.	116/09	6663	3,25	4,30	
	Hol. Fm.	4/10	6842	3,65	2,17	
	Hol. Fm.	124/09	6658	6,75	2,63	
	Hol. Fm.	125/09	6841	7,00	3,67	2,68
	Hol. Fm.	126/09	6664	7,25	3,48	
	Hol. Fm.	129/09	6661	8,90	2,83	4,15
	Hol. Fm.	130/09	6665	10,70	5,95	2,92
	Hol. Fm.	131/09				3,91
	Hol. Fm.	7/10	6844	14,50	3,25	4,20
	Hol. Fm.	6/10	6843	16,50	4,18	2,53
Vesuv	Batt. Fm.	164/09	164/09	Bunn	2,14	3,20
	Batt. Fm.	163/09	163/09	topp	2,45	3,07
Holmsenfjellet	Gru Fm.	61/09	6325		0,51	
	Hol. Fm.	46/09	6646	0,15	1,93	1,57
	Hol. Fm.	47/09	6333	0,30	2,42	2,28
	Hol. Fm.	49/09	6329	1,30	2,70	1,66
	Hol. Fm.	50/09	6846	1,60	2,05	
	Hol. Fm.	52/09	6328	2,40	0,69	3,00
	Hol. Fm.	56/09	6310	4,10	1,96	2,75
	Hol. Fm.	59/09	6309	5,60	1,87	4,25
	Hol. Fm.	60/09	6323	6,80	2,00	1,39
	Hol. Fm.	62/09	6332	8,25	3,61	2,46
	Hol. Fm.	64/09	6847	8,75	1,93	2,28
	Hol. Fm.	71/09	6299	10,30	2,15	1,59
	Hol. Fm.	70/09	6335	10,75	2,54	1,57

	Hol. Fm.	69/09		11,40		
	Hol. Fm.	66/09	6311	13,00	1,59	2,23
	Hol. Fm.	74/09	6336	13,15	2,52	1,18
	Hol. Fm.	76/09	6308	15,50	1,67	2,02
	Hol. Fm.	78/09	6331	17,60	2,63	2,26
	Hol. Fm.	81/09	6330	22,75	2,11	1,15
	Hol. Fm.	83/09	6334	23,90	2,12	1,54
	Hol. Fm.	84/09	6327	24,75	2,41	1,38
	Hol. Fm.	86/09	6324	26,00	2,16	2,22
	Hol. Fm.	87/09	6326	26,60	2,27	2,53
Trodalen	Gru. Fm.	21/10	6857		0,71	
	Hol. Fm.	1/10	6848	0,25	2,19	
	Hol. Fm.	2/10	6849	1,20	2,26	
	Hol. Fm.	3/10	6850	2,20	2,13	
	Hol. Fm.	6/10	6851	5,00	1,70	
	Hol. Fm.	7/10	6852	5,50	3,14	3,92
	Hol. Fm.	10/10	6853	8,50		7,57
	Hol. Fm.	14/10	6854	15,65	2,58	3,00
	Hol. Fm.	17/10	6855	17,90	2,85	
	Hol. Fm.	19/10	6856	18,90	2,32	2,74
Tillbergfjellet Batt.	Batt. Fm.	1/10	6868		1,77	1,99
Tillbergfjellet Vest	Hol. Fm.	2/10	6859	0,00	2,44	
	Hol. Fm.	4/10	6860	1,40	2,63	
	Hol. Fm.	5/10	6862	2,50	2,44	2,40
	Hol. Fm.	9/10	6861	5,90	2,14	1,43
	Hol. Fm.	13/10	6863	8,75	2,83	
	Hol. Fm.	14/10	6864	10,20	3,06	3,33
	Hol. Fm.	16/10	6865	13,50	4,20	2,60
	Hol. Fm.	17/10	6866	14,60	4,91	3,25
	Hol. Fm.	18/10	6867	15,60	6,15	2,92
	Gru. Fm.	1/10	6858		0,76	0,77
Gangdalen Sør	Gru. Fm.	1/10	6869		0,99	2,22
	Hol. Fm.	3/10	6870	2,75	2,03	
	Hol. Fm.	4/10	6871	3,50	1,31	
	Hol. Fm.	5/10	6872	4,00	1,92	
	Hol. Fm.	7/10	6873	5,90	2,47	
	Hol. Fm.	8/10	6874	7,25	2,01	4,03
	Hol. Fm.	10/10	6875	10,10	3,68	3,52
	Hol. Fm.	11/10	6876	10,25	2,50	
	Hol. Fm.	12/10	6877	12,00	2,23	1,34
	Hol. Fm.	13/10	6878	13,15	1,63	1,96
	Hol. Fm.	14/10	6879	14,50	2,52	
	Batt. Fm.	16/10	6880		2,89	2,51
Tverrdalen	Gru. Fm.	1/10	6881		0,79	

	Gil. Mb.	11/10	6887		1,44	
	Hol. Fm.	2/10	6882	0,20	1,47	
	Hol. Fm.	4/10	6883	1,40	1,67	2,36
	Hol. Fm.	6/10	6884	2,25	2,26	3,80
	Hol. Fm.	7/10	6885	3,25	0,96	2,31
	Hol. Fm.	10A/10	6886	4,80	3,55	3,36

Appendix 6: Standard log sheme applied in the field analysis

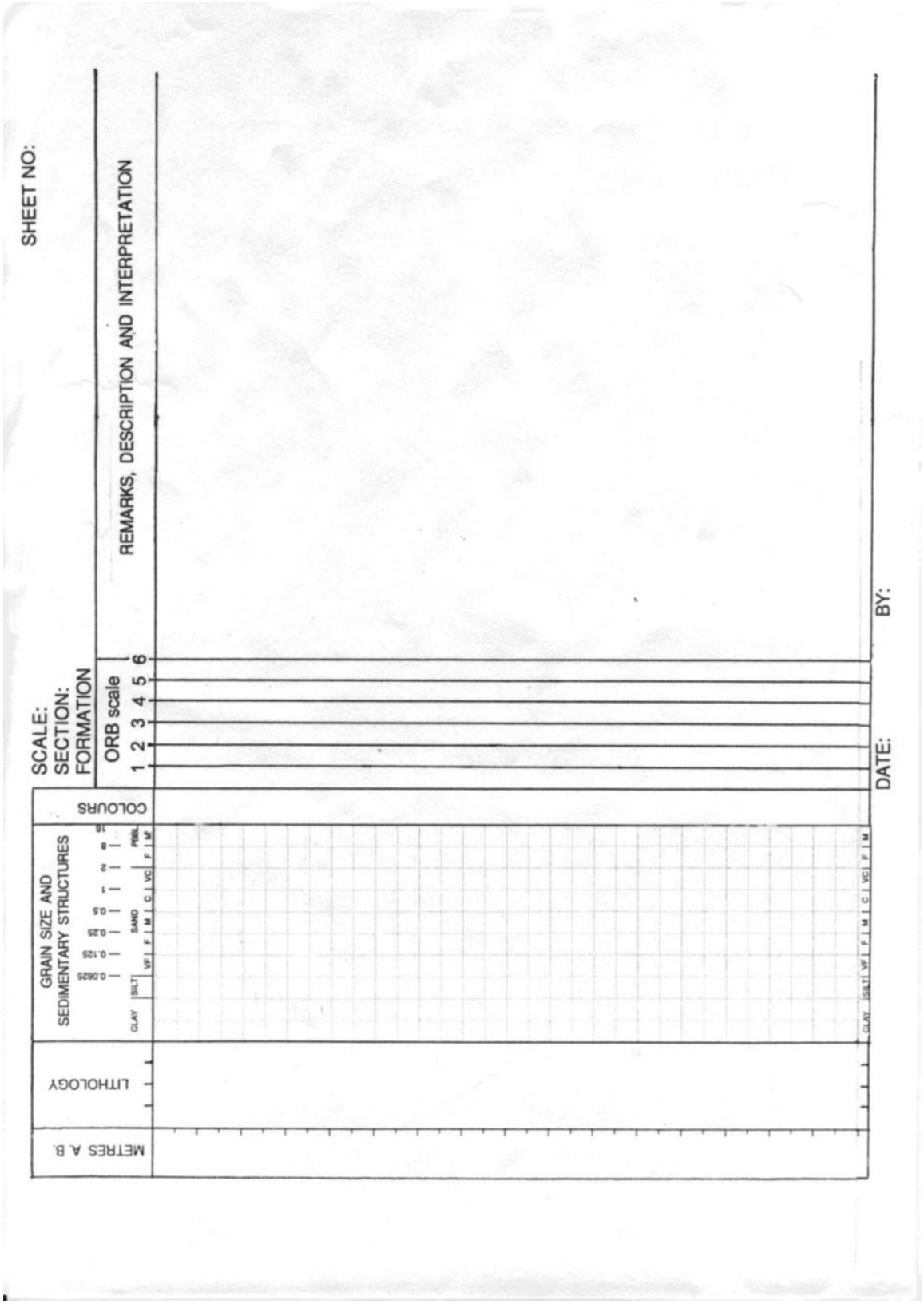

Appendix 7

Appendix 7: Paleocurrent measurements of ripples and cross-bedding. Note that measurements conducted in 2009 are not found in the logs. All logs from 2009 were re-logged in 2010.

Outcrop/height (m)	Structure	Paleocurrent	Year
oppkuvbekken			
2,5	Cross-bedding	335	2010
4	Cross-bedding	260	2010
4	Cross-bedding	300	2010
5	Low-angle cross-bedding	250	2010
1,1	Low-angle cross-bedding	136	2009
6	Asymmetrical ripples	330	2009
Vestalbekken			
1,5	Asymmetrical ripples	120	2010
3,75	Asymmetrical ripples	260	2010
2,75	Asymmetrical ripples	142	2009
3	Asymmetrical ripples	135	2009
3	Asymmetrical ripples	225	2009
3,5	Asymmetrical ripples	142	2009
3,75	Cross-bedding	40	2009
3,8	Cross-bedding	110	2009
3,9	Cross-bedding	74	2009
3,9	Asymmetrical ripples	135	2009
4,9	Cross-bedding	135	2009
5	Cross-bedding	1	2009
Holmsenfjellet			
0,75	Asymmetrical ripples	88	2009
9,75	Asymmetrical ripples	210	2009
11,4	Asymmetrical ripples	130	2009
12,5	Asymmetrical ripples	120	2009
19	Asymmetrical ripples	152	2009
19,25	Asymmetrical ripples	130	2009
19,6	Asymmetrical ripples	130	2009
24	Asymmetrical ripples	200	2009
Trodalen			
5,75	Symmetrical ripples	62/242	2010
5,8	Symmetrical ripples	75/255	2010
7,25	Cross-bedding	98	2010
9	Asymmetrical ripples	315	2010
12,25	Symmetrical ripples	88/268	2010
16	Asymmetrical ripples	165	2010
Tillbergfjellet Vest			
2,55	Low-angle cross-bedding	278	2010

13,25	Cross-bedding	75	2010
14	Asymmetrical ripples	120	2010
14,5	Asymmetrical ripples	270	2010
Gangdalen Sør			
7,4	Symmetrical ripples	175/366	2010
Tverrdalen			
1,4	Symmetrical ripples	150/330	2010
2	Symmetrical ripples	20/200	2010

Appendix CD